

## **ABSTRACT**

Merritt, Carey Reid. A Pneumatically Actuated Brace Designed For Upper Extremity Stroke Rehabilitation (Under the direction of Dr. Eddie Grant)

Nearly 700,000 people suffered from stroke last year and those who survived were left with any number of disabilities. One of the most common disabilities in stroke is paralysis of the upper arm. Since therapy for this disability is expensive, patients are finding rehabilitation difficult to afford and manage. This thesis proposes an inexpensive pneumatic wearable garment for the patient to use for stroke rehabilitation. Unlike most rehabilitation robots, which are large, non-compliant, and expensive, this device will enable the patient to purchase the garment and move freely within their own home while rehabilitating their affected arm. In this thesis, a wearable elbow device similar to the proposed wearable garment was designed using an inexpensive elbow brace. The elbow brace used custom made artificial air muscles also known as McKibben Artificial Muscles to substitute for the biceps and triceps, which are responsible for flexion and extension of the human elbow. These artificial muscles were chosen for their low-cost, compliance, lightweight, and large force capabilities. The air muscles were designed and developed especially for this device and cost less than \$3.00 to make and weigh approximately 11 g. This pneumatically actuated elbow brace was controlled using solenoid valves in conjunction with a Mitsubishi M32/83C 16-bit micro controller to achieve flexion and extension of the elbow. Experiments on the pneumatic elbow brace have shown that it is capable of moving a passive patient's arm within a 110° range, which is adequate for rehabilitation of the elbow.

**A PNEUMATICALLY ACTUATED BRACE DESIGNED FOR UPPER EXTREMITY  
STROKE REHABILITATION**

by  
**CAREY REID MERRITT**

A thesis submitted to the Graduate Faculty of  
North Carolina State University  
in partial fulfillment of the  
requirements for the Degree of  
Master of Science

**COMPUTER ENGINEERING**

Raleigh

April 2, 2003

**APPROVED BY:**

Two handwritten signatures in cursive script, one on the left and one on the right, positioned above a horizontal line.A handwritten signature in cursive script, positioned above a horizontal line.

Chair of Advisory Committee

# Dedication

*To Carol...*

## **Biography**

Carey R. Merritt, born on August 17, 1978 in Wilmington, NC, received both his Bachelor of Science and Masters of Science in Computer Engineering from North Carolina State University in Fall 2001 and Spring 2003 respectively. He is a member of Phi Kappa Phi, Tau Bata Pi, Golden Key Club, and Eta Kappa Nu.

# Acknowledgments

I thank my parents for their support and keeping me in their prayers. I thank Dr. Grant for his support and advice during the course of my research. I thank my committee: Dr. Dean and Dr. White.

I thank Tim Vanschaick and Spero Karas for their efforts in helping me obtain the donated elbow braces from DonJoy, and I owe thanks to DonJoy for their donation. I also thank Dr. Little for the donated mannequin arm that was used for testing the pneumatic brace and I thank Mitsubishi for the donated M32/83C MCU.

I am grateful for Andrew Nelson's help on the test platform in making the aluminum block and mounting the rotary potentiometer. I also thank Zheng Li for his help with several of the experiments and for making some of the air muscles. I thank Tim Slusser for his help on the accelerometers. Finally, I thank Dr. Carol Giuliani for her advice and great contacts.

# Table of Contents

<b>LIST OF FIGURES .....</b>	<b>viii</b>
<b>LIST OF TABLES.....</b>	<b>xi</b>
<b>LIST OF ABBREVIATIONS .....</b>	<b>xii</b>
<b>CHAPTER 1. INTRODUCTION .....</b>	<b>1</b>
<b>1.1 Motivation.....</b>	<b>1</b>
<b>1.2 Thesis Goals.....</b>	<b>2</b>
<b>1.3 Outline of Thesis .....</b>	<b>2</b>
<b>CHAPTER 2. LITERATURE REVIEW .....</b>	<b>4</b>
<b>2.1 Medical Professionals’ Roles in Stroke Rehabilitation .....</b>	<b>4</b>
2.1.1 Physicians .....	4
2.1.2 Rehabilitation Nurses.....	5
2.1.3 Physical Therapists .....	5
2.1.4 Occupational Therapists.....	5
<b>2.2 Upper Limb Rehabilitation for Hemiplegic patients.....</b>	<b>6</b>
2.2.1 Activities of Daily Living (ADLs).....	6
2.2.2 Range of Motion (ROM) .....	7
2.2.3 Stroke Rehabilitation Tests .....	9
2.2.4 Stroke Rehabilitation Strategies.....	9
<b>2.3 Current Rehabilitation Robots for Stroke Patients.....</b>	<b>9</b>
2.3.1 MIT-MANUS .....	10
2.3.2 Wrist Robot.....	12
2.3.3 MIME.....	13
2.3.4 ARM Guide.....	14
2.3.5 GENTLE/S.....	15
2.3.6 Bimanual Lifting Rehabilitator for the arm .....	17
2.3.7 Java Therapy – Joystick.....	19
2.3.8 Artificial Muscle Manipulator .....	20
<b>2.4 Virtual Reality Rehabilitation .....</b>	<b>22</b>
2.4.1 PHANToM.....	23
2.4.2 Immersion Products .....	25
2.4.2.1 CyberGlove™ .....	25
2.4.2.2 CyberGrasp™.....	26
2.4.2.3 CyberForce™.....	27

2.4.3 Rutgers Master II-ND Force Feedback Glove .....	28
2.4.4 Orthotic Upper Limb using Particle Mechanical Constraint (PMC) .....	29
<b>2.5 Actuators for Rehabilitation Robots .....</b>	<b>31</b>
2.5.1 DC Motors .....	32
2.5.2 Air Muscles .....	33
2.5.3 Pleated Air Muscles .....	34
<b>2.6 Human to Machine Interfaces for Rehabilitation Robots.....</b>	<b>36</b>
<b>2.7 Literature Review Summary .....</b>	<b>38</b>
<b>CHAPTER 3. OUTLINE OF SYSTEM DESIGN.....</b>	<b>39</b>
<b>3.1 Design Basis For Elbow Brace Prototype.....</b>	<b>39</b>
<b>3.2 Pneumatic System Design .....</b>	<b>42</b>
3.2.1 Pneumatic Circuit.....	43
3.2.2 Tubing and Connectors .....	43
3.2.3 Pneumatic Artificial Muscles (PAMs).....	45
3.2.3.1 Pneumatic Artificial Muscle Assembly .....	46
3.2.4 Valves .....	49
3.2.5 Pressure Transducers.....	50
<b>3.3 Hardware Design .....</b>	<b>54</b>
3.3.1 M32C/83 Micro-controller.....	54
3.3.2 Solenoid Valve Driver Circuit .....	56
3.3.3 Pressure Transducer Circuit.....	57
<b>CHAPTER 4. PNEUMATIC ACTUATOR CHARACTERISTICS AND CONTROL..</b>	<b>59</b>
<b>4.1 Air Muscle Control.....</b>	<b>59</b>
4.1.1 PWM Control.....	59
4.1.2 Bang-Bang Control .....	59
4.1.3 Antagonistic Muscle Pair.....	60
<b>4.2 Test Platform.....</b>	<b>61</b>
4.2.1 Experimental Operation .....	62
4.2.1.1 Single Muscle Pulling a Constant Mass.....	63
4.2.1.2 Air Muscle Positioning a Wooden Arm.....	64
<b>4.3 Test Platform Experiments with Air Muscles.....</b>	<b>65</b>
4.3.1 Response Time.....	65
4.3.2 Valve Response Time .....	67
4.3.3 Leakage .....	68
4.3.4 Exhausting the valve .....	69

4.3.5 Flow Experiments and Results.....	72
<b>4.4 Characteristics of the Air Muscle.....</b>	<b>74</b>
4.4.1 Static Characteristics.....	74
4.4.2 Dynamic Characteristics .....	76
<b>CHAPTER 5. ELBOW ACTUATOR DESIGN AND EXPERIMENTS .....</b>	<b>79</b>
<b>5.1 Design of modified elbow brace.....</b>	<b>79</b>
<b>5.2 Muscle Attachment.....</b>	<b>82</b>
<b>5.3 Experiments and Results.....</b>	<b>84</b>
<b>5.4 Control of Pneumatic Brace.....</b>	<b>90</b>
<b>CHAPTER 6. CONCLUSIONS AND FUTURE RESEARCH .....</b>	<b>95</b>
<b>6.1 Concluding Remarks .....</b>	<b>95</b>
<b>6.2 Future Research.....</b>	<b>96</b>
<b>CHAPTER 7. REFERENCES .....</b>	<b>101</b>
<b>CHAPTER 8. APPENDICES .....</b>	<b>107</b>
<b>8.1 Test Platform Construction .....</b>	<b>107</b>
8.1.1 Required Materials.....	107
8.1.2 Test Platform Design .....	107
<b>8.2 Controller and Experiment code.....</b>	<b>114</b>
8.2.1 Main.h and Main.c .....	114
8.2.1.1 Main.h .....	114
8.2.1.2 Main.c.....	114
8.2.2 Serial1.h and Serial1.c .....	122
8.2.2.1 Serial1.h .....	122
8.2.2.2 Serial1.c.....	123
8.2.3 adc.h and adc.c .....	125
8.2.3.1 adc.h .....	125
8.2.3.2 adc.c .....	125
8.2.4 Board.h.....	126
8.2.5 Timer.h and Timer.c .....	127
8.2.5.1 Timer.h.....	127
8.2.5.2 Timer.c .....	127



# List of Figures

Figure 2.1 MIT-MANUS Planar robot with two DOF .....	11
Figure 2.2 MIT-MANUS Screw-driven Spatial Module to add third dimension.....	12
Figure 2.3 MIT Wrist Robot.....	13
Figure 2.4 MIME uses a PUMA 560 for the patient’s impaired limb.....	14
Figure 2.5 ARM Guide.....	15
Figure 2.6 GENTLE/S.....	16
Figure 2.7 Bimanual Rehabilitator for the affected arm.....	18
Figure 2.8 Java Therapy using Force Feedback Joystick.....	19
Figure 2.9 Artificial Muscle Manipulator.....	20
Figure 2.10 Artificial Muscle Manipulator Frame Assignment.....	21
Figure 2.11 Control scheme for an Artificial Muscle Manipulator (a) Control system for each joint (b) 7-b PCM digital control valve.....	22
Figure 2.12 Stroke Rehabilitation with PHANToM.....	24
Figure 2.13 CyberGlove™.....	26
Figure 2.14 CyberGrasp™.....	26
Figure 2.15 CyberForce™.....	27
Figure 2.16 Rutgers Master II-ND.....	28
Figure 2.17 RMII-ND Haptic Control Interface.....	29
Figure 2.18 PMC Upper-arm movements.....	30
Figure 2.19 Structure of the PMC upper-arm orthotic.....	31
Figure 2.20 Air Muscle (a) Rubber tube with braided sleeve (b) Standard Air Muscle.....	33
Figure 2.21 Pleated Air Muscle.....	35
Figure 2.22 Pleated Air Muscle ‘pumpkin’ shape.....	36
Figure 3.1 Farris Ankle-Foot Orthosis.....	40
Figure 3.2 Inspired by Farris Ankle foot orthosis.....	40
Figure 3.3 Rehabilitative Garment.....	41
Figure 3.4 A Pneumatic Circuit for Pneumatic Artificial Muscles.....	43
Figure 3.5 New Air Muscle Design.....	46
Figure 3.6 Materials required for new air muscle design.....	47
Figure 3.7 Open tube end of air muscle pushing through braiding.....	48
Figure 3.8 Loop formed on plugged end of air muscle.....	49
Figure 3.9 Isonic 2-way solenoid valve and manifold.....	49
Figure 3.10 Motorola Pressure MPX5700GP-ND Transducer.....	51
Figure 3.11 Pressure Transducer response to PSI.....	53
Figure 3.12 MSV1632/83 - SKP Starter Kit Plus™.....	55
Figure 3.12 Mead Isonic® 2-way solenoid driver circuit.....	56
Figure 3.13 Recommended power supply decoupling and output filtering.....	58
Figure 4.1 Antagonistic Pair.....	61
Figure 4.2 Test platform (a) setup for lifting a mass (b) setup for positioning an arm with either one or two muscles.....	62
Figure 4.3 Test Platform Options (a) hanging mass (b) single muscle with arm (c) antagonistic muscles with arm.....	63

Figure 4.4 1 lb zip-lock bag of bee-bees.....	64
Figure 4.5 Antagonistic muscle pair controlling the wooden arm.....	65
Figure 4.6 Response Time To Fill Muscle at 0 lb.....	66
Figure 4.7 Response time for doubled 7 ¼" - 11" air muscles .....	67
Figure 4.8 Valve response time ≈ 8 – 10 ms for various pressures and a zero load.....	68
Figure 4.9 Average Leakage from air muscle with a 0 lb, 1 lb, 5 lb load over ½ second samples for 2 minutes .....	69
Figure 4.10 Exhausting a 7 ¼" - 11" air muscle .....	70
Figure 4.11 Exhausting a 7 ¼" - 11" air muscle at 40 and 70 PSI with different loads. ....	71
Figure 4.12 Exhausting doubled 7 ¼" - 11" muscles.....	72
Figure 4.13 Flow response curves combined (0 lb, 1 lb, 5 lb).....	73
Figure 4.14 Force vs. Length for 5 5/16" – 7 ½" air muscle .....	75
Figure 4.15 Force vs. Length for 7.25" – 11" muscle used on pneumatic brace .....	76
Figure 4.16 Damping for 60 PSI with 5 lb, 10 lb, 15 lb loads.....	77
Figure 4.17 Damping for 80 PSI with 5 lb, 10 lb, 15 lb loads.....	78
Figure 5.1 Don Joy IROM Elbow.....	79
Figure 5.2 AutoCad drawing of aluminum shoulder piece.....	80
Figure 5.3 Elbow joint aluminum shape.....	81
Figure 5.4 Insertions and origins of the air muscles (a) Origin of biceps and triceps on aluminum shoulder section (b) Insertion of biceps and triceps on aluminum ‘c’.....	83
Figure 5.5 Wooden block with screw in the top.....	85
Figure 5.6 Angle measurements .....	85
Figure 5.7 Three experiments for testing flexion and extension (a) Shoulder at 0° testing flexion (b) Shoulder at 35° testing flexion (c) Shoulder at -90° testing extension.....	86
Figure 5.8 Flexion experimental results.....	87
Figure 5.9 Extension experiments with single and doubled air muscles .....	88
Figure 5.10 Estimated Joint Force vs. change in length for biceps during flexion.....	89
Figure 5.11 Estimated Force on triceps vs. change in length with Extension angle for comparison.....	90
Figure 5.12 Pressure changes during flexion and extension.....	91
Figure 5.13 Brace angles using antagonistic pair (a) Fully extended [ $P_1 = P_{MIN}$ $P_2 = P_{MAX}$ ] (b) Flexion at approx. 50° [ $P_1 = P_2$ ] (c) Fully flexed at approx. 110° [ $P_1 = P_{MAX}$ $P_2 = P_{MIN}$ ].....	92
Figure 5.14 Antagonistic Controller Schematic.....	93
Figure 5.15 Flexion and extension using control scheme (a) Extension (b) Flexion .....	94
Figure 6.1 Analog Devices ADXL311 Accelerometer.....	96
Figure 6.2 ADXL311 Accelerometer with circuit developed in lab.....	97
Figure 6.3 JRehabilitor GUI using Java3D.....	98
Figure 6.4 File Menu.....	99
Figure 6.5 Options Menu .....	99
Figure 6.6 Connection Dialog.....	99
Figure 8.1 Building the platform body (a) top view connecting the sides to the back (b) back view showing screw placement and eyebolt hole position (c) bottom view middle support and eyebolt installed .....	108
Figure 8.2 Placing legs on body (a) side view (b) front view with feet (c) back view with feet .....	109

Figure 8.3 aluminum block (a) side view (b) top/bottom view .....	109
Figure 8.4 Pulley wheel with holes drilled and aluminum block outline .....	110
Figure 8.5 Top view of platform.....	111
Figure 8.6 1" length 3/8" diameter hex nut with hard wood screwed into the nut .....	111
Figure 8.7 Assembling the pulley (a) front view showing pulley connected to aluminum block and steel bolt (b) top view of platform showing the stops screwed into the aluminum block .....	112
Figure 8.8 Wooden armholes with aluminum block and pulley wheel outlined .....	113
Figure 8.9 Attaching air muscles to device (a) rear muscle attachment to spring link (b) muscle attachment to pulley wheel.....	114

## List of Tables

Table 2.1 Average normal ROMs for upper extremity.....	8
Table 2.2 Strategies that help patients regain use of impaired limbs.....	9
Table 2.3 GENTLE/S Measurements .....	16
Table 2.4 GENTLE/S 3 Modes of Control.....	17
Table 2.5 Four modes of physical therapy for Artificial Muscle Manipulator.....	22
Table 2.6 Advantages of Air Muscles.....	34
Table 2.7 Pleated Air Muscle comparison to Standard Air Muscles.....	35
Table 3.1 Air Muscles for rehabilitation garment.....	42
Table 3.2 Tubing and Connectors used for pneumatic circuit.....	44
Table 3.3 Shadow Air Muscle Prices.....	45
Table 3.4 Pneumatic Artificial Muscle Materials.....	46
Table 3.5 Specifications for Isonic® V1B02RW1 .....	50
Table 3.6 MPX5700GP-ND Specifications.....	52
Table 4.1 Four States of control for an air muscle using two solenoid valves .....	60

## List of Abbreviations

- ADC - Analog to Digital Converter
- ADLs - Activities of Daily Living
- API - Application Programming Interface
- CI - Constrained Induced Therapy
- DOF - Degrees of Freedom
- GUI - Graphical User Interface
- JNDs - Just Noticeable Differences
- MCU – Micro Controller Unit
- NIH - National Institute of Health
- PCM - Pulse Code Modulation
- PID - Proportional-Integral-Derivative Control
- PMC - Particle Mechanical Constraint
- POT - Potentiometer
- PPAM - Pneumatic Pleated Artificial Muscle
- PWM - Pulse Width Modulation
- ROM - Range of Motion
- TENS - Transcutaneous Electrical Nerve Stimulation
- USB - Universal Serial Bus

# Chapter 1. Introduction

## 1.1 Motivation

Stroke is the third leading cause of death in the United States (Slaughter 2002). Approximately 700,000 people have suffered from stroke in the past year and only two thirds of these people have survived to suffer from disabilities (*Post-Stroke Rehabilitation* 2000, p.1). The most common disability found among these stroke sufferers is paralysis (*Post-Stroke Rehabilitation* 2000, p.3). In order to recover from paralysis, rehabilitation nurses, physical therapists, and occupational therapists must carry out intensive rehabilitation therapy. Unfortunately, this intensive rehabilitation requires time and money, which decreases individuals' access to therapy due to the economic pressures on our health care system (Reinkensmeyer 2002, p.1). As a result, there is a demand for a cost effective alternative solution to stroke rehabilitation. Over the past decade several researchers have attempted to improve the cost effectiveness and availability of stroke rehabilitation by using robotics. Researchers chose to use robotics because many of the traditional physical and occupational therapy methods could be automated due to their repetitiveness (Reinkensmeyer 1993, p.185). However, today's rehabilitation robots, even though effective, are still costly, large, and require a substantial workspace (Reinkensmeyer 2001c, p.1). As a result, the motivation of this thesis is to provide an inexpensive, small, and lightweight upper extremity rehabilitative robotic device for stroke patients. This device should allow the patient to take the device home and spend less time and money in therapy. Other motivation for this thesis is to take some of the monotony out of therapist's jobs so that they can take on more patients and monitor the patient's recovery more carefully. Lastly, future use of this device will

include the motions of the hand combined with a virtual reality interface for complete rehabilitation of the upper extremity.

## **1.2 Thesis Goals**

The objectives of this thesis are to describe the:

- Current rehabilitative robotics and the need for an alternative.
- Design and construction of the pneumatically controlled elbow brace.
- Design and construction of the pneumatic control interface in conjunction with the MCU.
- Development and implementation of control software for MCU control of the pneumatic brace.
- Demonstration of the functionality of the pneumatic brace showing the range of motion accomplished by the device.

## **1.3 Outline of Thesis**

In Chapter 2, the literature pertaining to this thesis is reviewed. In this literature review, the main focus will be on the rehabilitation of the arm and hand due to the immense importance of the upper extremity in everyday functions. This literary review will discuss the current medical professionals' roles and treatments for the upper extremity, the current rehabilitation robots for stroke patients, actuators for rehabilitation robots, and the possible human to machine interfaces for rehabilitation robots.

In Chapter 3, the outline of the system design is discussed by describing the overall future goal of this project and the hardware involved in such a system.

In Chapter 4, the test platform experiments with the custom made air muscles are described to show the characteristics of the muscle to help control the muscles that were added to the device.

In Chapter 5, the pneumatic elbow actuator design is described giving details on the construction, testing, and control algorithm used for flexion and extension of the elbow.

In Chapter 6, conclusions are drawn and future suggestions are made for the development of a better device.

Finally, in the appendices the construction details of the test frame and the software for the experiments and control algorithm are given.



## **Chapter 2. Literature Review**

### **2.1 Medical Professionals' Roles in Stroke Rehabilitation**

Rehabilitation efforts are initiated in the hospital about 24 to 48 hours after the stroke has occurred and the patient's medical condition has stabilized (*Post-Stroke Rehabilitation* 2000, p.3, Reddy, p.1742). Stroke patients recover neurological functionality the most rapidly within the first three months of the onset of stroke (Reddy, p.1744). As stated earlier, one of the most common types of stroke is paralysis. More specifically, stroke patients usually suffer from a one-sided paralysis called hemiplegia, which is due to brain damage on the opposing side of the brain (*Post-Stroke Rehabilitation* 2000, p.3). The medical professionals that are the most involved with helping patients recover from hemiplegia are physicians, rehabilitation nurses, physical and occupational therapists (*Post-Stroke Rehabilitation* 2000, p.8).

#### **2.1.1 Physicians**

Physicians are the primary people responsible for managing the patient's health after stroke. This responsibility includes recommending specific rehabilitation programs, caring for the patient's health, and providing guidance in preventing another stroke (*Post-Stroke Rehabilitation* 2000, p.8). During hospitalization, Neurologists lead acute-care stroke teams, direct patient care and sometimes continue to remain in charge of long-term rehabilitation (*Post-Stroke Rehabilitation* 2000, p.8). Physiatrists often care for stroke patients after the acute stage of stroke by providing rehabilitation (*Post-Stroke Rehabilitation* 2000, p.8).

### **2.1.2 Rehabilitation Nurses**

Rehabilitation Nurses are involved in the overall care for stroke patients starting from the acute stage. The following is a list of responsibilities for rehabilitation nurses that was taken from the NIH *Post-Stroke Rehabilitation* pamphlet.

- Help patients relearn the basic activities of daily living (ADL)
- Educate survivors on routine health care like following a medication schedule, skin care, and how to transfer from bed to wheelchair
- Help survivors take measures to reduce the risk of a second stroke
- Provide training for caregivers
- Manage personal care issues like bathing and controlling incontinence

### **2.1.3 Physical Therapists**

Physical therapists are mainly concerned with treating motor and sensory impairments of stroke sufferers. They first assess the stroke patient's current condition and design a specific rehabilitation program for the patient (*Post-Stroke Rehabilitation* 2000, p.10). Each rehabilitation program involves helping the patient regain the use of impaired limbs, teaching strategies to compensate for motor impairment, and teaching ongoing exercises that help patients maintain their improved state and re-learned skills (*Post-Stroke Rehabilitation* 2000, p.10). The Physical therapist emphasizes 'repetitive' movements that require coordination and balance and activities that are goal-directed like games (*Post-Stroke Rehabilitation* 2000, p.10-1).

### **2.1.4 Occupational Therapists**

Occupational Therapists are similar to physical therapists because they work mainly on helping to improve a stroke patient's motor abilities. They focus more on the patient's

learning and re-learning of motor skills for everyday activities like eating, drinking, housecleaning, and personal hygiene (*Post-Stroke Rehabilitation* 2000, p.11). These therapists also teach patients how to compensate for limited movements and how to change their environment to make it safer, non-obstructive, and more physically functional for them to live in (*Post-Stroke Rehabilitation* 2000, p.12).

## **2.2 Upper Limb Rehabilitation for Hemiplegic patients**

Stroke Rehabilitation involves assessment, therapy, and testing. For upper limb rehab, the therapist must assess the patient's motor control, spasticity, range-of-motion, balance, and the patient's ability to tolerate exercise (Cerello 1986, p.99). Once the patient is assessed then the therapist will design a therapy program to improve the patient's condition. Finally, the patient's recovery is tested using one or more of the standard tests like the Fugl Meyer test or the Functional Independence Measure (FIM).

Upper limb rehabilitation is an extremely important focus for rehabilitation due to the importance of using both arms for everyday activities like eating, drinking, bathing, and using the bathroom. As a result, some of the main goals of rehabilitation of the upper extremity are restoration of motor function in the affected limb, improvement in ADLs, and recovery of previously performed functions (Cerello 1986, p.101).

### **2.2.1 Activities of Daily Living (ADLs)**

Stroke Rehabilitation that utilizes activities of daily living (ADLs) is extremely important for helping the patient relearn how to take care of themselves and perform everyday tasks. These tasks include mobility, self-care, management of environmental devices, and home activities (Pedretti 1985, p.141). Training ADLs requires that the therapist tailor to the patients learning style and ability (Pedretti 1985, p.143). The therapist will break

most activities down into smaller steps and slowly demonstrate and assist with each step (Pedretti 1985, p.143). During therapy these activities are repeated several times “to achieve skill, speed, or retention of learning” (Pedretti 1985, p.143). One example of a technique of ADL training is “backward chaining” where the therapist helps the patient with each step up and requires the patient to independently finish the last step to give them a goal (Pedretti 1985, p.143). Other ADL therapies may help teach a patient how to deal with impairment by giving them assistive devices to work with like modified knives, swivel spoons, writing aids, and long handled bathroom sponges.

### **2.2.2 Range of Motion (ROM)**

Range-of-motion is an important measure and means of rehabilitation for stroke patients. Range-of-motion exercises consist of moving the patient’s limb so that a specific joint rotates through its range of joint angles. There two types of range-of-motion exercises: passive and active. Passive range-of-motion exercises are exercises where the therapist actively helps a patient move a limb repeatedly where as active range-of-motion exercises are those in which the patient receives no help from the therapist (*Post-Stroke Rehabilitation* 2000, p.2). Stroke patients benefit from these repetitive exercises because repetition encourages brain plasticity i.e. the rewiring of the brain to adapt to change (*Post-Stroke Rehabilitation* 2000, p.10).

Since stroke patients do not have full control of their muscles for stability, moving their arm through the full range-of-motion could harm the patient and cause more pain. As a result, precautions must be taken when assisting in range-of-motion exercises. One main precaution is to limit the shoulder abduction and flexion from 0° to 120° instead of taking their shoulder all the way to an unsafe 180° according to C. Giuliani (personal

communication, Sept. 12, 2002). Another range-of-motion precaution is to limit shoulder horizontal adduction from 0° to 130° since larger angles are unnatural and stretch muscle according to C. Giuliani (personal communication, Sept. 12, 2002). Table 2.1 lists the average normal ROMs for the upper extremity with a few safety levels for stroke patients indicated in red.

**Table 2.1 Average normal ROMs for upper extremity**

<b>Joint</b>	<b>ROM</b>	<b>Associated girdle motion</b>	
<b>Shoulder</b>			
Flexion	0° - 170° (120°)	Abduction, lateral tilt, slight elevation, slight upward rotation	
Extension	0° - 60°	Depression, adduction, upward tilt	
Abduction	0° - 170° (120°)	Upward rotation, elevation	
Adduction	0°	Depression, adduction, downward rotation	
Horizontal abduction	0° - 40°	Adduction, reduction of lateral tilt	
Horizontal adduction	0° - 130°	Abduction, lateral tilt	
Internal Rotation		Abduction, lateral tilt	
Arm in abduction	0° - 70°		
Arm in adduction	0° - 60°		
External Rotation		Adduction, reduction of lateral tilt	
Arm in abduction	0° - 90°		
Arm in adduction	0° - 80°		
<b>Elbow</b>		<b>Fingers</b>	<b>ROM</b>
Flexion	0° - 135°, 150°	MP flexion	0° - 90°
Extension	0°	MP hyperextension	0° - 15°, 45°
<b>Forearm</b>		PIP flexion	0° - 110°
Pronation	0° - 80°, 90°	DIP flexion	0° - 80°
Supination	0° - 80°, 90°	Abduction	0° - 25°
<b>Wrist</b>		<b>Thumb</b>	
Flexion	0° - 80°	DIP flexion	0° - 80°, 90°
Extension	0° - 70°	MP flexion	0° - 50°
Radial deviation (abduction)	0° - 20°	Adduction, radial and palmar	0°
Ulnar deviation (adduction)	0° - 30°	Palmar abduction	0° - 50°

Data adapted from Pedretti, *Occupational Therapy*, which came from the American Academy of Orthopaedic Surgeons.  
DIP – Distal interphalangeal, MP – metacarpophalangeal, PIP – proximal interphalangeal

### 2.2.3 Stroke Rehabilitation Tests

Patients undergoing stroke rehabilitation are evaluated by several tests to determine their state of recovery. These tests help therapists measure improvement and overall functionality. The tests that are most commonly used in stroke rehabilitation are the Fugl Meyer, Wolf Motor Function Test, and the Jebson Hand Test according to C. Giuliani (personal communication, Sept. 12, 2002).

### 2.2.4 Stroke Rehabilitation Strategies

Therapists use several strategies to help patients to regain the use of their impaired limbs. Table 2.2 lists the main strategies and provides a description of each.

**Table 2.2 Strategies that help patients regain use of impaired limbs**

<b>Strategy</b>	<b>Description</b>
Cutaneous Sensory Stimulation	Tapping or stroking the weak area to activate, facilitate, or inhibit a motor response ( <i>Post-Stroke Rehabilitation</i> 2000, p.10, Cerello 1986, p.102)
Range-of-motion exercises (ROM)	Repetitive passive and active exercises that utilize the person's range-of-motion and stimulate recovery
Constrained Induced therapy (CI)	Restraint of healthy limb to force patient to use affect limb in performing tasks ( <i>Post-Stroke Rehabilitation</i> 2000, p.10, Reinkensmeyer 2002a, p.2)
Transcutaneous electrical nerve stimulation (TENS)	Uses a small current generating probe to stimulate nerve activity in the impaired limb ( <i>Post-Stroke Rehabilitation</i> 2000, p.10)

## 2.3 Current Rehabilitation Robots for Stroke Patients

Over the past decade several robots have been developed for stroke rehabilitation. The following is a list of current rehabilitation robots for stroke rehabilitation.

- MIT-MANUS
- Wrist Robot
- MIME
- ARM Guide
- GENTLE/S
- Bimanual Rehabilitator for the arm
- Java Therapy – Joystick
- Artificial Muscle Manipulator

### **2.3.1 MIT-MANUS**

The MIT-MANUS (Fig. 2.1) is a planar robotic manipulator consisting of a direct five bar-linkage SCARA mechanism that allows two translational degrees-of-freedom (DOF) and is designed mainly for hemiplegic stroke rehabilitation (Krebs 1998, p.76). In order to stabilize the patient so that they can successfully use this robot, the designers include a chair with three seat belts, an adjustable footrest, a lower arm Teflon orthosis, and a custom-made hand holder for weak hands.

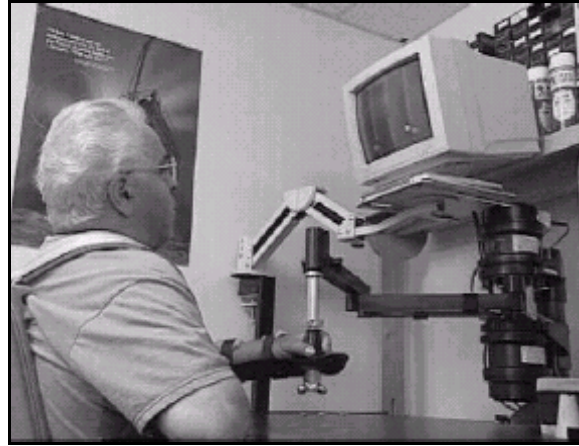


**Figure 2.1 MIT-MANUS Planar robot with two DOF**

This rehabilitator utilizes low intrinsic end-point impedance (i.e. back-drivable) so that the patient is able to move the end-effector freely (Reinkensmeyer 2002a, p.3). Using this impedance control the MIT-MANUS can safely move, guide, or resist the movement of the patients shoulder and elbow (Krebs 1998, p.75). This robot also uses built-in precision potentiometers, dc-tachometers, and torque sensors to measure the patient's hand position, velocity, and forces exerted on the end-effector (Krebs 1998, p.76). These measurements are sent to a PC so that the controller software can control the arm and update the graphical user interface. The graphical user interface consists of several video games designed to give the patient fun goals to achieve. If the user does not respond to the visual or audio cues from the game, then the robot will begin to assist the user and guide their hand through the exercise (Krebs 1998, p76). Examples of the games are drawing a circle, moving a circle through windows, etc.

Mounting a screw-driven spatial module onto the end of the planar module creates three DOF. This spatial module (Fig. 2.2) gives the device a much-needed 3D range so that the patient can practice more exercises and perform better on tests like the Fugl-Meyer.



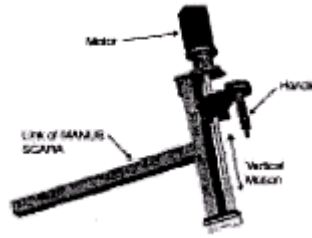


**Figure 2.2 MIT-MANUS Screw-driven Spatial Module to add third dimension**

The MIT-MANUS has been clinically tested for more than 5 years at the Burke Rehabilitation Hospital in White Plains, NY (Reinkensmeyer 2002a, p.3). Results of MIT-MANUS therapy using the planar module compared to traditional therapy have shown much improvement and patients have gained arm strength, reduced motor impairment, and increased functional independence. There are no reports of major clinical testing of the additional spatial module that allows three DOF.

### **2.3.2 Wrist Robot**

The MIT Wrist Robot (Fig. 2.3) focuses on the rehabilitation of the wrist, which is commonly ignored in most rehabilitation robots that usually use a splint on the entire wrist-hand for support. This robot is still in the developmental phase and only exists as a design solution for therapy on the wrist. The Wrist Robot was designed to have low impedance for free range of motion and to accommodate all of the possible motions of the wrist (Krebs 2001b, p.1336). The design specifies brush-less DC motors for the actuator in combination with several types of gears and an incremental high-resolution encoder for feedback (Krebs 2001b, pp. 1337-8).

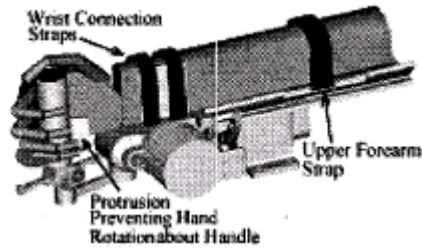


**Figure 2.3 MIT Wrist Robot**

### **2.3.3 MIME**

The MIME (Fig. 2.4) was created by VA Palo Alto in collaboration with Stanford University as a solution to upper limb rehabilitation therapy (Burgar 2001). This rehabilitator was designed using a PUMA-560 robot for the hemiplegic arm and a simple 3-D arm support for the unaffected arm. These two devices were placed on opposite sides of a table so that the patient could hold onto both robot and arm support via forearm-wrist splints (Burgar 2001). The PUMA-560 robot and the arm support allow the patient to work in a 3-D workspace and the PUMA is fully capable of supporting the limb during 3-D movements (Burgar 2001). The PUMA is connected with a 6-axis force transducer to monitor the force from the patient. A 6-axis position digitizer is placed on either device depending on the rehabilitation mode.

The MIME utilizes three unilateral modes and one bimanual mode. When the MIME is in bimanual mode, the 6-axis position digitizer is attached to the orthosis on the arm support and allows the unimpaired limb to act as the controller of the mirror image PUMA. The unilateral modes, only using the PUMA, are passive, active-assisted, active-resistive, and self-guided therapy modes.



**Figure 2.4 MIME uses a PUMA 560 for the patient's impaired limb.**

Rehabilitation with the MIME starts with 5 minutes of stretching without robot assistance and is followed by tracing circles, polygons, and several 3-D targeted reaching movements with robot aid (Burgar 2001). The movements progress from passive, active-assisted, self-guided, to the hardest mode, active-resistive. In clinical testing this rehabilitation regime was compared to rehabilitation therapy that included stretching, weight bearing, cutaneous and proprioceptive stimulation, and games like cone stacking, and ball tossing (Burgar 2001).

### **2.3.4 ARM Guide**

The ARM Guide (Fig. 2.5) is a linear guide that has three DOF (Reinkensmeyer 2001b, p.1344). These three degrees of freedom are a linear track in the reaching direction (R), an elevation axis (P), and the yaw (Y) about the shoulder (Reinkensmeyer 2001b, p.1344). The position of each axis measured by optical encoders and sent back to the computer (Reinkensmeyer 2001b, p.1344). The DC servo-motor (M) controls the position of the arm in the reaching direction via a chain driven counter-balanced linear track (Reinkensmeyer 2001b, p.1344-5). The elevation axis (P) and the yaw axis (Y) are each controlled by a magnetic particle brake that is coupled to elastic components. The lower arm

is strapped into a trough and hand piece orthosis (S) that is coupled to the linear track and a six-axis load cell (F) that measures the forces and the torques produced by the patient. This device can also assist and resist in arm movement similar to the MIT-MANUS and the MIME (Reinkensmeyer 2002a, p.5).



**Figure 2.5 ARM Guide**

The ARM Guide was designed specifically to assist the arm in creating smooth hand trajectories that are similar to normal point-to-point motions (Reinkensmeyer 2001b, p.1346). In a clinical test the ARM Guide was slightly more effective in improving the smoothness of arm movements. Also, the ARM Guide was found to help the patient generalize movements so that several activities of daily living (ADLs) could be performed. Results also suggested that the unassisted, rather than robot assisted, repetitive attempt to move stimulates recovery (Reinkensmeyer 2001b, p.1344). However, these results are dependant on the severity of the stroke.

### **2.3.5 GENTLE/S**

The GENTLE/S (Fig. 2.6) is a robotic system sponsored by the European Commission that is comprised of a three translational degrees-of-freedom Haptic Master robot arm by Fokker Control Systems, a computer for establishing an interactive virtual

environment, an overhead frame for supporting the patient’s arm and mounting of the Haptic Master, and a chair (Hawkins 2002, p.86, Mak 2002, p.60). A passive 3-DOF gimbal connects the patient’s arm to the robot and is “attached to the forearm by a moulded splint” (Mak 2002, p.60). Constant tension cords that are attached to the overhead frame support the forearm and upper arm via an elbow orthosis. As a result, this system allows non-resistive three-dimensional arm movements (Mak 2002, p.60). Measurements made by this robotic system are given in Table 2.3.



**Figure 2.6 GENTLE/S**

**Table 2.3 GENTLE/S Measurements (Mak 2002, p.60)**

<b>Measurement</b>	<b>Measuring Device</b>	<b>Device</b>
roll, pitch, yaw	3-potentiometers	gimbal
elbow angle	potentiometer	elbow orthosis
force feedback	three-axis force transducer	Haptic Master end effector

The GENTLE/S robotic system was designed for rehabilitation of stroke patients using haptic interface technologies (Hawkins 2002, p.85). This use of haptic technologies

allows the patient to work in a virtual environment and perform three modes of therapy exercises found in Table 2.4.

**Table 2.4 GENTLE/S 3 Modes of Control (Mak 2002, p.60)**

<b>Mode Number</b>	<b>Type of Movement</b>	<b>Description</b>
1	Passive	Robot moves patients inactive arm passively through a predetermined trajectory
2	Assisted	Robot assists the patients arm in completing a smooth trajectory
3	Resisted	Robot provides resistance or varies speed of movement to help strengthen the patient's arm.

The therapist can select exercises from a menu or they can create new exercises to customize a therapy program for individual patients. The pre-defined exercises are modeled after several activities of daily living that patients wish to improve on the most, such as reaching, lifting, pushing (Mak 2002, p60).

### **2.3.6 Bimanual Lifting Rehabilitator for the arm**

The Bimanual Lifting Rehabilitator (Fig. 2.7) is a two degree-of-freedom robotic manipulator that assists the affected arm of a stroke patient. Two handles are connected to link 2 via force transducers to measure the vertical forces applied by both hands (Reinkensmeyer 1995, p.167). Link 2 is connected to link 1 with a bearing that provides an object tilt of  $\theta_2$  that is measured with a potentiometer.

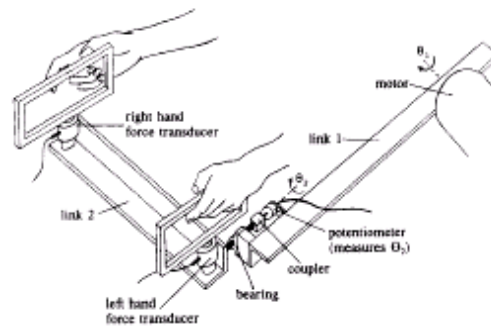


**Figure 2.7 Bimanual Rehabilitator for the affected arm.**

This bearing allows the DC motor that is mounted on link 1 to aid the weak side. The motor provides the vertical assisted lift by rotating link 1 by  $\theta_1$  (the vertical position measured by a potentiometer). The rehabilitator only assists the patient in lifting an object when there is a difference between the two force transducers, i.e. the affected arm needs assistance to keep up with the unaffected arm. The controller for this rehabilitator is controlled with a Proportional-Derivative controller with a  $1.5^\circ$  deadband to reduce the oscillations when the tilt  $\theta_2$  is less than 1.5 degrees (Reinkensmeyer 1995, p.168).

The rehabilitator was tested and worked properly for a completely disabled left hand and a fully able left hand. However, the motor force lagged behind when a partially disabled left hand used the manipulator. This insufficient compensation was due mostly to the control laws and the use of the  $\theta_2$  as feedback (Reinkensmeyer 1995, p.171).

Unfortunately, this rehabilitator is limited to repetitive lifting movements that may help ADL's requiring two hands. Further research on this rehabilitator seems to have seized soon after its conception.

### **2.3.7 Java Therapy – Joystick**

The Java Therapy – Joystick (Fig. 2.8) is a cost effective solution to robotic rehabilitation that uses a commercial force feedback joystick in combination with online games designed for hemiplegic stroke rehabilitation patients. A special hand-wrist orthosis is mounted on the joystick to give the patient support for playing the games. During these games, the force feed back on the joystick is controlled through a Java applet and Immersion Corporation's FEELtheWEB software, which is an ActiveX control for browsers and can receive function calls through HTML (Reinkensmeyer 2001c, p.3).



**Figure 2.8 Java Therapy using Force Feedback Joystick**

Java Therapy tests speed, coordination, strength, and finger speed. The speed test requires the patient to move the cursor into a target as fast as they can. The coordination test requires the user to trace a figure eight while software measures the tracing error. The strength test requires the user to hold the joystick still while the software applies forces to the joystick and measures the distance moved. The Java Therapy games are: Breakout therapy (Pong), Blackjack card game, Othello, and TailGunner (Reinkensmeyer 2001c, p.4). The



patient's progress is monitored throughout these games and is displayed in several progress reports.

Testing of the Java Therapy consisted of several stroke patients using the Joystick from home three times a week for four weeks (Reinkensmeyer 2001c, p.3). One patient improved his movement speed by 40% and performed over 1600-targeted movements in the speed test (Reinkensmeyer 2001c, p.5). Since this rehabilitator is web-based and uses a low-cost commercially available force feedback joystick, large populations now have access to exercise programs for stroke rehabilitation and testing.

### **2.3.8 Artificial Muscle Manipulator**

The Artificial Muscle Manipulator (Fig. 2.9) is a 2 degree-of-freedom manipulator that uses pneumatic rubber artificial muscle actuators. The pneumatic artificial muscles were chosen because robots must be safe and flexible contrary to common industrial robots (Noritsugu 1997, p.259). This manipulator was designed for rehabilitation and can demonstrate four modes of physical therapy using an impedance control system consisting of a PID position control (Noritsugu 1997, p.259).

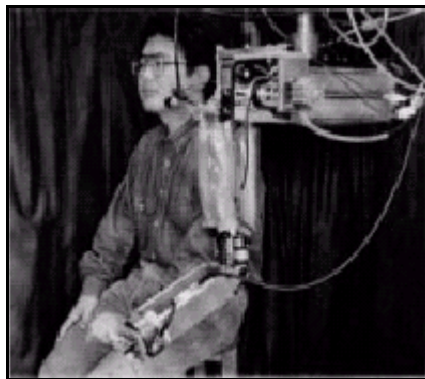


**Figure 2.9 Artificial Muscle Manipulator**

The manipulator (Fig. 2.10) has two links ( $L_1 = 410\text{mm}$  and  $L_2 = 385\text{ mm}$ ) that are similar in length to the human arm. The patient is supposed to sit next to the manipulator with their upper arm next to  $L_1$ , their lower arm next to  $L_2$ , and their hand grasping the manipulator's end-effector.

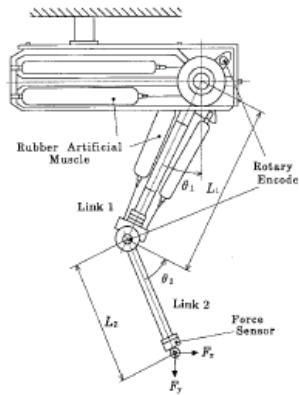


**Figure 2.10 Artificial Muscle Manipulator Frame Assignment.**

The two joints of the rehabilitator are each controlled by an actuator in an antagonist artificial muscle pair. For example,  $L_1$  has two muscles on opposite sides of the link. One of the muscles contracts while the opposite muscle extends in order to move  $L_2$  about an angle of  $\theta_2$  and keep the link steady. The designers chose to use rotary encoders with a resolution of  $0.009^\circ$  and  $0.011^\circ$  to measure the joint angles  $\theta_1$  and  $\theta_2$  (Noritsugu 1997, p.260). A six-axes-type force sensor is mounted on the end-effector to measure the subjected horizontal and vertical forces  $F_x$  and  $F_y$  (Noritsugu 1997, p.260). Each actuator is controlled by a 7-bit pulse code modulation (PCM) digital control value, which is supposed to be an equivalent proportional valve using only ON-OFF valves (Noritsugu 1997, p.260). The robot's four modes of physical therapy are described in Table 2.5. Unfortunately, there was no report of

clinical tests to validate the rehabilitator for helping patients recover. Besides the lack of clinical testing, this manipulator is limited in its use because it only works in two dimensions.

**Table 2.5 Four modes of physical therapy for Artificial Muscle Manipulator (Noritsugu 1997, p. 262)**

Mode	Description
Isometric Mode	Robot arm receives force from the patient in stationary state.
Isokinetic Mode P (Patient Passive)	Robot arm moves at a constant speed regardless of force from the patient.
Isokinetic Mode A (Patient Active)	The patient moves arm at constant speed while the robot while the robot assists.
Isotonic Mode	The arm gives the patient a constant force to increase muscular strength.

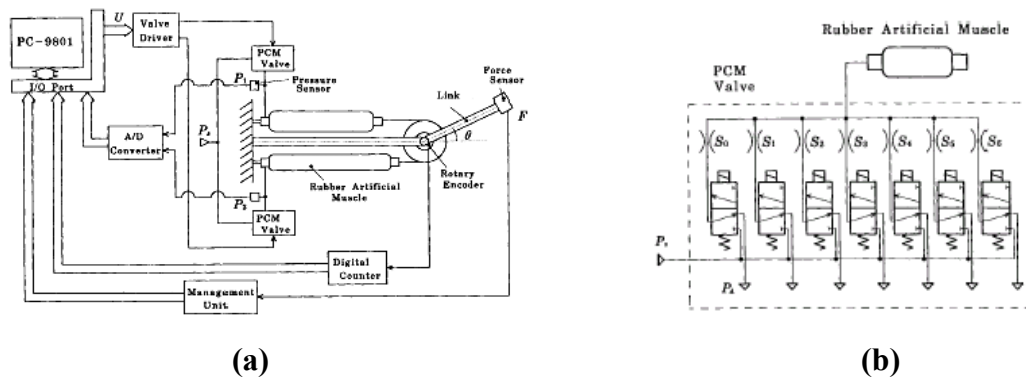


**Figure 2.11 Control scheme for an Artificial Muscle Manipulator (a) Control system for each joint (b) 7-b PCM digital control valve**

## 2.4 Virtual Reality Rehabilitation

Recently robot assisted training has been found to enhance stroke rehabilitation using virtual reality (Jack 2001, p.308). According to David Jack, virtual reality “provides the capability to create an environment in which the intensity of feedback and training can be

systematically manipulated and enhanced in order to create the most appropriate, individualized learning paradigm” (Jack 2001, p.309). Since patient motivation is the key to recovery from stroke, virtual reality rehabilitation exercises can place the patient in a stimulated world and evoke patient interaction (Jack 2001, p.309).

Several virtual reality haptic interfaces have been developed for use with the arm and hand. Currently, researchers are experimenting with the PHANToM, CyberGlove™, Rutgers Master II ND, and an Orthotic Upper Limb using Particle Mechanical Constraint (PMC). For example, researchers like Jack are experimenting with using both the Rutgers Master II ND and CyberGlove™ for stroke rehabilitation exercises in a virtual environment.

Since the cost of virtual reality equipment has decreased, there is the increasing possibility of using this technology for stroke rehabilitation in more convenient locations like the patients home (Jack 2001, p.309). As a result of the lower prices and successful research in virtual reality, more research is being done with haptic devices for rehabilitation. The following describes the four haptic devices (PHANToM, CyberGlove™, Rutgers Master II ND, and an Orthotic Upper Limb using Particle Mechanical Constraint (PMC)) that are being used for rehabilitation research.

#### **2.4.1 PHANToM**

The PHANToM arm (Fig. 2.12) is currently the most common haptic interface for virtual reality (Bouzit 2002). Created by in the MIT Artificial Intelligence Laboratory, the PHANToM measures fingertip position and is capable of exerting a controlled force on the finger for feeling virtual objects (Massie 1994). The finger is placed in a thimble that is connected to a passive 3-DOF gimbal, which is driven by three DC brushed motors via

tension cables. The overall device has 6-DOF and allows the user to work in a three dimensional virtual environment.

The PHANToM is currently being studied for use with vocational rehabilitation for people with disabilities. This device requires small forces that can slightly increase the patient's manipulation ability while substantially increasing the number of jobs a patient can perform (Pernalette 2002, pg.1269). Some of the examples for functional development include moving virtual blocks from one side to another and target force constrained assistance (Pernalette 2002, pg.1270-1).

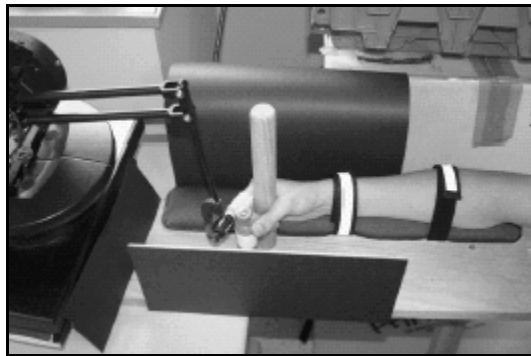


**Figure 2.12 Stroke Rehabilitation with PHANToM**

Since the PHANToM responds well to just noticeable differences (JNDs) in movements, it is suitable for assisting people who are weak and disabled (Allin 2002). Students at *Carnegie Mellon University* are experimenting with using the PHANToM (Fig. 2.12) for stroke rehabilitation. They are attempting to use the JNDs to provide the user motivational feedback for minute differences in motion to gradually help the user overcome their limitations. Gradually the patient should gain control and increase movements while the

motivational feedback decreases. Their goal is to create a ‘distorted’ virtual environment that “extends limitations by perceptually undetectable amounts” (Allin 2002).

The PHANToM also has disadvantages due to its size and actuator selection. Since this device is small it has a small workspace that limits the freedom of motion (Bouzit 2002). The PHANToM is also incapable of sustaining high forces because the DC brushed motors will overheat (Bouzit 2002). Besides overheating at high forces, this device lacks dexterity because only one finger is used for force feedback (Bouzit 2002). Using only one finger can also result in the ‘Phantom’ effect where objects can be felt with the finger but the hand can physically pass through the object (Massie 1994).

## **2.4.2 Immersion Products**

Immersion Co. has designed and built several virtual reality based products that can be used for rehabilitation: CyberGlove™, CyberGrasp™, and CyberForce™. These three main products are built on top of each other to sense the position of individual fingers and provide force-feedback to the hand and arm.

### **2.4.2.1 CyberGlove™**

The CyberGlove™ (Fig 2.13) is an instrumented glove that provides up to 22 high-accuracy joint-angle measurements using a proprietary resistive bend sensing technology to convert hand and finger motions into real-time digital joint-angle data (Immersion 2002). This digital joint-angle data is sent to a computer via RS-232 or Ethernet to Immersion’s VirtualHand® Studio which displays the movements and position of the hand graphically. The CyberGlove is constructed out of stretch fabric and has a mesh palm for ventilation.



**Figure 2.13 CyberGlove™**

#### **2.4.2.2 CyberGrasp™**

The CyberGrasp™ (Fig. 2.14) originally developed under STTR contract by the United States Navy is a lightweight force-reflecting exoskeleton device that fits on top of the CyberGlove™ to provide force-feedback. This extension of the CyberGlove™ lets the operator grasp and feel objects in a virtual world. These grasp forces are produced by a network of tendons connected to each fingertip by way of the exoskeleton (Immersion 2002). There are five independently controlled actuators connected to each finger to prevent the user from “crushing virtual objects” and provide force feedback (Immersion 2002). This extension permits full range-of-motion of the hand and fingers, does not obstruct the wearers movements, and is fully adjustable to fit several hand sizes.



**Figure 2.14 CyberGrasp™**

### 2.4.2.3 CyberForce™

The CyberForce™ (Fig. 2.15) is a force feedback external armature that provides realistic grounded forces to the hand and arm and also provides 6-DOF positional tracking to measure the translation and rotation of the hand in three dimensions (Immersion 2002). This device is designed to work with the CyberGrasp™ exoskeleton to add external forces to the hand and arm so that the virtual environment is more natural to the user. According to Immersion Co., “you can literally ‘hang your hand’ on a virtual steering wheel, sense weight and inertia while picking up a "heavy" virtual object, or feel the impenetrable resistance of a simulated wall” (Immersion 2002).



**Figure 2.15 CyberForce™**

Since the addition, CyberForce™, people are now capable of picking up virtual objects and manipulating them. As a result, Immersion’s products are applicable in medicine, mainly surgery and possible rehabilitation. Unfortunately, since rehabilitation requires all three components, the combination of the CyberGlove™, CyberGrip™, and CyberForce™ is expensive (Bouzit 2002).



### 2.4.3 Rutgers Master II-ND Force Feedback Glove

The Rutgers Master II-ND (RMII-ND) is an improvement of the previous Rutgers Master II force feedback glove. Since all the mechanics of the RMII-ND are placed in the palm, the RMII-ND is limited to a virtual environment i.e. rehabilitation could not consist of picking up real objects.



**Figure 2.16 Rutgers Master II-ND**

The RMII-ND connects custom pneumatic actuators between the palm and thumb, index, middle, and ring fingers as shown in figure 2.16 (Bouzit 2002). These actuators can apply up to 16 N of force when pressurized at 100 psi and are driven by pneumatic pulse-width modulated servo-valves, which result in better force control (Bouzit 2002, Jack 2001, pg 308).

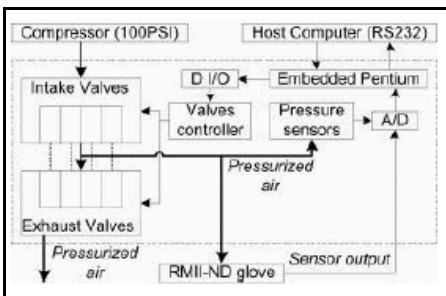


**Figure 2.17 RMII-ND Haptic Control Interface**

Sensors that are placed in the palm measure the finger-actuator positions for feedback control. The RMII-ND uses two Hall-effect sensors to measure flexion, abduction, and adduction angles and one infrared sensor to measure piston translation inside the air cylinder for each actuator (Bouzit 2002). Since these sensors are non-contact sensors, they do not produce any oppositional frictional forces that may prevent the user from moving freely (Bouzit 2002).

The haptic control interface (Fig. 2.17) utilizes an embedded 233MHz Pentium PC with a PC104 bus. This embedded computer uses Pulse-Width Modulation (PWM) running at a frequency of 500 Hz to control the valves that are connected to the pneumatic actuators on the fingers (Bouzit 2002). The embedded computer communicates with a host computer using an RS-232 serial port that runs at baud-rates from 38,400 to 115,200 bps (Bouzit 2002). The host computer sends action commands and receives sensor data to and from the embedded computer. The sensor readings are used to relate the physical environment to the virtual environment displayed on the computer screen.

#### **2.4.4 Orthotic Upper Limb using Particle Mechanical Constraint (PMC)**

Several researchers are developing an orthotic upper limb using PMC. A PMC is a soft vinyl tube that envelops Styrofoam beads and is driven by vacuum pressure (Mitsuda

2002). By varying the air pressure inside the PMC, its tube like structure can compress, elongate, bend, and twist to provide 6-DOF. Since PMC's do not create power by themselves they are 'intrinsically' safe. A PMC is soft, lightweight, and safe making it suitable for human interaction for use with a virtual environment. As a result, researchers are using PMC technology to construct a wearable upper limb orthosis to constrain upper limb motion and exert a stiffness or viscosity on the joints.



**Figure 2.18 PMC Upper-arm movements**

The current prototype allows the operator to move and rotate their hand freely due to the passive characteristics of PMC (Mitsuda 2002). This orthosis is being developed for haptic display, sport trainings, rehabilitation, and welfare issues (Mitsuda 2002). Figure 2.19 shows the structure of the upper-arm orthosis, Figure 2.18 shows the possible constraining movements of the upper-arm orthosis.

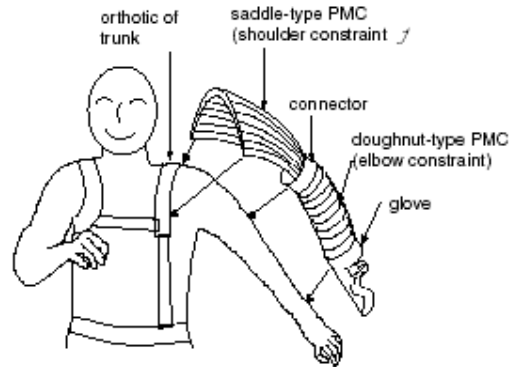


**Figure 2.19 Structure of the PMC upper-arm orthotic**

## 2.5 Actuators for Rehabilitation Robots

Rehabilitation robots are driven by actuators that control how they rotate or translate in a given space. Most common rehabilitation robots use revolute joints that provide one degree-of-freedom between two links. There are several types of actuators that control the rotation between the links of a robot which include: pneumatic, hydraulic, piezoelectric, and DC motors. The requirements to drive a ‘human motion mimicking machine’ like a rehabilitator are the following:

- Low weight
- High Power
- Smooth and elegant movement
- Compliance
- Safe

The rehabilitator must be lightweight and have high power to be agile and strong (Daerden 2001a, 738). Also, a rehabilitator must have smooth and elegant movements in order to copy to human motions (Daerden 2001a, 738). Besides having smooth and elegant

movements, a rehabilitator must have compliance, which is the capability to store and release energy or give in to the patient, so that the robot responds to the patient more naturally. Finally, safety is a major requirement when patients work with robots. For example, an unsafe rehabilitator might use a DC motor that is connected directly to the joint of a manipulator via a transmission that adds additional weight, which contributes to unwanted inertia and possibly backlash (Daerden 2001a, p.738). This section will examine two types of actuators, DC Motors and Air Muscles, for use in rehabilitation robotics.

### **2.5.1 DC Motors**

The DC motor is commonly used for rehabilitation robotics due to its rotational nature and availability. Since DC motors generate maximum power at high speeds they must be geared down to convert their high speeds into a lower speed/higher torque so that slow movements with larger forces can be achieved in therapy (Reinkensmeyer 2002b, p.12). Back-drivability, the ability to manually drive a robot without any opposing force, is hard to achieve because adding gears to a motor increases the frictional resistance of the gear train (Reinkensmeyer 2002b, p.12). The only alternative to using a high-g geared DC motor is to use a larger motor or develop another type of transmission system.

DC motors have a difficult time comparing well to the required characteristics for a robotic rehabilitator. Instead of being lightweight, DC motors are heavy due to either using a transmission system or having large sizes to achieve higher torques. As a result, DC motors make the rehabilitator strong, but not agile. Also, smooth and elegant movement is difficult to achieve with DC motors because they are rigid drives (Daerden 2001a, p.738). Besides lacking smooth and elegant movements, DC motors are not compliant due to their physical

characteristics and they are unsafe unless engineered to perfection in order to prevent backlash and extra inertia (Daerden 2001a, p.738).

DC motors not only have trouble with meeting the ideal requirements for a robotic rehabilitator but they are also difficult to control. Force control is a major complication for DC motors because they require “complicated and state-of-the-art feedback control and sensory equipment to achieve this” (Daerden 2001a, p.738).

### **2.5.2 Air Muscles**

Air muscles (Fig. 2.20) are pneumatic actuators that use a rubber tube inside of a hollow braided sleeve that is made out of either Nylon or Kevlar. When the rubber tube fills with air, it expands and the outer sleeve begins to contract like a human muscle. Air muscles have power-to-weight ratios as high as 400:1, which overshadows pneumatic cylinders and DC motors that can only provide ratios of 16:1 (Shadow Robot Co. 2002). The advantages of air muscles are listed in Table 2.6.



**Figure 2.20 Air Muscle (a) Rubber tube with braided sleeve (b) Standard Air Muscle**

**Table 2.6 Advantages of Air Muscles\***

<b>Advantage</b>	<b>Description</b>
Lightweight	Weigh as little as 10g - particularly useful for weight-critical applications.
Low cost	Cheaper to buy and install than other actuators and pneumatic cylinders.
Smooth Movement	Air muscles have no 'stiction' and have an immediate response. This results in smooth and natural movement.
Flexible	Can be operated when twisted axially, bent round a corner, and need no precise aligning.
Powerful	Produce an incredible force especially when fully stretched
High Force/Low Speeds	Can operate with high forces at low speeds (Daerden 2001a, p.738).
Damped	Air Muscles are self-dampening when contracting (speed of motion tends to zero), and their flexible material makes them inherently cushioned when extending.
Compliant	Can be used to store and release energy during separate phases of running due to gas compressibility and the dropping force-displacement characteristics (Daerden 2001a, p.738, Daerden 2001b, p.1958).
Failure mechanism	Continues to work even if there is a tear in the muscle
Easy to install	Loops in the ends of the air muscle can attach to just about anything. Can connect directly to the joint without any gears (Daerden 2001b, p1958).

\*Table adapted from Shadow Robot Company website

Since no actuator is perfect, there are also problems that arise with any type of actuator. The standard air muscle exhibits hysteresis when expanding and contracting due to the friction between the rubber tube and the braiding (Daerden 2001a, p.738). This friction also causes wear on the braiding and the rubber tube that can lead to poor performance or possibly even bursting. As a result, the air muscle must be controlled with complex control algorithms (Daerden 2001a, p.738). Besides friction and hysteresis, air muscles have a non-linear relationship between force and displacement. Fortunately, air muscles have a linear relationship between pressure and force i.e. air muscles only require pressure sensors for control of movement distance (Shadow Robot Co. 2002).

### **2.5.3 Pleated Air Muscles**

Pleated Air Muscles (PPAMs) (Fig. 2.21) were recently developed by the Dept. of Mechanical Engineering at Vrije Universiteit Brussel (Daerden 2001b, p.1958). PPAMs are an enhancement of the standard air muscle and are distinguished by their pleated design for

the hollow outer netting. The pleated membrane or sleeve is made out of Kevlar®49 quasi-unidirectional fabric lined with a polypropylene film which gives it a high tensile stiffness and makes it gas-tight (Daerden 2001a, p.740). Since this pleated membrane has its fold faces laid out in a radial pattern, there is no friction byproduct during the folding-unfolding stage (Daerden 2001a, p.739). This unfolding of the membrane makes the PPAM look like a pumpkin when it is fully contracted and allows for maximum displacements of up to 50% of the initial length (Fig. 2.22) (Daerden 2001a, p. 739, Daerden 2001b, p.1958). The benefits of removing the friction component compared to standard air muscles are listed in table 2.7 below.

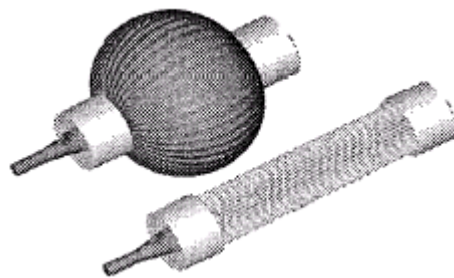


**Figure 2.21 Pleated Air Muscle**

**Table 2.7 Pleated Air Muscle comparison to Standard Air Muscles**

<b>Pleated Air Muscles</b>	<b>Standard Air Muscles</b>
No Hysteresis	Hysteresis
Maximum displacement 50%	Maximum displacement 20%-30%
Wide range of gas pressures 10 kPa – 300 kPa/1.45 PSI – 43.5 PSI	Threshold at 90 kPa/13 PSI if hard rubber Only low pressures if soft rubber
Requires simple PI control	Requires more complex control algorithms
No rubber tube necessary	Rubber tube wears out

Comparison derived from Daerden’s “Pleated Pneumatic Artificial Muscles: Compliant Robotic Actuators 2001”



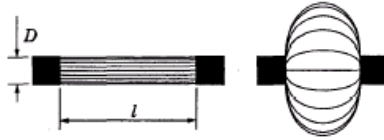


**Figure 2.22 Pleated Air Muscle ‘pumpkin’ shape**

## **2.6 Human to Machine Interfaces for Rehabilitation Robots**

Today the most common human to machine interface, as seen above, is a virtual representation of the patient’s upper arm. This virtual representation can be as simple as a ball that represents the position of the patients hand or as complex as displaying the patients physical hand in a virtual reality environment. With decreasing costs, advances in virtual reality, and the strong influence on patients, virtual reality is becoming the preferred choice for human to machine interfaces.

Since the virtual environment requires values from the physical environment in order to interact with the user, the rehabilitation robot must interface with a computer. The values from the physical environment are measurements recorded by the sensors placed on the rehabilitation robot. The values from the sensors can be sent to the computer either by an A/D Converter (ADC) PC card or interfacing an embedded microprocessor via either serial communication (RS-232, USB) or Ethernet. Once the virtual environment receives the values, it can respond to changes in the physical environment.

The virtual environment can interact with the patient by creating user-defined or predefined games that motivate the patient. There are games like moving a circle or sphere around a target, picking up balls and placing them with other balls, and pushing a box. However, VR games are not limited to simple spheres and cubes. VR games can be complex, displaying a whole new world. For example, Nearlife, Inc has created a Virtual FishTank™

using Java 3D to allow people to create and release their own digital fish into a virtual aquarium and interact with their own fish via motion sensitive cameras (Gehring 2002, p. 5).

There are several virtual reality languages and utilities for creating a virtual environment. The following is a list of some of the virtual reality development environments.

- Java 3D SDK
- Ghost SDK
- Virtual Hand SDK
- AutoCAD
- OpenInventor
- Performer
- OpenGL

Fortunately, Sun Microsystems has created a platform independent, free, and easy to use standard development kit for virtual reality called Java 3D. Java 3D is a high level programming API that allows developers to focus on what to draw instead of how to draw (Gehring 2002, p.3). One major advantage over other 3D APIs is that Java 3D can be utilized on the world-wide-web via Java Applets. Java 3D has several advantages over other 3D API. For example, everyone will immediately have the most updated software because the software resides on the server's side. Also, anyone with a Java enabled browser, regardless of platform, and the Java 3D runtime environment can view Java 3D. Plus, unlike other APIs, Java 3D is free to the public. Java 3D can utilize single-processor and multi-processor units and utilize 3D hardware accelerators.

## 2.7 Literature Review Summary

Since stroke is the leading cause of impairment, there is a demand for post-stroke rehabilitation. Medical professionals such as physicians, occupational and physical therapists, and rehabilitation nurses help patients recover from impairment so that they can take care of themselves and function in the real world. Recently, researchers have attempted to automate some of the repetitive exercises that are used in rehabilitation by using robots. Clinical results have shown that using robots for stroke rehabilitation actually helps the patient recover. The most effective rehabilitation robots use virtual reality computer games that give the patient fun, stimulating, and goal driven tasks using the robot as a haptic interface. Unfortunately, most of these rehabilitation robots are driven by DC-motors, which are not idealistic for human-machine interaction. Fortunately, pneumatic actuators like air muscles are more suitable for human-machine interaction because they are lightweight, strong, provide smooth and elegant movement, compliant, and safe to use with people.

## **Chapter 3. Outline of System Design**

The system design for the pneumatic elbow brace prototype was derived from the overall goal or design basis for this project in the future. This chapter first discusses the design basis for the elbow brace prototype and then describes the pneumatic and electronic hardware involved in the design.

### **3.1 Design Basis For Elbow Brace Prototype**

Most rehabilitative devices for the upper extremity use an external slave robot as the manipulator. Unfortunately, these devices have many disadvantages: expensive, large, non-compliant, and they have difficulties controlling the joints of the arm and shoulder on an individual basis. As a result, researchers are still trying to find a solution to combat these disadvantages and better serve the unfortunate sufferers of stroke, spinal cord injury, etc. Our solution to designing a better rehabilitative device for the upper extremity is to use a lightweight pneumatic actuator known as the McKibben Artificial Muscle or PAM. Air muscles are lightweight, cheap, compliant, and are comparable to the human muscle. Instead of using an external device to house the air muscles we have chosen to design a garment capable of housing the air muscles and allowing the patient to move freely and comfortably.



**Figure 3.1 Farris Ankle-Foot Orthosis**

The idea for the pneumatic device came from researching the Ankle-foot orthosis (Fig. 1) with artificial pneumatic muscles developed by Dan Farris at the *University of Michigan Dept. of Movement Science and Dept. of Biomedical Engineering*. The Ankle-foot orthosis is made out of lightweight carbon fiber (or polypropylene) and titanium fittings for the air muscles. This design inspired the following drawing (Fig. 3.2) for a similar rehabilitative device for the upper extremity. Basically, just imagine your arm fitting in the device shown in Fig. 3.1 and you get Fig. 3.2.

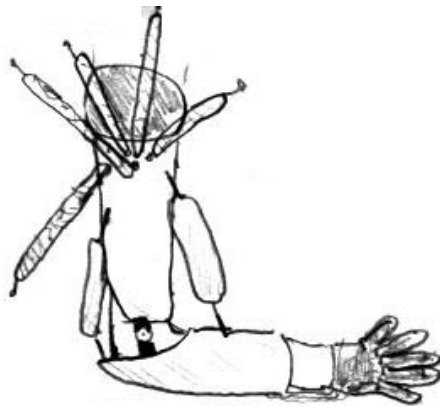


**Figure 3.2 Inspired by Farris Ankle foot orthosis**

While this solution may seem somewhat viable, the carbon fiber that Farris used was expensive and each device must be custom fit to the patient. One possible solution to making the wearable arm cheaper may be to make the device out of textiles that are strong enough for the air muscles to attach to and structured to direct loads over a broader area to keep from hurting the patient. The drawing (Fig. 3.3) attempts to show a rehabilitative device with around 15-17 air muscles strategically placed to achieve individual joint control. Table 3.1 summarizes the air muscles with their function that are in the drawing.

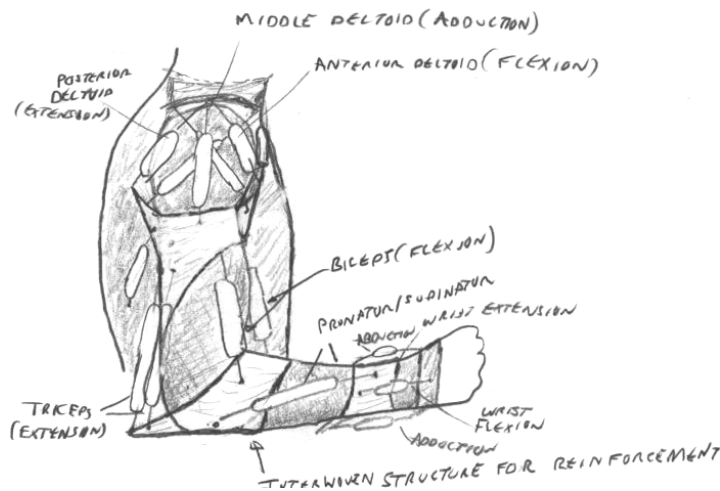


**Figure 3.3 Rehabilitative Garment**

In the drawing, the lighter areas of origin and insertion for the air muscles are an interwoven durable material designed to manage loads without stretching and squeezing the arm. The darker shaded area of the garment is the textile material that covers the body like a jacket or a shirt.

The most complicated part of the design is the shoulder. The main concern of the shoulder portion is where and how to place the origins of the deltoids on the shoulder without having the air muscles squeezing on the patient's deltoids. Currently, our solution is to

connect Bowden cables, which are similar to bicycle brake cables, to the arm running them over the shoulder and connecting them to the air muscles that could then be mounted along the patient's upper back. The use of Bowden cables would keep the air muscles from pressing on the patient's shoulder and allow for larger and longer muscles that could then be mounted on the patient's back.

**Table 3.1 Air Muscles for rehabilitation garment.**

<b>Air Muscle</b>	<b>Function</b>
2 Parallel Biceps	Flexion of elbow
2 Parallel Triceps	Extension of the elbow
Middle Deltoid	Abduction
Anterior Deltoid	Flexion of shoulder
Posterior Deltoid	Extension of shoulder
Undecided	Lateral Rotation of shoulder
Undecided	Medial Rotation of shoulder
Pronator	Pronates the forearm/wrist
Supinator	Supinates the forearm/wrist
Wrist Adduction Muscle	Wrist Adduction
Wrist Abduction Muscle	Wrist Abduction
Wrist Flexion Muscle	Wrist Flexion
Wrist Extension Muscle	Wrist Extension

### **3.2 Pneumatic System Design**

Since air muscles are pneumatic, a pneumatic system was designed to control the air muscles required for the device. The following pneumatic components are required for the pneumatic system:

- Pneumatic Circuit
- Tubing and Connectors
- Pneumatic Air Muscles (PAMS)
- Valves

- Pressure Transducers

### 3.2.1 Pneumatic Circuit

The pneumatic circuit for the rehabilitative device was designed to control the artificial muscles that are attached to the device using 2-way solenoid valves. Since solenoid valves are either on or off, two valves are required to control one artificial muscle. One valve lets air into the muscle causing it to contract while the other valve releases the air out to the environment causing it to extend and reach a resting position. In order to measure the air pressure in each muscle, a pressure transducer was placed in the circuit at each muscle inlet. A tank and an air filter were combined to provide the air supply to each muscle in the circuit. An example pneumatic circuit for two air muscles is illustrated in figure 3.4.

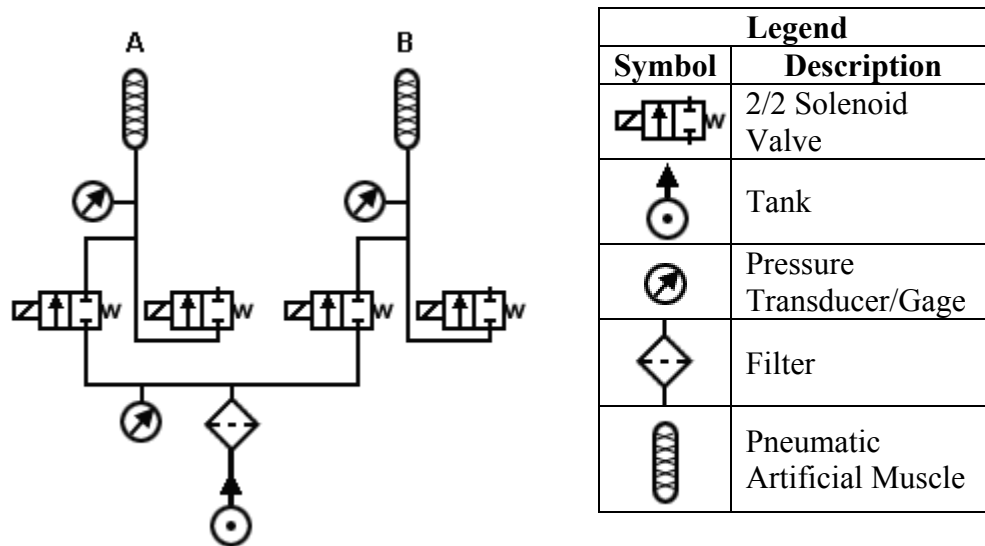


Figure 3.4 A Pneumatic Circuit for Pneumatic Artificial Muscles

### 3.2.2 Tubing and Connectors




The pneumatic circuit needed to be small and flexible so that the air muscles could be mounted on the device without being in the patient's way. Since the valves have 5/32"



diameter inlet and outlet push-fit connectors the 5/32" tubing size for the circuit was chosen for all of the connectors and the tubing.

The tubing that was used to connect the pneumatic components for the device was 5/32" Nycoil tubing. Three push-fit connectors were also required for connecting the components together. One 5/32" Union "Y" was used to connect the inlet and exhaust valves to the air muscle. Also one unequal tee was used to connect the pressure transducer to the tubing that was directed to the air muscle. Since the pressure transducer required 1/4" tubing, the unequal tee's diameters were 1/4" for the unequal tube while the equal tube-to-tube diameter was 5/32" like the rest of the circuit. Finally, the tubing coming from the unequal tee was connected to an equal tube-to-tube connector, which plugged directly into the muscle's hose barb. The tubing and connectors used in the pneumatic circuit are listed in table 3.2.

**Table 3.2 Tubing and Connectors used for pneumatic circuit**

<b>Graphic</b>	<b>Model Number</b>	<b>Item</b>	<b>Company</b>	<b>Unit Price</b>
	65233	5/32" OD Flexible Nylon Tubing Blue	Nycoil	\$0.12 /ft
	3140-04-00	5/32" Union "Y"	Legris	\$1.83
	3104-04-56	5/32" – 1/4" Unequal Tee	Legris	\$2.89
	3106-04-00	5/32" Equal Tube to Tube Connector	Legris	\$1.90

### 3.2.3 Pneumatic Artificial Muscles (PAMs)



The actuator of choice for the device was the pneumatic artificial muscle known as the McKibben Air Muscle. The main reason for choosing this actuator over other actuators namely DC motors is because of their advantages and capabilities for producing a force that is similar to the human muscle. Instead of using a large gearbox and structure to convert a dc-motor's rotational motion into linear motion, air muscles were chosen to compliment the patient's own muscles by strategically attaching them to the device.

There are only a few air muscle manufacturers that exist so purchasing an air muscle is costly and difficult compared to custom making and designing them. For example, the most popular air muscle manufacturer, Shadow Robot Company, is located in the United Kingdom so shipping would be an additional expense. Prices for their air muscles are shown in table 3.3.

**Table 3.3 Shadow Air Muscle Prices**

Size	Stretched Length (mm)	Price
Small	150	\$10
Medium*	210	\$40
Large	290	\$100

\* This is approximately the preferred size for the wearable device's muscles

The preferred muscle size for the wearable device is the medium size costing \$40. Unfortunately, there are over 15 muscles needed just for actuating the arm and shoulder so the cost for the muscles alone would be around \$600. Since one of the goals of this device is affordability for the patient, other alternatives must be considered.

Our alternative for obtaining inexpensive air muscles was to make them. Fortunately, the University of Washington Bio-Robotics Laboratory provides a simple guide to making air

muscles. Their guide helped us to develop our own muscle design that enabled us to produce large numbers of muscles that are cheap, easy to make, and lightweight weighing only 11 g for a 180mm ( $\approx 7$ " ) length muscle. This new design of muscle, figure 3.5, for a 180mm air muscle costs only \$2.70. This cost is calculated from the price of the required materials, table 3.4, used in building a 180mm air muscle. The cost calculation is the following:

$$\frac{7''}{300''} \cdot \$31.00 + \frac{13''}{300''} \cdot \$8.75 + 2 \cdot \$0.61 + 2 \cdot \$0.19 = \$2.70$$

**Table 3.4 Pneumatic Artificial Muscle Materials**

<b>Model Number</b>	<b>Item</b>	<b>Company</b>	<b>Diameter</b>	<b>Length/Quantity</b>	<b>Price</b>
EW-95802-07	Platinum-Cured Silicone Rubber Tubing	Cole-Parmer	ID 5/32" OD 7/32" Wall Thickness 1/32"	25'	\$31.00
-	Protecto PE Braided Sleeving	Cable Organizer	1/2" Diameter	25'	\$8.75
3122-04053	Barbed Connector for Unequal Tube	Legris (Air Power Inc.)	Tube OD 5/32" Barb OD 1/8"	2	\$0.61
OE 10100008	7-9 Two-Sided Hose Clamp	Air Power Inc.	5/16"	2	\$0.19



**Figure 3.5 New Air Muscle Design**

### 3.2.3.1 Pneumatic Artificial Muscle Assembly

For an example of artificial muscle assembly, the actuator will have a resting length of about 14 cm and a stretched length of 18 cm and will be capable of producing forces up to 200N according to University of Washington Bio-Robotics Laboratory air muscle website.

Air muscle assembly requires nippers, scissors, and a lighter. The materials for construction are listed in table 3.3 and shown in figure 3.6. The steps for assembly are listed below.



**Figure 3.6 Materials required for new air muscle design**

1. Cut a 16.0 cm piece of silicone rubber tubing for the inner bladder.
2. Cut a 30.0 cm piece of the braided sleeving for the outer braided shell.
3. Use the lighter to singe the ends of the braided sleeving to keep the ends from unraveling.
4. To make the plug take a barbed connector and cut about a 1/4" off the tube end and melt the shortened end of the barb tube until the hole is closed.
5. Insert the plug and another barbed connector into both ends of the silicone rubber tubing.
6. Insert the silicone rubber tubing inside the braided sleeving.
7. Form a loop at the barbed connector end with the open tube and push the tube through the braiding like in figure 3.7.



**Figure 3.7 Open tube end of air muscle pushing through braiding**

8. Slide a 7-9 hose clamp on the other end of the braiding and slide it over the loop until it is flush with the middle of the barb where the barb stops and the barb tube begins. There should be a little ring or ridge to indicate this area. Clamp both sides of the clamp using a pair of nippers.
9. Slide the other 7-9 hose clamp on the other end
10. Slide the other end of the braiding up on the tubing a certain amount so when the tubing is stretched it goes to 18 cm and relaxes back to around 14 cm. Grab the middle of the barb connector when doing this making sure not to let go.
11. Form a loop on the end and slide the 7-9 hose clamp over the loop until the clamp is flush with the middle of the barb like in step 8. Clamp both ends of the clamp using the nippers. See figure 3.8 for end result.



**Figure 3.8 Loop formed on plugged end of air muscle**

### 3.2.4 Valves

The Mead Fluid Dynamics Isonic® 2-way solenoid valves, figure 3.9, were used for controlling the artificial muscles on the device. The main reasons for choosing this particular valve were because it was inexpensive, small and lightweight, and provides an easy connection to pneumatic circuit.

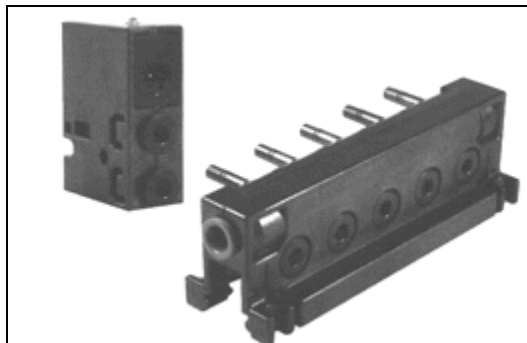


**Figure 3.9 Isonic 2-way solenoid valve and manifold**

Most solenoid valves prices range from \$30 to \$500 resulting in an expensive system especially when multiple valves are needed. Fortunately, Mead makes the Isonic® 1000 series for a little more than \$20 depending on the options selected like the optional LED. The

cost of the 2-way Isonic® valve model V1B02RW1 that was used in this thesis was \$23.34. Due to the low cost of these valves the total cost for all the valves for the device was much lower.

Since these valves are made out of glass-impregnated Ultem thermoplastic they are extremely lightweight unlike the industrial valves made out of stainless steel. The dimensions of the device are about the size of a Zippo® cigarette lighter and are given in table 3.5. The small and lightweight characteristics of the valves allow for a lightweight device and possibly a belt of valves that could go around the patient’s waist.

The easy connection of the built in push-in fittings eliminated the need for fasteners, adhesives, gaskets, and inserts. As a result, the 5/32" Nycoil tubing was plugged directly into the push-in fittings on the valve in one step and there were no additional costs for connectors.

**Table 3.5 Specifications for Isonic® V1B02RW1**

Voltage	5 VDC
Amps	320 mA
Resistance	18 Ω
Cycle Life	50,000,000 cycles
Orifice Size	0.90 mm
Flow	0.02 C <sub>v</sub>
Max Pressure	120 PSI
Tubing	5/32"
Dimension (in)	1-9/32 x 1-3/4 x 5/8
Weight	1.5 oz
Response Time	10 ms

### 3.2.5 Pressure Transducers

The pressure transducer that was chosen for measuring the pressure of each muscle was the Motorola MPX5700GP-ND. The MPX5700 series is a piezoresistive monolithic

silicon pressure transducer designed for use with a MCU with A/D inputs. The output signal is conditioned for a range of 0 – 4.7V and is proportional to the applied pressure. The main reasons for choosing this sensor over others are because of its low price, small size, minimum circuitry for interfacing with a MCU, and easy connection to pneumatic circuit.



**Figure 3.10 Motorola Pressure MPX5700GP-ND Transducer**

The prices of pressure transducers range generally from \$50.00 to \$1000.00. These high prices defeat the goals of this thesis to develop a device that is inexpensive for the patient. Extensive research on pressure transducers revealed the Motorola MPX5700 series, which is small and economical in comparison to most pressure transducers. The Motorola MPX5700GP-ND can be purchased from DigiKey for \$18.19, which is more than a factor of 10 cheaper than most pressure sensors.

The Motorola pressure transducer is also small enough to be mounted on the device next to the air muscle. As a result, the pressure transducer takes up minimal space and helps keep the device design more mobile and lightweight. Also, connecting the transducer to the pneumatic circuit is simple because of the port extending from the package. This port fits approximately 1/4" diameter tubing allowing the device to be plugged into the pneumatic circuit via an unequal tube tee connector shown in table 3.2.



The specifications for the Motorola pressure transducer are given in table 3.6. These specifications comply with the 5V power supply and the Mitsubishi MCU, which has an ADC reference voltage of 5V. The pressure range of 0 – 101.5 PSI also meets the requirements for the artificial muscle’s pressure range of 0 – 90 PSI.

**Table 3.6 MPX5700GP-ND Specifications**

<b>Supply VDC</b>	5 V
<b>Pressure</b>	0 – 101.5 PSI
<b>Output</b>	0 – 4.7 V
<b>Response Time</b>	1ms
<b>Pressure Type</b>	Gage

The equations for pressure related to voltage are given below.

The equation given by the datasheet for output voltage related to pressure is:

$$V_{OUT} = V_S(0.0012858P_{kPA} + 0.04) \pm \varepsilon \quad (3.1)$$

The following equations for Voltage in terms of PSI and ADC are derived below.

$$P_{kPA} = \frac{P_{PSI}}{0.14504}$$

$$V_{OUT} = V_S(0.0088651407P_{PSI} + 0.04) \pm \varepsilon \quad (3.2)$$

$$V_{OUT} = \frac{ADC \cdot V_S}{2^N}$$

The equations for the A/D value in terms of PSI and vice-versa are derived below.

$$ADC = \frac{V_{OUT}}{V_S} 2^N$$

$$\frac{ADC \cdot V_S}{2^N} = V_S(0.0088651407P_{PSI} + 0.04) \pm \varepsilon$$

$$ADC = (0.0088651407P_{PSI} + 0.04)2^N \pm \frac{2^N \cdot \varepsilon}{V_S} \quad (3.3)$$

$$P_{PSI} = \frac{\left( \frac{ADC \pm \frac{2^N \cdot \varepsilon}{V_S}}{2^N} - 0.04 \right)}{0.0088651407} \quad (3.4)$$

$V_S = 5 \text{ V}$

$N = 10 \text{ bits (10 bit analog to digital converter)}$

$\varepsilon = \text{error offset (small value)}$

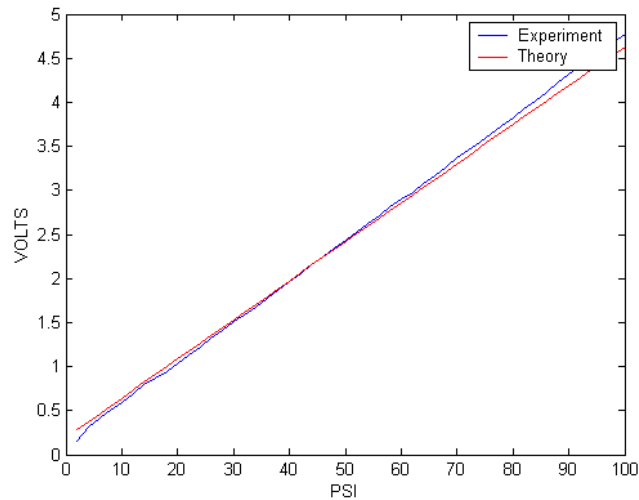


**Figure 3.11 Pressure Transducer response to PSI**

In order to show the linear response of the pressure transducer, voltage data was collected at 2-PSI increments from 0 – 100 PSI. The data was graphed in figure 3.11 along with data generated from the typical response data sheet equation 3.2. This figure shows that the pressure transducer’s response to pressure is extremely linear and fits the equation almost

perfectly. There was a slight deviation at pressures 80-100 PSI but, fortunately, the air muscles typically operate between 0-75 PSI.

### **3.3 Hardware Design**

The hardware required for controlling the pneumatic system consists of a micro-controller, solenoid valve driver circuit, and pressure transducer noise filtering circuit.

#### **3.3.1 M32C/83 Micro-controller**

The M32C/83 micro-controller (MCU) is a member of the Mitsubishi M16C platform. This 144-pin chip features:

- 20 MHz clock frequency
- 108 instructions
- 16 MB memory space
- 11 16 bit timer/counters
- 5 Serial I/O channels for UART, IE bus and I<sup>2</sup>C bus
- 34 A/D Pins
- 2 Independent 8-bit D/A Converters
- 4 Groups of Intelligent I/O for waveform generation, serial I/O, and IE bus
- 1 Channel CAN Module
- 4 Channel DMAC

Mitsubishi donated a single MSV1632/83 – SKP Strater Kit Plus™ shown in figure 3.12, which included the MCU, two serial ports, a 16x2 LCD, push buttons, and a 150-Pin DIN header for easy access to the 144 pins on the MCU. The convenience of this kit made

the M32C/83 easy to use and allowed all of its features to be exploited. The main features of attraction for the rehabilitative device are the 20 MHz clock speed, 16 MB memory space, and abundant I/O for the sensors and control of the solenoid valves.

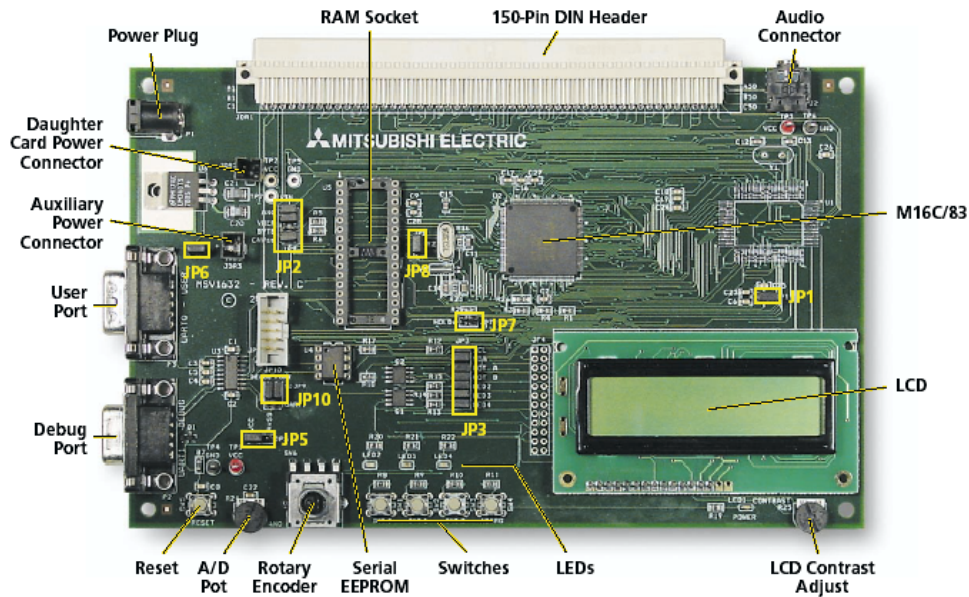


**Figure 3.12 MSV1632/83 - SKP Starter Kit Plus™**

Since control of each muscle required several sensors and the device required multiple muscles, the 34 A/D pins and fast sampling rate offered more than enough support for data acquisition. As a result, no extra data acquisition board was required for using this MCU for this application. Besides requiring A/D pins for the sensors, each muscle required a two output pins for control of the inlet and exhaust valves. Several pins are provided by the MCU and control possibilities are enhanced with the Intelligent I/O feature of the MCU. For example, the popular pneumatic control strategy PWM with the solenoid valves was possible through the use of Intelligent I/O waveform generation.

The serial channel debug port made programming the MCU simple and also allowed for outputting experimental data back to the computer for data collection. Also, the additional serial channels are appropriate for communicating data with a computer running a virtual reality environment for later use with the device.

### 3.3.2 Solenoid Valve Driver Circuit

The following circuit is used to switch the Mead Isonic® 2-way solenoid valve on/off via a MCU. A single NPN transistor switches the solenoid valve on/off by using a digital output pin from the MCU. A rectifier diode (1N4001) is connected across the valve leads to prevent any damage to the transistor due to inductance. The 4.7K $\Omega$  resistor is connected to the output pin to ensure that the output goes low while the R<sub>B</sub> resistor drops the current going through the base junction to reduce the current on the collector side. The Mitsubishi M32C/83 MCU has an I/O current of 5mA and voltage of 5V so that would give the solenoid a current of 5A. The R<sub>B</sub> resistor should drop this current down thus reducing power consumption. The solenoid driver circuit is illustrated in the following figure.

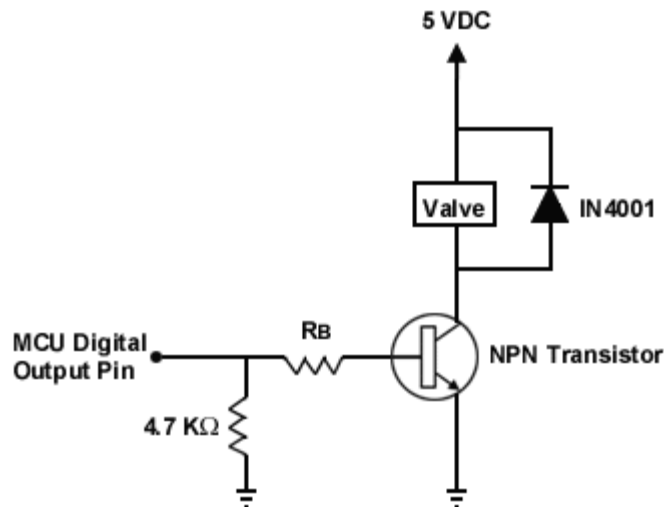


**Figure 3.12 Mead Isonic® 2-way solenoid driver circuit**

To solve for  $R_B$  the following two equations were used.

$$I_C = h_{FE} I_B \quad (3.5)$$

When the digital output pin is raised high by the MCU the voltage is 5V. A KVL around the Base-Emitter loop results in the equation for  $R_B$  in terms of  $I_B$ .

$$-5V + I_B R_B + 0.7V = 0 \quad (3.6)$$

$$R_B = \frac{5V - 0.7V}{I_B} \quad (3.7)$$

$$R_B = \frac{(5V - 0.7V) h_{FE}}{I_C} \quad (3.8)$$

The current gain,  $h_{FE}$ , for the NPN transistor is approximately 200 and the required  $I_C$  for the solenoid is 320 mA according to their respective data sheets. Now  $R_B$  can be solved for using equation (x-4)

$$h_{FE} = 200$$

$$I_C = 320mA$$

$$R_B = \frac{(5V - 0.7V) 200}{320mA} = 2.69K\Omega$$

### 3.3.3 Pressure Transducer Circuit

The circuitry for interfacing the pressure transducer with the MCU is a simple filter circuit using capacitors. Since the output is already conditioned to range from 0 – 4.7 V, the only work left to do is to filter the noise from the signal to achieve clear and accurate outputs. The recommended circuitry from Motorola's data sheet is given in figure 3.13. This circuitry was implemented for each pressure transducer connected to the pneumatic circuit.

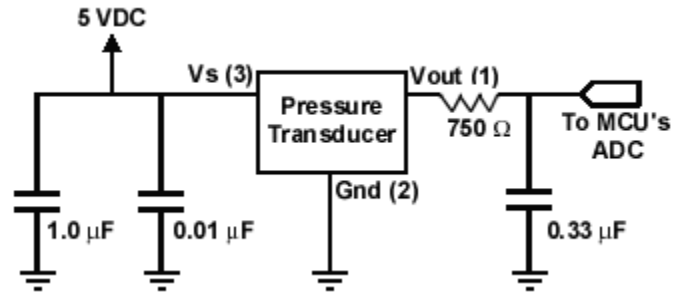


Figure 3.13 Recommended power supply decoupling and output filtering

# Chapter 4. Pneumatic Actuator Characteristics and Control

## 4.1 Air Muscle Control

Controlling an air muscle with solenoid valves deserves special attention because extra work must be done to make the muscle respond smoothly and achieve a desired length. Currently there are two popular types of control schemes for an air muscle with two solenoid valves: PWM and Bang-Bang control.

### 4.1.1 PWM Control

Recently the most popular type of control scheme for a valve controlling an air muscle is PWM. PWM for an on/off valve uses a fixed frequency and varies the duty cycle of a binary waveform in order to control the pressure in an air muscle. Since an air muscle requires two valves for operation, the duty cycle of each valve must coordinate so that air fills the muscle when desired. The duty cycle generally works within a range given the response time of the valve to open and close i.e. if the duty cycle is smaller than the valve response time then the valve will never open or close (van Varseveld et al. 1997, p. 1197). These duty cycles generally increase to achieve a faster rate of airflow into the muscle. Since the duty cycle determines the flow in an air muscle, air muscles can be easily controlled in a smooth fashion by using small duty cycles that are larger than the response times of the valves.

### 4.1.2 Bang-Bang Control

Bang-Bang control is an extremely simple control algorithm that uses only the sign of the error to determine whether to make a change to the system. This type of control for air



muscles uses the sign of pressure error to decide from three possible types of states: In, Exhaust, and Leak. The In state, where the inlet valve is opened, occurs when the pressure error is positive. The Exhaust state, where the exhaust valve is opened, occurs when the pressure error is negative. When this error is zero or within a preset dead-band region then the Leak action occurs in which both the valves are closed.

Cham has offered a modified version of bang-bang control adding a Flow state to the three existing types of states. Since the air muscle requires two valves, there are a total of four possible states for the air muscle (Cham 1999). Table 4.1 shows the binary representation of each state. Each bit is attributed to each valve so if the binary value is ‘0’ then the valve is off and if the value is ‘1’ then the valve is on.

**Table 4.1 Four States of control for an air muscle using two solenoid valves**

<b>Inlet</b>	<b>Exhaust</b>	<b>State</b>
0	0	Leak
0	1	Exhaust
1	0	In
1	1	Flow

Cham uses an estimate of the current state and a model of the delays for each state and predicts the future errors for each transition. The controller finally picks the transition with the smallest predicted error.

### **4.1.3 Antagonistic Muscle Pair**

Another important means for controlling the position of a joint like and elbow is the use of an antagonistic pair of muscles. An antagonistic pair like a human muscle can provide the power to achieve a specified angle and also restore the device to an initial angle in a controlled fashion.

The antagonistic pair of air muscles, figure 4.1, works by varying the pressure in both muscles to achieve a desired angle. Ideally, when both pressures are the same ( $P_1 = P_2$ ) in two identical air muscles the forces exerted by them should cancel out and the angle should be zero (Daerden 2001b, p. 1961). However, if the pressure in one muscle is greater than the pressure in the other muscle then the angle will increase in its favor and vice versa if the pressure decreases.

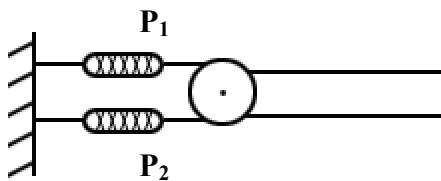


**Figure 4.1 Antagonistic Pair**

## **4.2 Test Platform**

A test platform, figure 4.2, was developed to run several experiments on the air muscles to determine their characteristics. This platform can be used for hanging weights on a single air muscle and for balancing a wooden arm with one or two air muscles. The steps and materials for the construction of the test platform are outlined in the appendices.

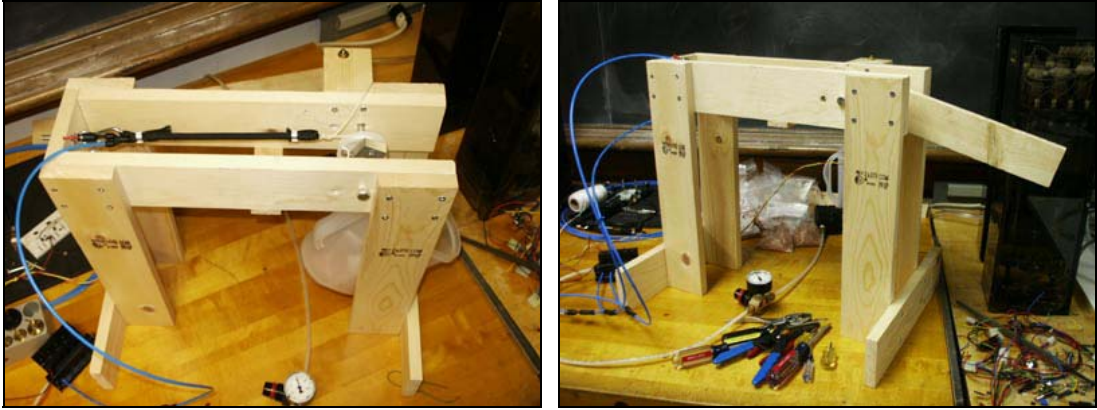


**Figure 4.2 Test platform (a) setup for lifting a mass (b) setup for positioning an arm with either one or two muscles**

#### **4.2.1 Experimental Operation**

The test platform was designed to be flexible so that it could support a variety of experiments. In order to support several experiments with one test platform, the platform was designed for two different configurations. This test platform can be configured for hanging a mass for force or it can be configured for positioning a wooden arm with one or two muscles. A graphical representation of these options is illustrated in figure 4.3.

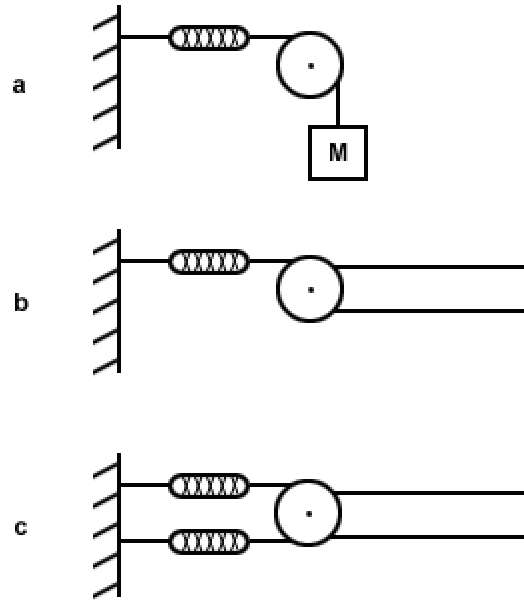


**Figure 4.3 Test Platform Options (a) hanging mass (b) single muscle with arm (c) antagonistic muscles with arm**

#### **4.2.1.1 Single Muscle Pulling a Constant Mass**

Option ‘a’ in figure 4.3 allowed for experiments with a single air muscle in order to measure the relationship between length, force, and pressure. This configuration was also useful for determining the characteristics of the air muscle during the four different pressure states: in, exhaust, flow, and leak. For example, recorded pressures when opening the in valve for two seconds revealed both the response time to fill the air muscle and confirmed the response time of the valve. Besides using this configuration for determining the response time of the air muscle, this configuration was also used to determine the damping of the muscle under test.

Instead of using expensive conventional weights, bee-bees were used to provide incremental weight to the single air muscle. This incremental unit of weight was 1 lb so 15

zip-lock bags were filled with 1 lb of 0.4g bee-bees, figure 4.4. As a result, tests were done with a 0 – 15 lb range weight by simply adding or removing 1 lb bags of bee-bees. These bags were placed in a plastic lightweight pitcher and were hung from the nylon string that usually connects to the second muscle. Figure 4.2 a shows the pitcher with several 1 lb bags being lifted by an air muscle.



**Figure 4.4 1 lb zip-lock bag of bee-bees**

#### **4.2.1.2 Air Muscle Positioning a Wooden Arm**

Option ‘b’ and ‘c’ in figure 4.3 allowed for control experiments with one or two air muscles. For example, the potentiometer measured the angle of the arm while the pressure transducer measured the pressure in the muscle to provide two error terms for both determining the duty cycle when using PWM and determining pressure states when using Bang-Bang control. Figure 4.5 shows two muscles controlling the wooden arm.



**Figure 4.5 Antagonistic muscle pair controlling the wooden arm**

### **4.3 Test Platform Experiments with Air Muscles**

Several experiments were set up for determining the characteristics of the air muscles that were built for the rehabilitative wearable arm. Since the response times of the valves and the air muscles are important for both Bang-Bang control and PWM control, tests were executed to measure the response times of both the valves and the air muscles. Experiments were also designed to measure the static and dynamic characteristics of the air muscles to understand the nature of these custom-made air muscles.

#### **4.3.1 Response Time**

Response time tests were done by using the test apparatus set up for hanging weights of 0 lb, 1 lb, and 5 lb on a single air muscle at pressures of 20-70 PSI in 10 PSI increments. The single air muscle was connected to an inlet valve, an exhaust valve, and a pressure regulator. The M32C/83 was programmed to open the high-pressure valve for 1.5 seconds and record the pressure transducer values during that time. Figure 4.6 shows the test results for response times for a 7 ¼" resting length and 11" stretched length (7 ¼" - 11") air muscle. In the figure, the solid black lines are drawn through the 90% steady-state values to

determine the response time for filling the air muscle. The response time for filling the air muscle was approximately 610 ms  $\pm$  20ms and was independent of the load on the muscle.

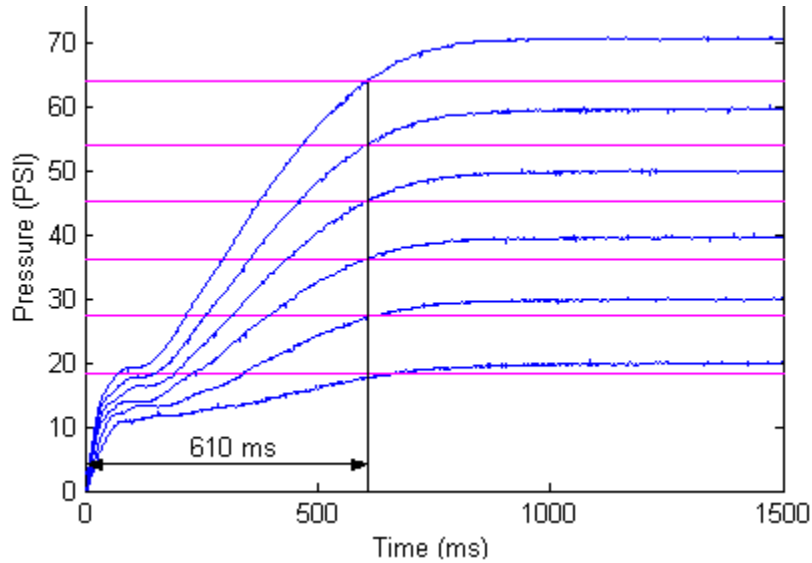


**Figure 4.6 Response Time To Fill Muscle at 0 lb**

A response time experiment was also done on two muscles connected in parallel to the same two valves. This experiment was intended for the doubled muscles that were later used on the device for improving the strength of the device for flexion and extension. Since the response time was independent of the load, the experiment only used a 1 lb weight. The results, figure 4.7, show that the response time increases by nearly double. Fortunately, elbow flexion and extension must be slow and controlled for rehabilitation and requires times greater than 1080 ms between each motion. As a result, both single and double muscles have response times that are fast enough to handle the slow rehabilitation of the elbow.

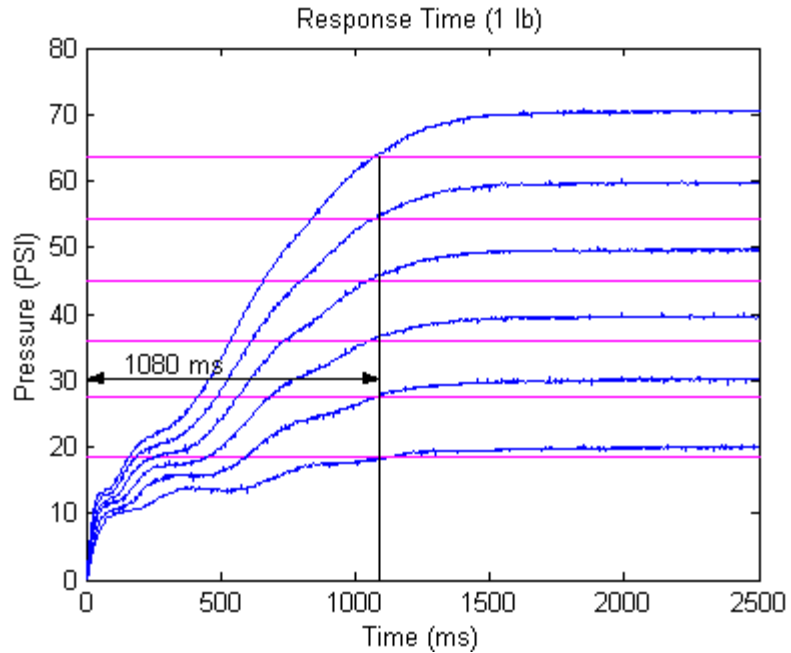


**Figure 4.7 Response time for doubled 7 1/4" - 11" air muscles**

### 4.3.2 Valve Response Time

The same data that was collected for figure 4.6 was analyzed to estimate and confirm the factory response time for opening the solenoid valve. According to the Mead specifications on the Isonic® 1000 valves the response time of the valve is 10 ms. The valve's approximate 10 ms response time is also shown in the previous data collected by zooming in on the plot for the first 20 ms. Results for the valve response time at various pressures is shown in figure 4.8. According to figure 4.8 the response time of the solenoid valve lies between 8 ms and 10 ms.



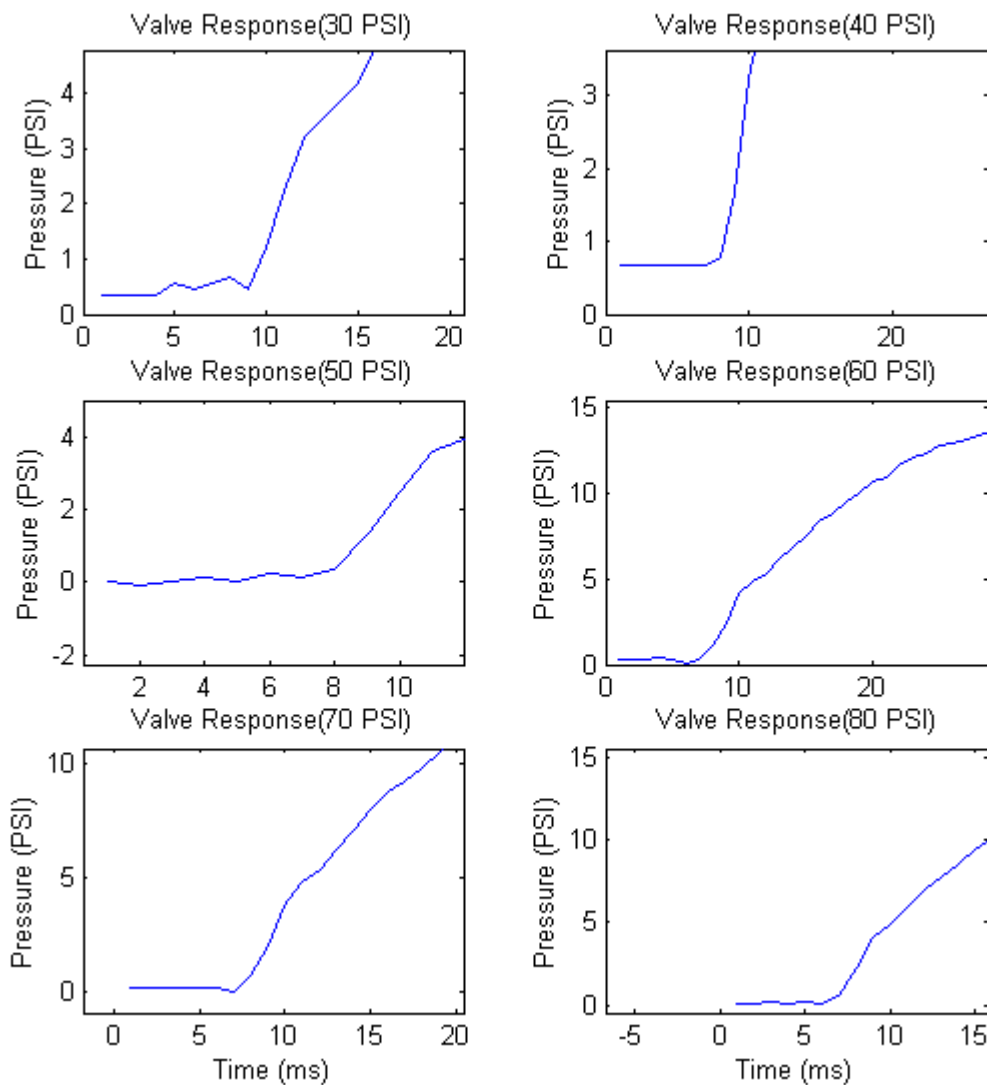


**Figure 4.8 Valve response time  $\approx$  8 – 10 ms for various pressures and a zero load.**

### 4.3.3 Leakage

Another important characteristic of the air muscle is the amount and rate of leakage during the leakage state when all the valves are closed and the air muscle is full of air. Several experiments to observe the leakage were conducted using 0 lb, 1 lb, and 5 lb loads each at set pressures from 20-70 PSI. First, the inlet valve was opened for two seconds to fill the muscle completely with the specified pressure. After two seconds the inlet valve was

closed and half-second pressure samples were taken for two minutes from the Motorola pressure transducer to measure the air leakage from the air muscle and its connections to the pneumatic circuit. These results were collected and plotted in figure 4.9.

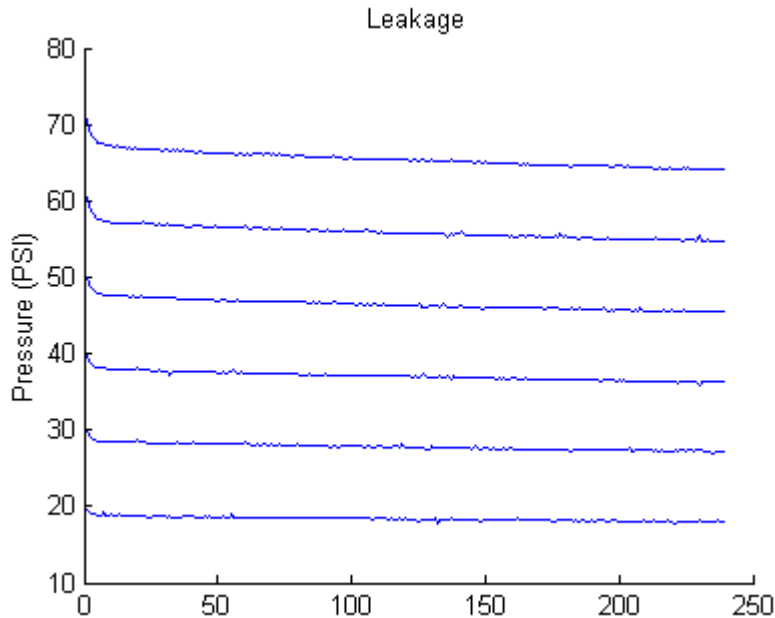


**Figure 4.9 Average Leakage from air muscle with a 0 lb, 1 lb, 5 lb load over ½ second samples for 2 minutes**

The results from these figures show that for higher pressures there is a small 2-3 PSI pressure drop approximately 10ms when the inlet valve closes. Fortunately, there is little concern over the leakage of the system because the pressure drops slowly over these two minutes. Leakage also appears to be independent of the load on the air muscle. These results indicate that maintaining a constant pressure in the air muscles should not be difficult.

#### **4.3.4 Exhausting the valve**

The third possible state when using a two-valve circuit with an air muscle is the exhaust state. When the air muscle is exhausted from a set pressure to 0 PSI, the time for

exhausting the muscle completely is important for developing a control scheme. As a result, experiments similar to the inlet valve response time experiments were done to capture the response time and nature of the system when the air muscle is depleting. First, the inlet valve was opened for two seconds to fill the air muscle completely. The inlet valve was then closed and 5 ms later the exhaust valve was opened for two seconds while values were read from the pressure transducer.

The results that are shown in figure 4.10 indicate that the higher the initial pressure the longer it takes for the muscle to deplete. Each pressure level tends to take the same response curve except time shifted to the right with increasing pressure. The rate of pressure decrease appears to slow down around 10 PSI, which is the max pressure for the silicone tubing. After reaching 10 PSI the tubing forces the air at a faster rate due to the tubing taking its natural form.

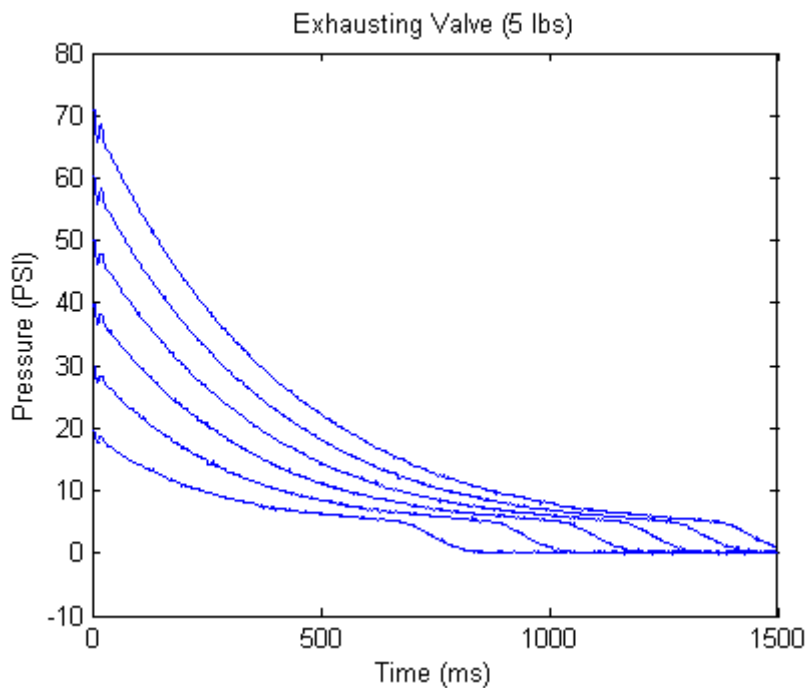


**Figure 4.10 Exhausting a 7 ¼" - 11" air muscle**

Figure 4.10 also indicates that the time to exhaust the air muscle is between 750 and 1500 ms. One possible way to speed this up may be to take 10 PSI as fully exhausted since the muscle does not contract with pressures equal to or less than 10 PSI. Another possible way to speed up exhausting the valve may be to either increase the exhaust port size or to add additional exhaust valves.

Figure 4.11 shows the trend when exhausting the air muscle from 40 PSI and 70 PSI with various loads. As the load increases the exhaust time decreases at times after the 10 PSI mark. This change in time is due to the weight stretching the tubing, which causes the diameter of the tubing to contract and force the air out faster. However, before the 10 PSI mark the curves are approximately the same for what this thesis is concerned with.

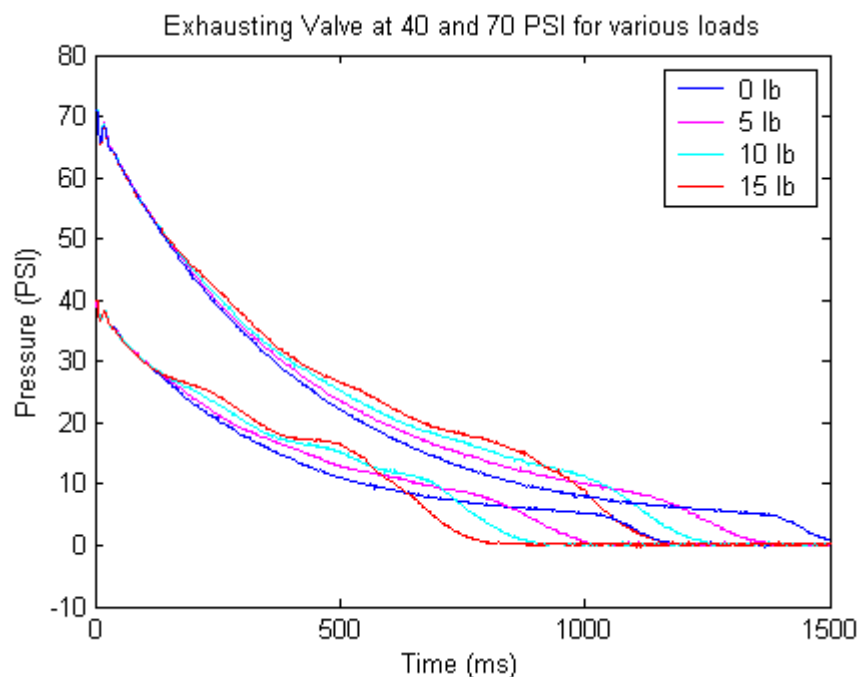


**Figure 4.11 Exhausting a 7 ¼" - 11" air muscle at 40 and 70 PSI with different loads.**

An Exhaust experiment was also conducted on the doubled muscles that were used on the device for increasing the strength and improving the angles achieved by the device. This

experiment was the same as the previous exhaust experiments except the only weight tested was a single 1 lb weight. The results for this experiment, shown in figure 4.12, reveal that the exhaust time for two muscles is around 1700 ms for the 70 PSI source if the 10 PSI mark is considered the fully exhausted state. Otherwise the time response for exhausting the muscle is around 2500 ms, which is almost a second later. As a result, the 10 PSI mark may be better suited for exhausting the doubled air muscles unless flexion and extension is really slow.

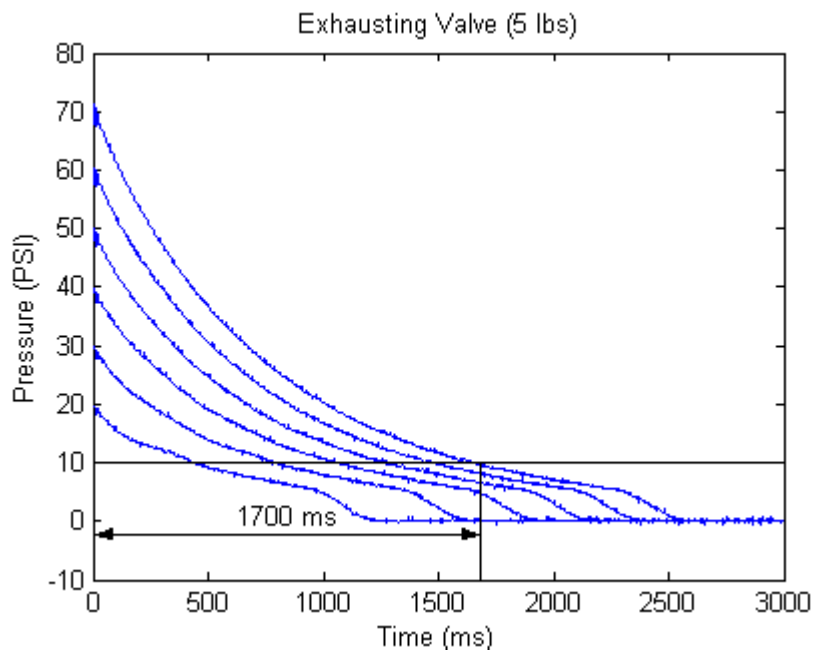


**Figure 4.12 Exhausting doubled 7 ¼" - 11" muscles**

#### **4.3.5 Flow Experiments and Results**

The final possible state (flow) for a two-valve system is when both valves are open. When both valves are opened with a preset pressure in the air muscle the pressure in the muscle drops by an amount dependant on the pressure level. Experiments were designed to measure the flow state's response over a two second time period with a 1 ms sample time. The MCU was programmed to open the inlet valve for two seconds to fill the air muscle to a

set pressure. After two seconds the inlet valve was left open while the exhaust valve was turned on and the pressure was measured from the Motorola pressure transducer. Results for the flow experiments are shown in figure 4.13. Figure 4.13 shows the tests for 0 lb at different set pressures as well as the tests for 1 lb and 5 lb. According to this plot the pressure change is independent of the load on the air muscle. Another observation is that the higher the initial pressure the larger the pressure drops in the system. For example, the pressure drops 20 PSI (70 PSI to 50 PSI) and drops only 10 PSI (20 PSI to 10 PSI). Also, the response time of the plots appears to converge to approximately 550 ms.

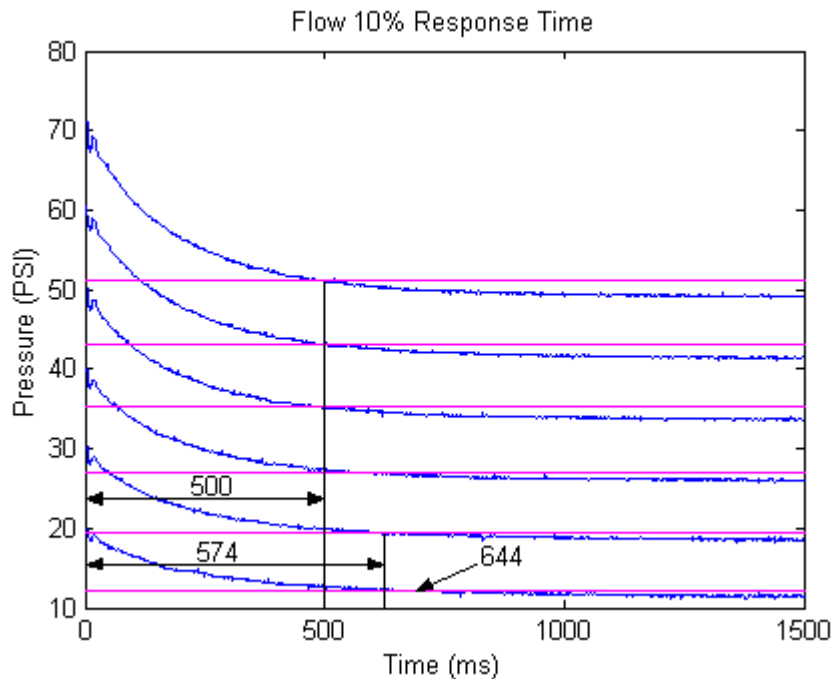


**Figure 4.13 Flow response curves combined (0 lb, 1 lb, 5 lb)**

## 4.4 Characteristics of the Air Muscle

### 4.4.1 Static Characteristics

Experiments were done to determine the force-length relationship of the muscles and to measure the hysteresis of the air muscles. Separate tests at 20 PSI increments from 20 PSI to 80 PSI were done with weight increments of 1 lb ranging from 0 lb to 15 lbs. For each test a pressure regulator that was connected to the air muscle was set to the desired pressure and weights were added starting from 0 lb to 15 lb and then removed from 15 lb to 0 lb. The pressure and change in length were recorded at each increment using the pressure transducer and potentiometer connected to the pulley wheel respectively. Since the angle was measured on the potentiometer, the change in length had to be calculated by first measuring the circumference of the pulley wheel and then finding the radius of the wheel.

$$C = 2\pi r \quad (4.1)$$

$$r = \frac{C}{2\pi} \quad (4.2)$$

The change in length was measured by taking the angle at 0 lb as the initial angle and subtracting it from the measured angles to get the change in angle from the start. Then the formula for calculating arc length was used to find the change in length from the starting 0 lb.

$$S = r(\theta_i - \theta_0) \quad (4.3)$$

Since the angles are converted from voltage to a 10-bit number the angle must be converted back to an angle in radians. This conversion takes place by multiplying the resolution ( $k_R$ ) in radians per bit by the ADC change in values.

$$S = r[k_R(ADC_i - ADC_0)] \quad (4.4)$$

$$k_R = \frac{Span}{2^N} \cdot \frac{\pi}{180} \quad (4.5)$$

Results for tests on a 5 5/16" – 7 1/2" sized muscle and a 7.25" – 11" sized muscle are shown in figures 4.14 and 4.15 respectively. Figure 4.14 indicates that the hysteresis for the air muscles is between 0.19" and 0.25". This value is poor compared to the same experiments using the Shadow muscles and could easily be observed by simply pulling on the muscle while it was attached to a mass. The reason for this hysteresis is due mostly to the friction between the braiding and the inner bladder. Figure 4.15 also shows even more hysteresis, 0.25" - 0.40" for the longer muscles that were actually used on the pneumatic brace. This leads to the conclusion that longer muscles give worse hysteresis because there is more braiding and tubing to create more friction when inflated. Based on this hysteresis, the elbow brace will exhibit larger angles when the device is flexed or extended without weight and then adding a weight vs. flexing and extending with the weight already on the arm.

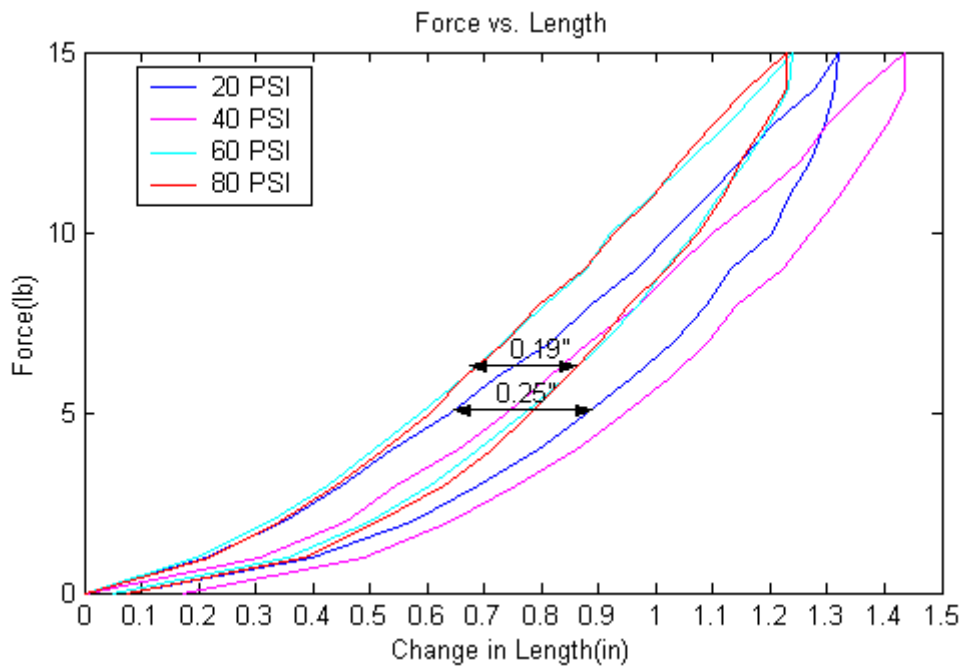


**Figure 4.14 Force vs. Length for 5 5/16" – 7 1/2" air muscle**



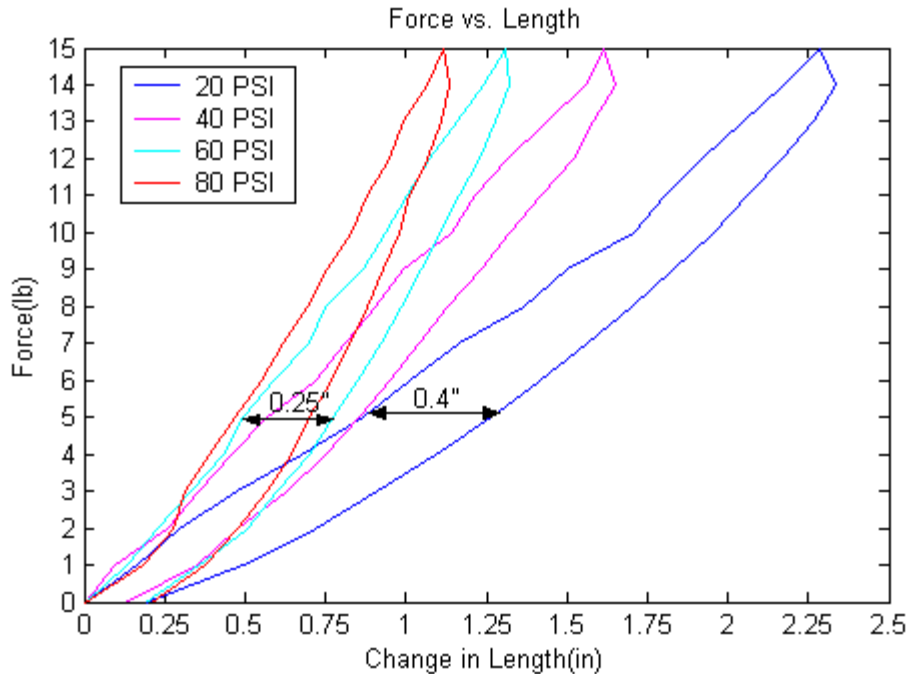


**Figure 4.15 Force vs. Length for 7.25" – 11" muscle used on pneumatic brace**

#### **4.4.2 Dynamic Characteristics**

An experiment was designed to measure the damping of the air muscles that were made for the pneumatic brace. This experiment consisted of hanging a mass from an air muscle that is filled with a constant pressure and displacing the mass to cause the muscle to oscillate until it reaches a steady state. During this time the potentiometer connected to the pulley wheel recorded the angles so that the change in length could be plotted versus time. Figures 4.16 – 4.17 show the results for the experiments, which use various constant pressures and weights from 5 lb, 10 lb, and 15 lb. According to each of these figures the damping increases with respect to an increase in load. Therefore, damping is not constant but could possibly be averaged since the change in damping for 5 lb increments is small.

These plots reveal that the muscles made for this project are much more damped compared to the Shadow's air muscles that were tested in Colbrunn's thesis. One possible reason for more damping is because the selected rubber tubing is silicone rubber instead of latex rubber, which is used in the Shadow air muscles. This silicone tubing is supposedly more durable and longer lasting than the latex rubber, but the friction between the braiding and the silicone rubber may be greater. The braiding may also be the difference that is causing the damping instead of the tubing but this is an uncertainty. Another possible reason for this additional damping may be attributed to the friction on the pulley wheel bolt that rotates through two wooden holes on the test frame. This type of friction could cause more damping but not any significant amount of friction since the pulley wheel rotates freely.

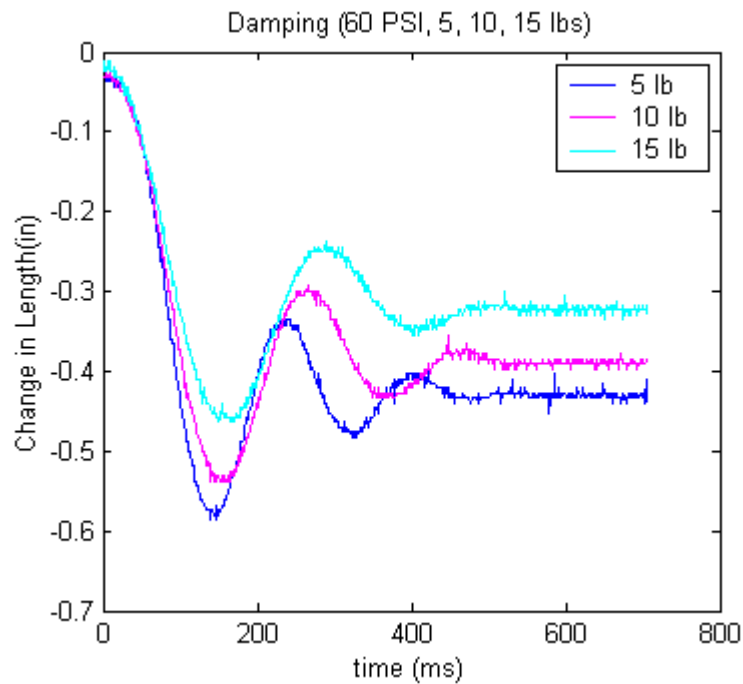


**Figure 4.16 Damping for 60 PSI with 5 lb, 10 lb, 15 lb loads**

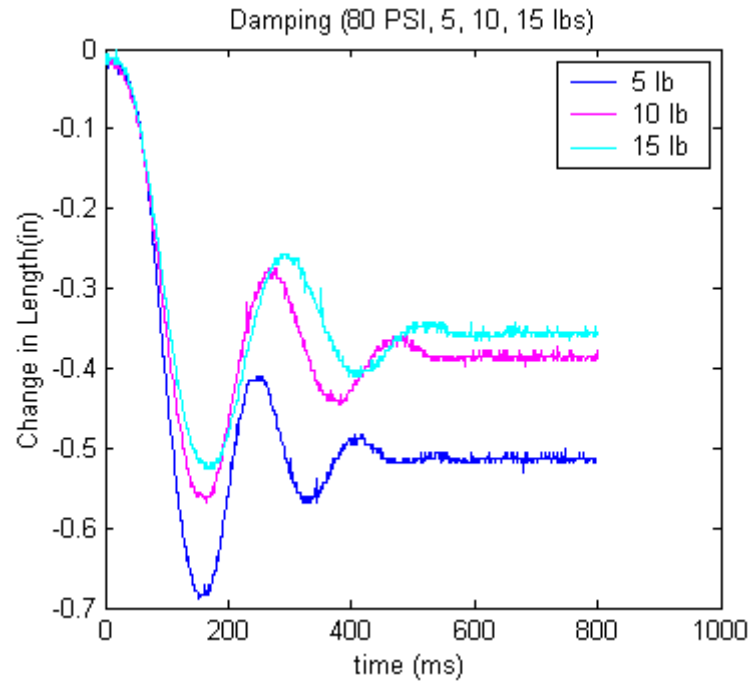


**Figure 4.17 Damping for 80 PSI with 5 lb, 10 lb, 15 lb loads**

# Chapter 5. Elbow Actuator Design and Experiments

## 5.1 Design of modified elbow brace

The rehabilitation device was built from an existing elbow brace called the IROM Elbow that was donated by Don Joy, figure 5.1. Modifications were made to the elbow brace to allow for muscle connections to certain areas of the device to achieve elbow flexion and extension. The two main modifications to the device are the addition of two aluminum shapes.



**Figure 5.1 Don Joy IROM Elbow**

An aluminum shoulder section was made for the origins of the biceps and triceps since the actual length of the section covering the mid-arm was not viable for longer air muscles with sufficient contraction ratios. This aluminum section, figure 5.2, was placed under the Velcro straps on the posterior side of the hinge and attached to the device using two  $\frac{1}{4}$ " x  $\frac{1}{2}$ " flat head bolts with washers on both sides of the device. The bolts were inserted from the inside of the brace under the foam padding and bolted on top of the Velcro straps. These bolts feature a flat round head to keep from hurting the patient and causing discomfort.





cover, which caused unstable motions and wasted muscle length that reduced the angle achieved by the muscle.

## **5.2 Muscle Attachment**

In order to achieve flexion and extension of the elbow, air muscles were added to the brace that mimic the biceps and triceps. These muscles were then doubled to provide ample force for moving the patient's arm since one muscle was insufficient in initial testing.

Each muscle was attached to both aluminum sections with nylon rope by drilling holes for the ends of the muscle and tying the nylon rope through the holes. Three holes were drilled in the aluminum shoulder section for the doubled pairs so that the muscles' air tubes could sit side by side. Also, two holes were drilled in the aluminum c-shape for each pair to share since space was limited and there was no tubing to avoid damaging.

Nylon rope with a 1/8" diameter was used to tie each muscle to the brace and act as a tendon. The rope was melted on both ends to avoid fraying and pushed through the air muscle's loop end. Then each end of the rope was pushed through the two appropriate holes and a triple knot was tied behind the aluminum to hold the muscle in place. Finally, the muscles were tightened so that the biceps were fully stretched in the 0° position and the triceps were fully stretched in the 120° position.

The actual sites for muscle origin and insertion are shown in figure 5.4. The biceps and triceps origins are located on the aluminum shoulder section located in figure 5.4 a. Since this device used a left arm elbow brace the biceps origins are located on the left side of the aluminum shoulder section while the triceps are located on the right. The insertions of the biceps and triceps are located on the aluminum 'c' shaped piece below the elbow joint and

are shown in figure 5.4 b. In this figure the biceps are located on the left tip of the aluminum 'c' and triceps are located on the right tip of the 'c'.

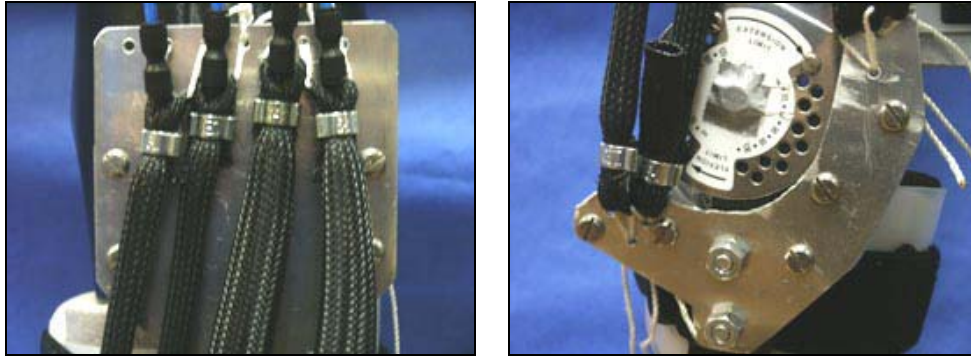


**Figure 5.4 Insertions and origins of the air muscles (a) Origin of biceps and triceps on aluminum shoulder section (b) Insertion of biceps and triceps on aluminum 'c'.**

The lengths of the biceps and triceps were determined by measuring the displacement from the insertions and origins while rotating the joint. The actual displacement required for the triceps was measured by measuring the diagonal created from the insertion site on the aluminum 'c' to the origin on the aluminum shoulder section while rotating the elbow the full 120°. This measurement resulted in a 2.5" – 2.75" diagonal and was rounded to 2.5". The same measurement was found for the biceps and was also rounded to 2.5". In order to calculate the length of the muscle required to displace something 2.5" the following equation was derived based on the average percent contraction of these air muscles. The derivation of the simple length equation is found below. The parameter 'L' is the actual length of the muscle, 'disp' is the displacement, and 'C' is the average percent contraction length for the type of air muscle used. The displacement of the air muscle is calculated by subtracting the stretched length by the contracted length in the following equation:



$$disp = L - C \cdot L \quad (5.1)$$

This is then rearranged to solve for the length of the muscle for a desired displacement.

$$L = \frac{disp}{1 - C} \quad (5.2)$$

The percent contraction,  $C$ , was calculated by measuring the contracted length percentages of air muscles with various lengths. The average contraction percentage for the muscles developed for this thesis was 0.76 (76%) so for a contraction of 2.5" the length using equation 5.2 would be:

$$L = \frac{2.5}{1 - 0.76} = 10.41"$$

The contracted length was found by subtracting the desired displacement from the length, which equaled 7.91". The final lengths of the muscle are 7.91"-10.41" for a muscle with a 2.5" contraction. The lengths for the biceps and triceps were actually expanded to 7.25" – 11" to increase the chances of actually constructing a muscle with a 2.5" contraction. The muscle was then constructed and the contraction was determined to be approximately 2.5". Finally, the air muscles were constructed, tested and placed on the device.

### **5.3 Experiments and Results**

The experiments used a mannequin arm donated from NCSU's Textile Apparel, which was cut at the elbow to allow the two sections of the arm to move freely. The shoulder-elbow portion of the arm was attached to a 1" x 4" block so that the shoulder could be fixed at desired angles. The block was then drilled into the side of a table to hold the arm up. A screw was also drilled in the top of the block so that a rope could be added to hold the brace up since the dummy arm has a slick hard surface unlike that of the human arm. The

brace was then added to the shoulder-elbow section and connected from the aluminum shoulder section to the screw in the block with nylon rope, figure 5.5.

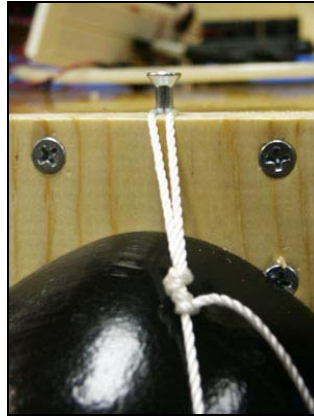


**Figure 5.5 Wooden block with screw in the top**

The experiments used the elbow brace's flexion and extension limit peg holes for measuring the angles produced by the air muscles. The angle is simply read by looking at where the forearm joint is located through the peg holes, which are labeled in  $10^\circ$  units. Figure 5.6 shows an example of the angle measurement technique that reads an angle of approximately  $90^\circ$ .



**Figure 5.6 Angle measurements**

Several experiments were designed using the setup with the mannequin arm to determine the effectiveness of the muscles and their positions on the device. A total of three experiments were designed for testing flexion and extension of the elbow and are shown in figure 5.7. The first two experiments were designed to test the flexion of the elbow at two different shoulder angles,  $0^\circ$  and  $35^\circ$ , with single air muscles acting for the biceps. The last experiment was designed to test the extension of the elbow at a shoulder angle of  $-90^\circ$  with both single and double air muscles acting for the triceps. Experiment one was also repeated using doubled muscles for the biceps.

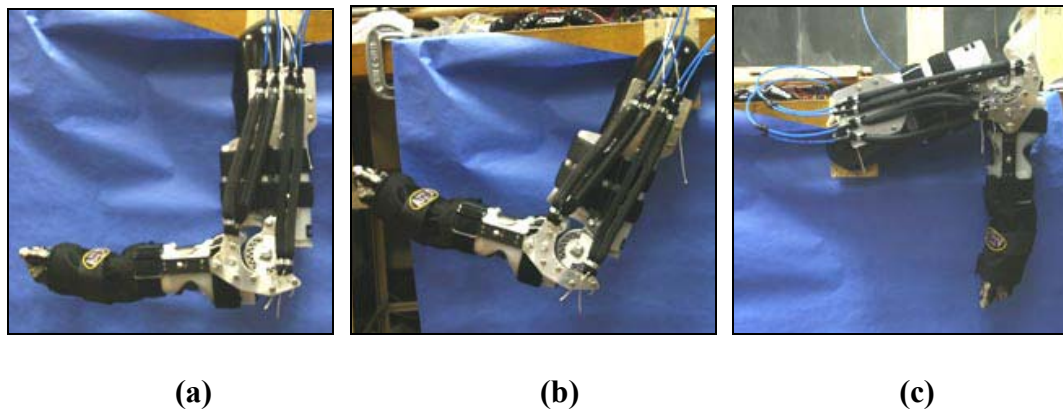


**Figure 5.7 Three experiments for testing flexion and extension (a) Shoulder at  $0^\circ$  testing flexion (b) Shoulder at  $35^\circ$  testing flexion (c) Shoulder at  $-90^\circ$  testing extension**

These experiments all used a pressure of 60 PSI and measured the angle of rotation for both flexion and extension while 1 lb incremental weights ranging from 0 lb to 10 lb were added to the wrist.

The first two experiments tested the flexion of the device with the shoulder at the  $0^\circ$  position i.e. the arm is pointing to the ground, figure 5.7a. The air muscles were initially deflated and then the biceps were filled to 60 PSI causing the arm to flex. The results for both

are shown in figure 5.8. Analysis of these results shows that the flexion of the elbow is rather limited when the shoulder is at 35° with single muscles, but this can be improved by adding another air muscle to make a pair. Adding another muscle to the device essentially doubles the force to help produce a better range of flexion when the forces on the elbow joint are large. The results of the doubled muscle experiments give a 10° improvement in flexion over the single muscle. One important point to make is that the forces required to move a passive patient's arm are usually less than 3 lb which are in the range where the device happens to perform extremely well.

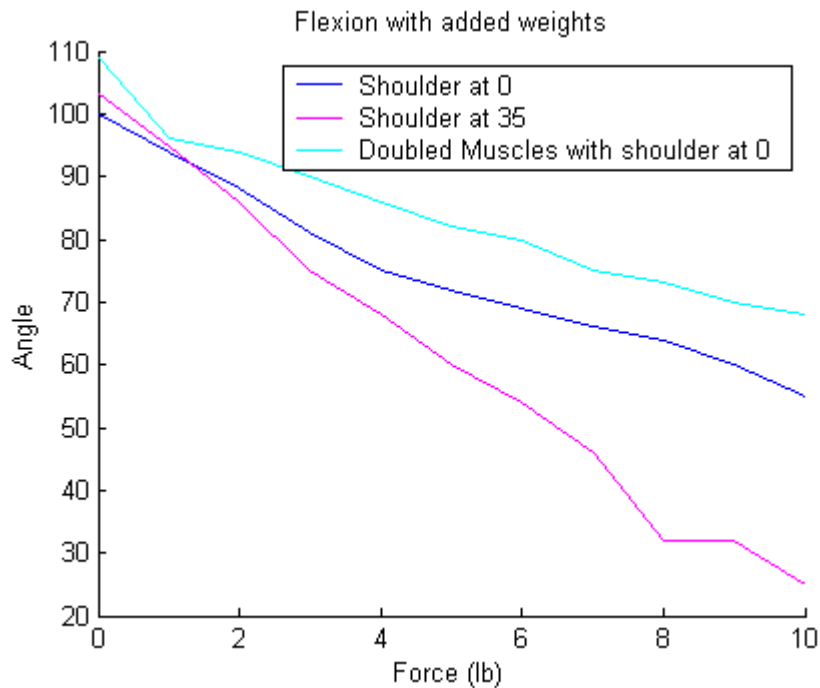


**Figure 5.8 Flexion experimental results.**

The next experiments set out to measure the angles produced by the triceps during extension of the elbow using both single and doubled air muscles. For these experiments the shoulder was rotated back -90°, figure 5.6c, so that the triceps could actuate the elbow from

approximately 110° to 0°. The results given in figure 5.9 show that both the single and doubled muscles perform well within the 0 lb to 3 lb range, however, the doubled muscles perform significantly better. The doubled muscles also give a 40° improvement over the single muscle for larger forces. As a result, the doubled muscles are better candidates for extending the elbow.

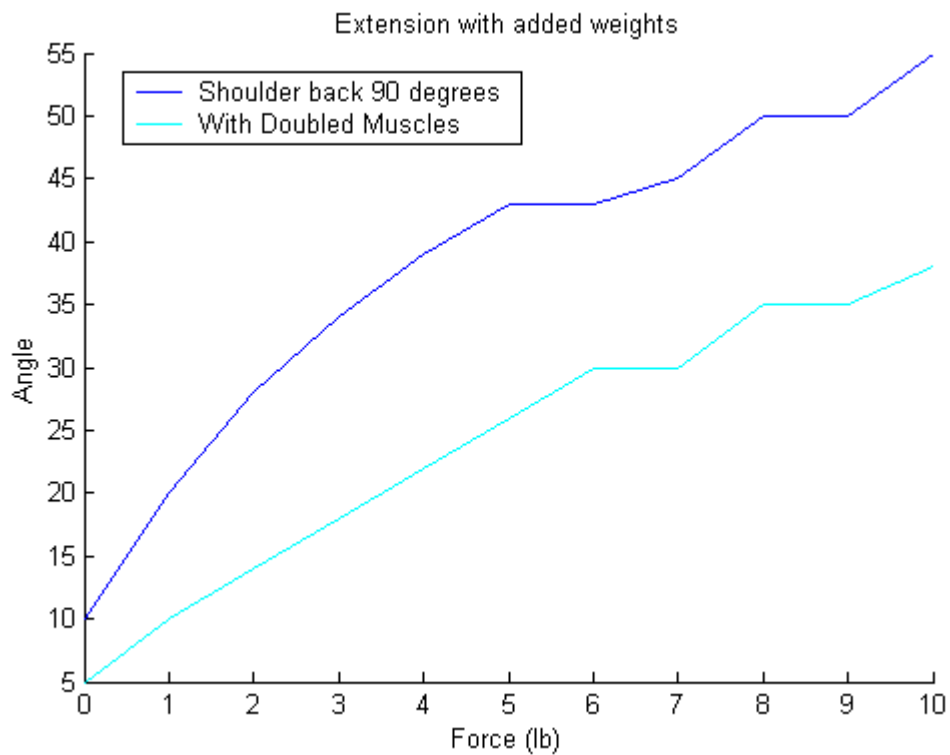


**Figure 5.9 Extension experiments with single and doubled air muscles**

The pneumatic brace was also tested without the dummy arm to compare the angles accomplished with no added force other than the brace to the previous experiments. The brace achieves 120° flexion and 0° extension which are the maximum angles that the brace will allow due to its design. Apparently the weight of the dummy arm is enough to bring the biceps max angle down to the 90° – 105° mark. Another reason for the loss of angle on

flexion and extension is due to the knots tightening during operation. When the knots tighten the rope extends just enough to reduce the angle of flexion by about 10°.

Muscle length data was also collected during the experiments where the shoulder was at 0° and -90° by using a tape measure and measuring from hose clamp to hose clamp. This data was collected to estimate the actual forces exerted on the muscle for both the biceps and triceps from the change in length from rest, which is 7 ¼". The relationship between force and length is given in figure 4.25. This relationship, also known as the stiffness of the muscle, is the slope of the line for 60 PSI located in the figure. The slope was approximately 10.67 lb/inch for the 60 PSI line when increasing in pressure. This slope from the static force vs. length data allows for the calculation of force by first finding the change in length and multiplying by the slope. The results for both flexion and extension experiments are shown in figures 5.10 and 5.11 respectively.

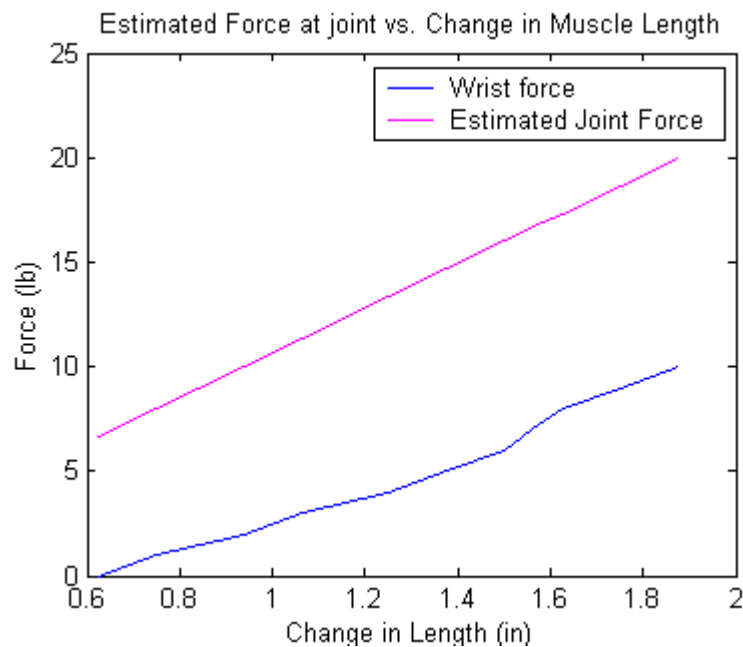


**Figure 5.10 Estimated Joint Force vs. change in length for biceps during flexion**

The actual forces on the joint are quite impressive ranging from 7 lb to 20 lb for flexion and 9 lb to 22 lb for extension. Since these forces are so large compared to the normal forces for the air muscle, the device will definitely perform better with doubled muscles. However, according to the figure the 1 lb to 3 lb range for a passive stroke patient only results in muscle forces of 7 lb to 14 lb. This range means that using single muscle should be capable of moving a patient's arm successfully but may suffer a loss of range of motion without the doubled muscles.

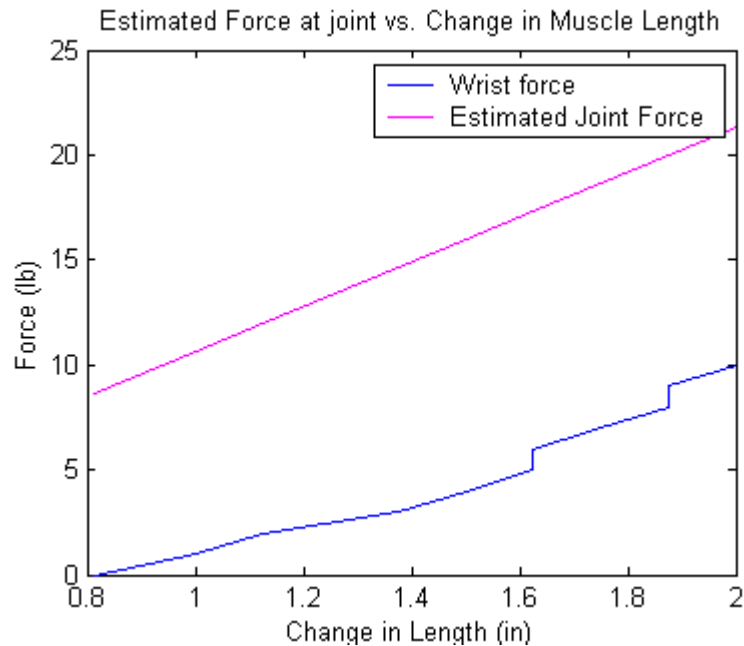


**Figure 5.11 Estimated Force on triceps vs. change in length with Extension angle for comparison**

## 5.4 Control of Pneumatic Brace

The pneumatic brace utilized an antagonistic pair of air muscles that required varying the pressure in each muscle to flex and extend the elbow. Since the air muscles work in an

antagonistic way, the pressure in the muscles is also antagonistic because they follow opposite paths. For example, when the desired angle is at a maximum, the pressure in one muscle is at the maximum pressure while the pressure in the opposite muscle is near zero. As a result, the waveform in figure 5.12 was derived to map out the paths that each pressure would take during flexion and extension. In this figure  $t_{FE}$  is the time for the device to completely flex or extend and  $t_D$  is the time between flexion and extension. The two pressures are represented as  $P_1$  and  $P_2$ , which are the pressures for the biceps and the triceps respectively.

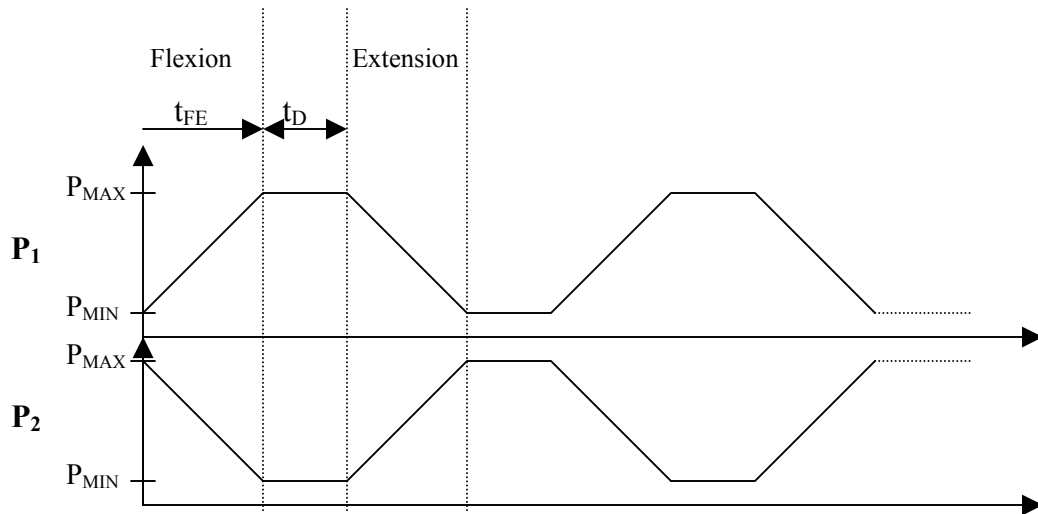


**Figure 5.12 Pressure changes during flexion and extension**

Examples of the brace angles accomplished for these pressure paths are shown in figure 5.13. Figure 5.13a describes the device fully extended where the pressure in the bicep,  $P_1$ , is at a minimum pressure while the pressure in the triceps,  $P_2$ , is at a maximum. Figure 5.13b shows the brace halfway flexed where the pressures are equal in both muscles while figure 5.13c shows the brace fully flexed where the pressure in the bicep is at a maximum and the pressure in the triceps is at a minimum.



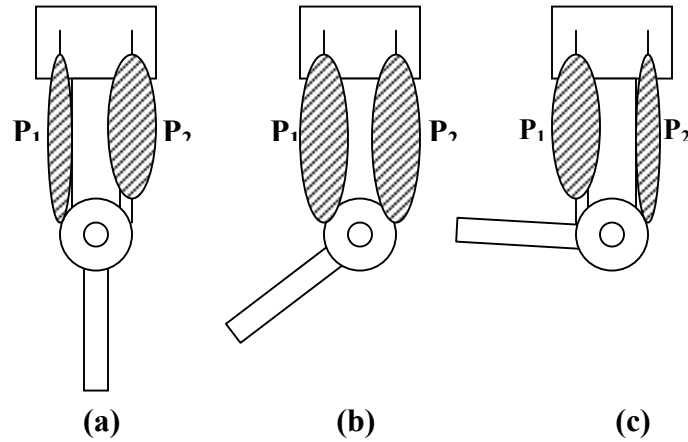


**Figure 5.13 Brace angles using antagonistic pair (a) Fully extended [ $P_1 = P_{MIN}$   $P_2 = P_{MAX}$ ] (b) Flexion at approx.  $50^\circ$  [ $P_1 = P_2$ ] (c) Fully flexed at approx.  $110^\circ$  [ $P_1 = P_{MAX}$   $P_2 = P_{MIN}$ ]**

A control scheme was designed to force the pressures in each muscle follow the paths depicted in figure 5.12. This control scheme, figure 5.14, used bang-bang control instead of PWM as the means for controlling the pressure in each muscle with a cycle time of 7ms. The controller begins with a signal generator, which either increases in value or decreases in value depending on whether the user pressure button one,  $B_1$ , or button two,  $B_2$ . Button one is reserved for flexion of the elbow while button two is reserved for extension of the elbow. If the user presses button one to flex the elbow then the signal generator increases the pressure in increments of the ADC value of the on board potentiometer divided by 100. As a result, the potentiometer could be used to set the speed of flexion by increasing the pressure increments. If button two for extension is pressed then the signal generator sets the pressure at a max value and decreases this value with the same potentiometer value, which is divided by 100. The output of this signal generator is always signal conditioned for both pressure paths. For the  $P_1$  pressure path, the signal conditioner uses the same value of the signal generator

except that it forces the pressure to conform to equal no less than the minimum pressure and be no more than the maximum pressure. The  $P_2$  pressure path takes the signal generator output and subtracts this value from the maximum pressure value and then ensures that it is no greater or less than the maximum and minimum pressures respectively. The signal-conditioned outputs, which are interpreted as desired pressures, are then sent to the bang-bang portion of the controller that calculates the errors between these outputs and the actual pressures read in from the Motorola pressure sensors. The bang-bang controller for each muscle finally makes a decision on which valves to open and closed based on the sign of the error and if it is outside of a 3-PSI threshold.

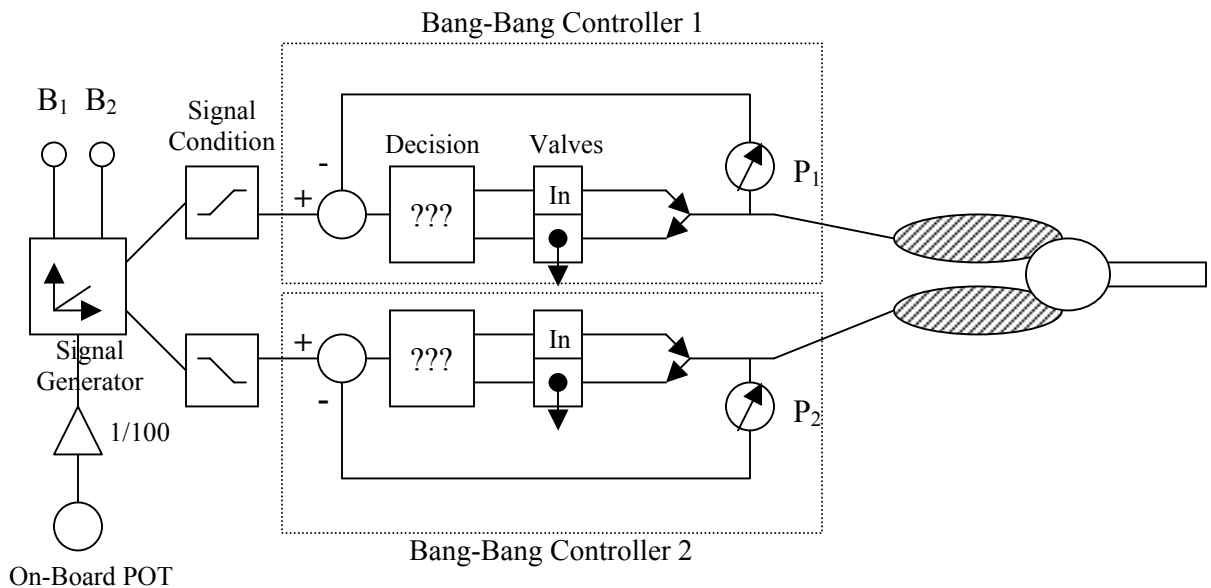


**Figure 5.14 Antagonistic Controller Schematic**

Values for  $P_{MAX}$  and  $P_{MIN}$  were 60 and 10 PSI respectively.  $P_{MIN}$  was set to 10 PSI instead of 0 PSI because the muscle was considered inflated or deflated at the 10 PSI mark that is indicated in the exhaust graphs in chapter 4. Besides, the time to exhaust the valve

from 10 PSI to zero results in a longer settling time according to figure 4.19. This minimum pressure also makes the movement of the muscles more stable for both flexion and extension because the tubing does not have to continue to break the 10 PSI maximum pressure barrier.  $T_{FE}$  was determined by the analog potentiometer and  $T_D$  depended on the time between the user pressing the flexion and extension buttons. Figure 5.15 shows the final results of pressing the flexion and extension buttons on the M32/83C board.

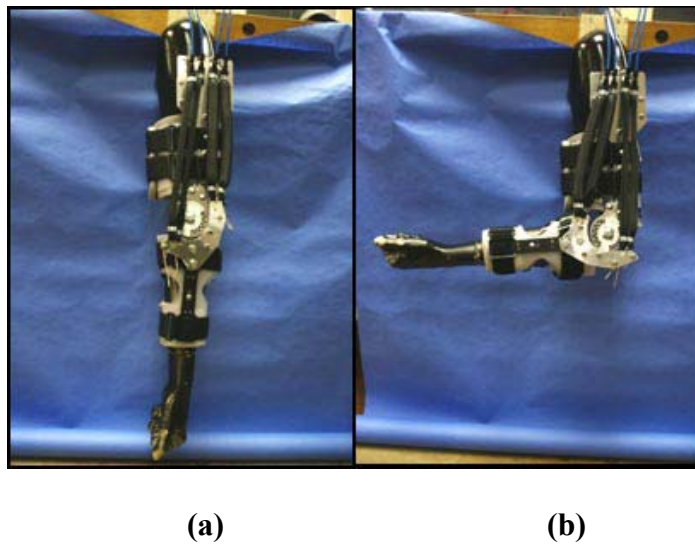


**Figure 5.15 Flexion and extension using control scheme (a) Extension (b) Flexion**

# Chapter 6. Conclusions and Future Research

## 6.1 Concluding Remarks

The pneumatic brace prototype for stroke rehabilitation demonstrates the capabilities of air muscles for achieving tasks that would normally require a large, external, expensive, dc-motor driven robot. Experimental results have shown that the pneumatic brace can both flex and extend a patient's elbow within an acceptable range and pace for rehabilitation. This prototype is worn just like the original elbow brace without any additional obstructions for the patient and maintains its lightweight characteristic attributed to the 11g air muscles. The \$2.70 air muscles are easy to make and are connected to the prototype by simply tying nylon rope through holes in the brace's aluminum sections. As a result, the muscles can be replaced easily and there is no inconvenience if one gets damaged.

The control scheme implemented on the MCU allows the patient to flex and extend their arm by simply pressing two buttons and adjusting a dial to increase the speed of flexion and extension. Since this device has position control capabilities and still maintains the fixed ROM capabilities of the original elbow brace this device may also be extended beyond stroke rehabilitation to other forms of therapy like sports injuries or to patients recovering from surgeries.

The design of this prototype will lead to the further research on developing the complete upper extremity stroke rehabilitation device and will hopefully become a reality in the near future to aid the overwhelming and increasing number of stroke sufferers.

## 6.2 Future Research

There are several possibilities for future research on this device. The main additions to this device are adding the actuation of the shoulder, developing a control scheme that responds to the patient's moves, and developing a virtual reality system for the patient to interface with.

Since this thesis focused mainly on developing a simple device using an existing elbow brace for actuation of the elbow and wrist, a more complex device including the motions of the shoulder deserves some attention. One suggestion is to use an existing vest for muscle attachment on the back and chest. Also, mentioned earlier in chapter 3, Bowden cables could be used for attaching the muscles on the shoulder to the back so that larger and longer muscles could be used.

Another important addition to this device is a control scheme that interacts with the patient. Since most controllers require position information to control each joint of a robotic device, carefully placed accelerometers on the device could be used to measure kinematics of the arm. One possible type of accelerometer is Analog Devices' ADXL311 accelerometer, which has several features that make it an excellent candidate for this device. For example, the accelerometer is tiny, lightweight, and cheap. Figure 6.1 shows the accelerometer for a size comparison to a dime.

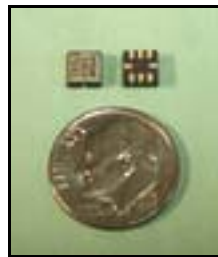


**Figure 6.1 Analog Devices ADXL311 Accelerometer**

Since the accelerometer signal conditions its two outputs, a simple circuit board like that shown in figure 6.2 can be easily mounted on the pneumatic device in an inconspicuous manor.

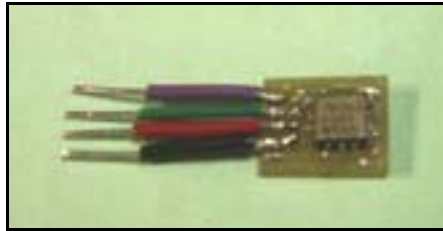


**Figure 6.2 ADXL311 Accelerometer with circuit developed in lab**

Another addition to the control scheme could be the use of EMG to measure the patient's muscle impulses. This will allow the device to know if the patient is trying to move but needs assistance. As a result, the device can kick in and assist the patient in reaching their goal.

Valve control could also be considered for a future improvement to the device. Currently there are two popular control methods for solenoid valves: Bang-Bang and PWM. The valves used in this thesis have slower response times of 10ms, however, other valves have response times of 1ms, which may improve the performance of both Bang-Bang and PWM. An example of such a valve is the Matrix 850 series. This valve has a speed-up configuration that allows for a 1ms response time. The only setback to faster valves is the size and cost. Since this thesis' aim is to develop a device that is inexpensive for stroke patients, only cheap solenoid valves were used.

Besides adding shoulder functionality and improved control of the device, a virtual environment could be developed to create fun and interactive games for the patient to play while using the rehabilitative device. One possible inexpensive virtual reality programming

environment is Sun's Java 3D. A simple example of a possible GUI using Java 3D was created and is shown in figure 6.3. It uses a standard GUI layout with a file menu, figure 6.4, for selecting an existing patient's profile or starting up a new patient's profile. The GUI also has an options menu, figure 6.5, for setting the individual patients preferences, viewing statistics to see if the patient has improved, and establishing a serial connection, figure 6.6, with the rehabilitative device. The most important feature of the GUI is the Java3D view where the patient can play games and select different games by choosing from the tree in the left hand column.

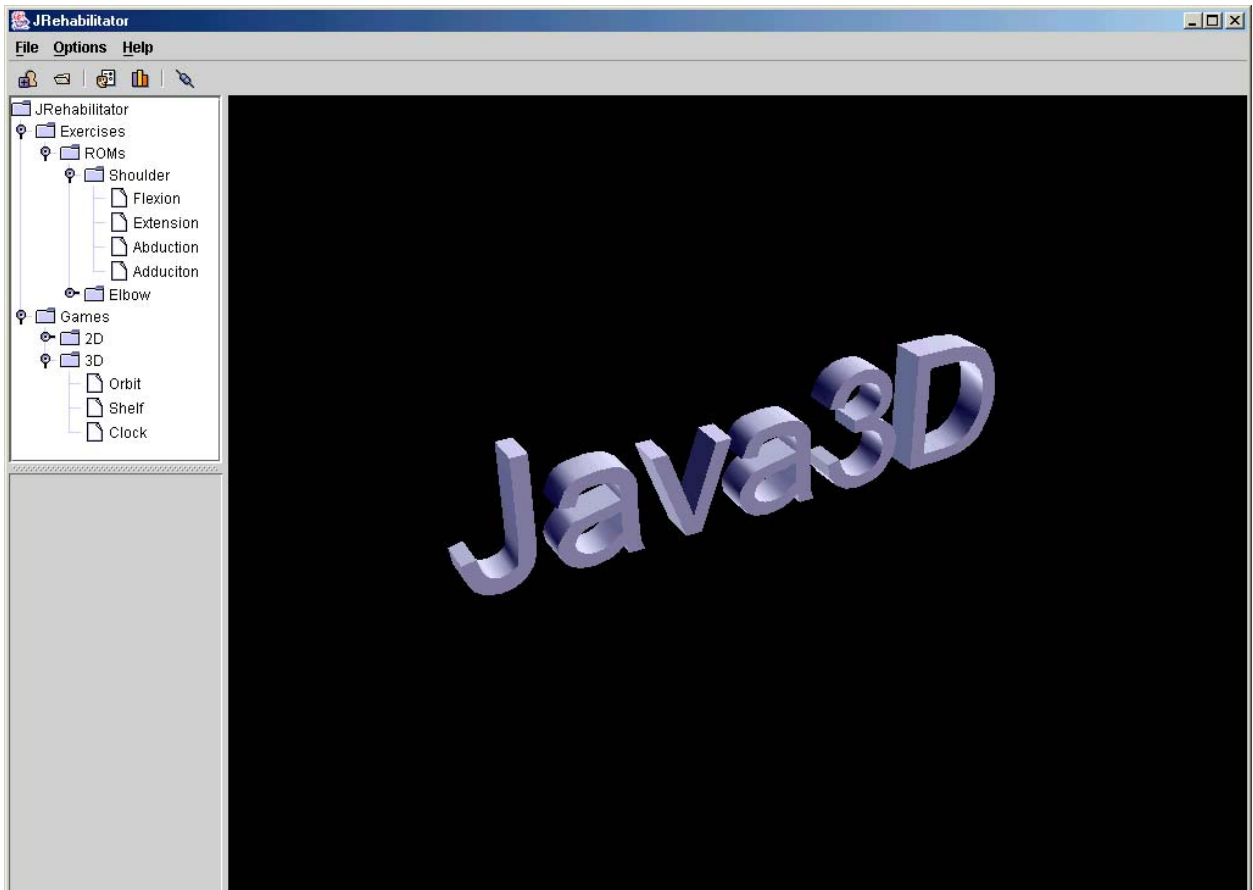


**Figure 6.3 JRehabilitator GUI using Java3D**

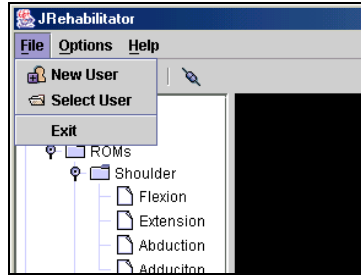


**Figure 6.4 File Menu**

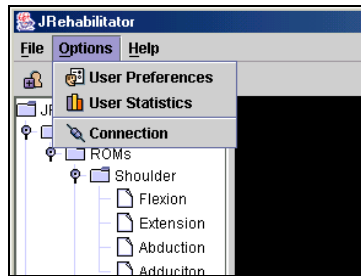


**Figure 6.5 Options Menu**

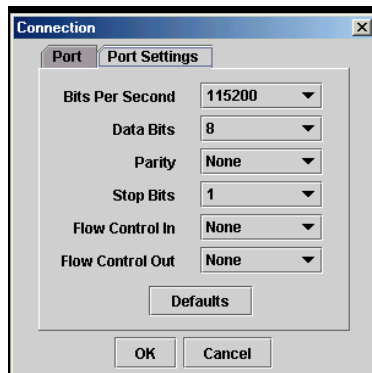


**Figure 6.6 Connection Dialog**

Finally, more research should be done to improve the performance and characteristics of the air muscles. The muscles in this thesis tended to explode more frequently than desired. The reason for these explosions was most likely due to the type silicone tubing used for the inner bladder. Also, the muscles only had contraction length percentages of only 76% (24%),



where as, real muscles have contractions closer to 50%. If the contraction ratio could be improved then shorter muscles could be placed on the device and reduce the need for adding extensions to accommodate longer muscles like the biceps and triceps used in this thesis. One suggestion is the use the pleated muscle idea mentioned in the literature review section on air muscles. Another suggestion is to use a material that acts more like a barrier for the braided sleeving instead of an elastic bladder. Robb Colbrunn suggests in his thesis to use a Mylar balloon material to act as the barrier.

## Chapter 7. References

Allin, S., Matsuoka, Y., Klatzky, R. (2002), 'Measuring Just Noticeable Differences For Haptic Force Feedback: Implications for Rehabilitation', Proceedings of the 10th Symposium On Haptic Interfaces For Virtual Environments. & Teleoperator Systems, 2002.

Bouzit, M., Popescu, G., Burdea, G., Boian, R. (2002), 'The Rutgers Master II-ND Force Feedback Glove', *Proceedings of IEEE VR 2002 Haptics Symposium*, Orlando FL, March 2002.

Burgar, C.G., Lum, P.S., Shor, P.C., Van der Loos, H.F.M. (Jan 9 2001), "Development of robots for rehabilitation therapy: The Palo Alto VA/Stanford experience", (VA Research and Development), Available: <http://www.vard.org/jour/00/37/6/burga376.htm> (Accessed: Aug. 29 2002).

Cerullo, L.J. (1986), *Stroke Rehabilitation*, Butterworth Publishing, Stoneham, MA.

Cham, Jorge. (1999), Jorge Cham's Qualifying Exam Technical Talk: "Control of a Linkage with Embedded Components", Available: [http://www-cdr.stanford.edu/biomimetics/documents/cham\\_qual/](http://www-cdr.stanford.edu/biomimetics/documents/cham_qual/) (Accessed: 2003, January 16).

Colbrunn, R. (2000), "Design and Control of a Robotic Leg with Braided Pneumatic Actuators, M.S. Thesis, Case Western Reserve University, Cleveland OH.

Daerden, F., Lefeber, D., Verrelst, B., & Van Ham, R. (2001a), 'Pleated pneumatic artificial muscles: actuators for automation and robotics', *2001 IEEE/ASME International Conference on Advanced Intelligent Mechatronics*, July 8 – 12 2001, vol. 2, pp. 738 – 43.

Daerden, F., Lefeber, D., Verrelst, B., & Van Ham, R. (2001b), 'Pleated pneumatic artificial muscles: compliant robotic actuators', *Proceedings of the 2001 IEEE/RSJ International Conference on Intelligent Robots and System*, Oct. 29- Nov 3, vol. 4, pp. 1958 – 63.

Eskiizmirli, S., Tondu, B., Darlot, C. (2001), 'Motor control of a limb segment actuated by artificial muscles', *Proceedings of the 23rd Annual International Conference of the IEEE Engineering in Medicine and Biology Society*, Oct. 25 – 28 2001, vol. 1, pp. 865 – 8.

Fairhurst, M.C., Smith, L., & Mitchell, J. (1995), "Automated image analysis in visuo-motor testing for the specification of an integrated evaluative and therapy support tool for rehabilitation", *IEEE Transactions on Rehabilitation Engineering*, vol. 3, no. 1, March 1995, pp. 103 – 11.

Ferris, D.P., Czerniecki, J.M., & Hannaford, B. (2001), 'An ankle-foot orthosis powered by artificial muscles', *Proceedings of 25th Annual Meeting of the American Society of Biomechanics*, August 8-11 2001, San Diego, CA.

Gehring, D., Walsh, A.E. (2002), *Java 3D: API Jump-Start*, Prentice Hall PTR, Upper Saddle River, NJ.

Hawkins, P., Smith, J., Alcock, S., Topping, M., Harwin, W., Loureiro, R., Amirabdollahian, F., Brooker, J., Coote, S., Stokes, E., Johnson, G., Mak, P., Collin, C., & Driessen, B. (2002) GENTLE/S project: Design and ergonomics of a stroke rehabilitation system, 1<sup>st</sup> Cambridge Workshop on Universal Access and Assistive Technology March 25-27 2002, pp. 85-90. Available: <http://rehab-www.eng.cam.ac.uk/cwuaat/02/15.pdf> (Accessed: April 1 2003).

Jack, D., Boian, R., Merians, A., Tremaine, M., Burdea, G., Adamovich, S. Recce, M., Poizner, H. (2001), "Virtual Reality-Enhanced Stroke Rehabilitation", *IEEE Transactions on Neural Systems and Rehabilitation Engineering*, vol. 9, no. 3, Sept. 2001, pp. 308-18.

Krebs, H.I., Hogan, N., Aisen, M.L., & Volpe, B.T. (1997), 'Technique to investigate ipsilateral functional activation in motor task', *18th Annual International Conference of the IEEE Engineering in Medicine and Biology Society*, 1996, vol. 5, pp. 2246 –7.

Krebs, H.I., Hogan, N., Aisen, M.L., & Volpe, B.T. (1998), "Robot-aided neurorehabilitation", *IEEE Transactions on Rehabilitation Engineering*, vol. 6 no. 1, March 1998, pp. 75 – 87.

Krebs, H.I., Hogan, N., Charnnarong, J., Srikrishna, P., & Sharon, A. (1992), 'MIT-MANUS: a workstation for manual therapy and training', *IEEE International Workshop on Robot and Human Communication*, June 12 1992, pp. 161 – 5.

Krebs, H.I., Buerger, S.P., & Hogan, N. (2001a), 'Characterization and control of a screw-driven robot for neurorehabilitation', *Proceedings of the 2001 IEEE International Conference on Control Applications*, Sept. 5-7 2001, pp. 388 – 94.

Krebs, H.I., Williams, D.J., & Hogan, N. (2001b), 'A robot for wrist rehabilitation' *Proceedings of the 23rd Annual International Conference of the IEEE Engineering in Medicine and Biology Society*, Oct 25-28 2001, vol. 2, pp. 1336 – 9.

Krebs, H.I., Volpe, B.T., Palazzolo, J., Fasofi, S., Ferraro, M., Edelstein, L., & Hogan, N. (2001c), 'Disturbances of higher level neural control - robotic applications in stroke', *Proceedings of the 23rd Annual International Conference of the IEEE Engineering in Medicine and Biology Society*, Oct. 25-28 2001, vol. 4, pp. 4069 – 74.

Mak, P., Gomes, G.T., Johnson, G.R. (2002), 'A robotic approach to neuro-rehabilitation-interpretation of biomechanical data', *Seventh International Symposium on the 3-D Analysis of Human Movement*, International Society of Biomechanics, Newcastle upon Tyne, England, July 10-12 2002.

Massie, T.H., Salisbury, J.K. (1994), 'The PHANTOM Haptic Interface: A Device for Probing Virtual Objects', *Proceedings of the ASME Winter Annual Meeting, Symposium on Haptic Interfaces for Virtual Environment and Teleoperator Systems*, Chicago, IL, Nov. 1994.

Mitsuda, T., Kuge, S., Wakabayashi, M., Kawamura, S. (2002), 'Wearable haptic display by the use of a Particle Mechanical Constraint', *Proceedings of the 10th Symposium On Haptic Interfaces For Virtual Environments. & Teleoperator Systems*, 2002.

Noritsugu, T. & Tanaka, T. (1997), "Application of rubber artificial muscle manipulator as a rehabilitation robot", *IEEE/ASME Transactions On Mechatronics*, vol. 2, no. 4, Dec. 1997, pp. 259 – 67.

Noritsugu, T., Tsuji, Y., & Ito, K. (1999), 'Improvement of control performance of pneumatic rubber artificial muscle manipulator by using electroreological fluid damper', *IEEE International Conference on Systems, Man, and Cybernetics*, 1999. vol. 4, pp. 788 – 93.

Pedretti, L.W., (1985), *Occupational Therapy: Practice Skills for Physical Dysfunction*, 2<sup>nd</sup> ed., C.V. Mosby Co., St. Louis, Missouri.

Pernalte, N., Yu, W., Dubey, R., Moreno, W. (2002) 'Development of a Robotic Haptic Interface to Assist the Performance of Vocational Tasks by People with Disabilities', *Proceedings of the 2002 IEEE International Conference on Robotics & Automation*, Washington, DC, May 2002.

Reddy, M.P, Reddy, V. "Stroke Rehabilitation", *American Family Physician*, vol. 55, no. 5, pp. 1742 – 8.

Reinkensmeyer, D.J., Lum, P.S., Winters, J. (2002a), *Emerging Technologies for Improving Access to Movement Therapy Following Neurologic Injury*, Emerging and Accessible Telecommunications, Information and Healthcare Technologies: Engineering Challenges in Enabling Universal Access, IEEE Press.

Reinkensmeyer D.J., (2002b), Rehabilitators, in: Kutz, M., *Biomedical Engineer's Handbook*, McGraw-Hill.

Reinkensmeyer, D.J., Kahn, L.E., Averbuch, M., & Rymer, W.Z.(2001a), ‘Comparison of robot-assisted reaching to free reaching in promoting recovery from chronic stroke.’, *Proceedings 7th International Conference on Rehabilitation Robotics*, April 25-27 2001, IOS Press, Amsterdam, pp. 39-44.

Reinkensmeyer, D.J., Kahn, L.E., Zyngman, M.L., & Rymer, W.Z.(2001b), ‘Effect of robot-assisted and unassisted exercise on functional reaching in chronic hemiparesis’. *Proceedings of the 23rd Annual International Conference of the IEEE Engineering in Medicine and Biology Society*, 2001, vol. 2, pp. 1344 – 7.

Reinkensmeyer, D.J., Pang, C., Nessler, J.A., & Painter, C.C. (2001c), ‘Java Therapy: Web-based robotic rehabilitation. Integration of Assistive Technology in the Information Age’, *Proceedings 7th International Conference on Rehabilitation Robotics*, April 25-27, IOS Press, Amsterdam, pp. 66-71.

Reinkensmeyer, D.J., Scheidt, R.A., Conditt, M.A., Rymer, W.Z., & Mussa-Ivaldi, F.A. (2000), “Persistence of motor adaptation during constrained, multi-joint arm movements”, *Journal of Neurophysiology*, April 28 2000, pp. 853 - 62.

Reinkensmeyer, D.J., Dewald, J.P.A., & Rymer, W.Z. (1999a), “Guidance-based quantification of arm impairment following brain injury: a pilot study”, *IEEE Transactions on Rehabilitation Engineering*, vol. 7, no. 1, March 1999, pp. 1 – 11.

Reinkensmeyer, D.J., Schmit, B.D., & Rymer, W.Z. (1999b), “Assessment of active and passive restraint during guided reaching after chronic brain injury”, *Annals of Biomedical Engineering*, vol. 27, no. 6, pp. 805- 14.

Reinkensmeyer, D.J. & Rymer, W.Z. (1997), ‘Using a mechanical guide to evaluate and treat workspace deficits after brain injury’, *Proceedings of the 19th Annual International Conference of the IEEE Engineering in Medicine and Biology Society*, Oct. 30 – Nov. 2 1997, vol. 5, pp. 1962 – 65.

Reinkensmeyer, D.J., Lum, P.S., & Lehman, S.L. (1995), ‘The bimanual lifting rehabilitator: an adaptive machine for therapy of stroke patients’, *IEEE Transactions on Rehabilitation Engineering*, vol. 3, no. 2, June 1995, pp. 166 –74.

Reinkensmeyer, D.J., Lum, P.S., & Lehman, S.L. (1993), “Robotic assist devices for bimanual physical therapy: preliminary experiments”, *IEEE Transactions on Rehabilitation Engineering*, vol. 1, no. 3, Sept. 1993, pp. 185 – 91.

Slaughter, A. (2002, June 26 – last update), “Ram Dass shares his battle against stroke”, (USA Today), Available: <http://www.usatoday.com/news/healthscience/health/2002-06-25-ramdass.htm> (Accessed: Sept. 4 2002).

van der Linde, R.Q. (1999), “Design, analysis, and control of a low power joint for walking robots, by phasic activation of McKibben muscles”, *IEEE Transactions on Robotics and Automation*, vol. 15. no. 4, Aug. 1999, pp. 599 –604.

van Varseveld, R.B., Bone, G.M. (1997), ‘Accurate Position Control of a Pneumatic Actuator Using On/Off Solenoid Valves’, *Proceedings of the 1997 International Conference on Robotics and Automation*, April. 1997, Albuquerque, New Mexico, pp. 1196 - 1201.

Webb, Y., Pethybridge, J., Baker, R., (2002), “Stroke rehabilitation: quality of care and levels of staff training”, *British Journal of Therapy & Rehabilitation*, vol. 9, no. 5, May 2002, pp. 171 – 5.

Shadow Robot Company: Air Muscles (2002, Sept 10 – last update), (Shadow Robot Company), Available: <http://www.shadow.org.uk/products/airmuscles.shtml> (Accessed: Sept. 18 2002).

“Biologically Based Robotics: McKibben Artificial Muscles Construction”. (University of Washington BioRobotics Laboratory), Available: [http://brl.ee.washington.edu/Research\\_Past/Biologically\\_Based/Device\\_01\\_McKibben/Mckibben\\_Costruction.html](http://brl.ee.washington.edu/Research_Past/Biologically_Based/Device_01_McKibben/Mckibben_Costruction.html) (Accessed: April 1 2003).

“Driver Simulation Environment for Arm Therapy”, (VA Palo Alto Rehabilitation R&D Center), Available: <http://guide.stanford.edu/Projects/seat/seat.html> (Accessed: 2002, September 18).

“Immersion Corporation - 3D Technologies Hardware” (2002), (Immersion Corporation), Available: <http://www.immersion.com/products/3d/interaction/hardware.shtml> (Accessed: Sept. 18 2002).

*Post-Stroke Rehabilitation*, (2000), U.S. Dept. Health and Human Services, Public Health Service, National Institutes of Health, Bethesda, Maryland.

“Stroke Rehabilitation Information”, (2001, July 1 – last update), (National Institute of Neurological Disorders and Stroke), Available: [http://www.ninds.nih.gov/health\\_and\\_medical/pubs/stroke\\_rehabilitation.htm](http://www.ninds.nih.gov/health_and_medical/pubs/stroke_rehabilitation.htm) (Accessed: Aug. 29 2002).

## **Appendix**

# Chapter 8. Appendices

## 8.1 Test Platform Construction

### 8.1.1 Required Materials

The materials required to make this platform are the following:

- Six 1" x 4" x 18" wood
- Two 14 1/2" wood
- One 1" x 4" x 4 1/2" wood
- One 3/8" x 2" x 4 1/2" wood
- Two 1/4" Eye bolts with 1/4" nut and two washers
- Screws
- Pulley wheel with 3/8" diameter hole
- 5 1/2" length 3/8" diameter bolt with 3/8" nut
- 1" length 3/8" diameter nut
- Nylon rope
- Two 1/4" spring links

### 8.1.2 Test Platform Design

The test platform was built from 1" x 4" wood purchased at a local hardware store. It consists of four 18" legs with two 14 1/2" feet and a body that is made from two 18" boards connected by a 4 1/2" board.

#### **Building the Body:**



1. Connect the 4 ½" back to the two 18" pieces of wood using two flat head Phillips 8 x 1 ½" wood screws on each side. The dashed circles in figure 8.1 b show the general placement of these screws.
2. Drill ¼" even spaced holes in the center of the back piece for the eyebolts, figure 8.1 b, and install the eyebolts from the inside with a washer on both sides of the wood and a ¼" nut on the outside.
3. Connect the 3/8" x 2" x 4 ½" piece of wood to the bottom of the body in the center like in figure 8.1 c using two flat head Phillips 8 x 1 ¼" screws.

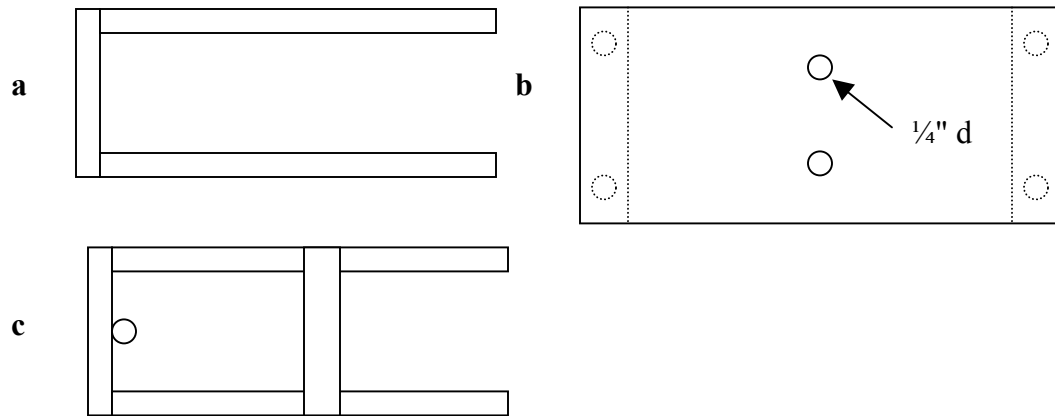


**Figure 8.1 Building the platform body (a) top view connecting the sides to the back (b) back view showing screw placement and eyebolt hole position (c) bottom view middle support and eyebolt installed**

#### **Adding the Legs:**

4. Connect the four 18" pieces of wood to the body so that they are flush with the corners and top of the body like in figure 8.2 a using four flat head Phillips 8 x 1 ¼" screws for each leg.

- Connect the two 14 1/2" pieces of wood to the legs on the front and back sections like in figure 8.2 b and c using the same type of screws.

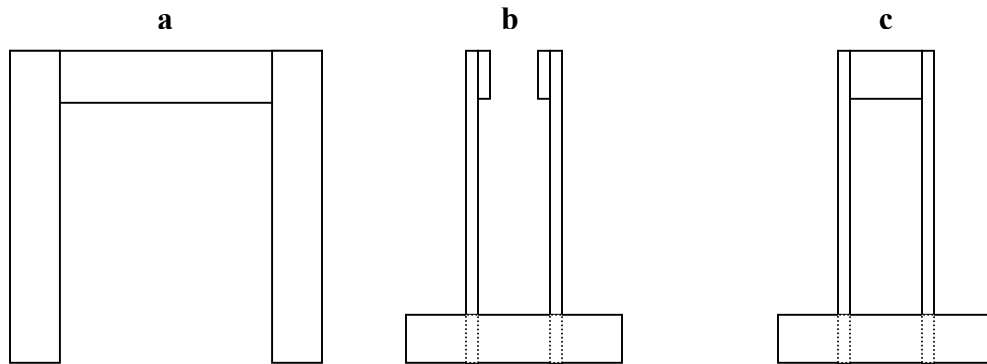


**Figure 8.2 Placing legs on body (a) side view (b) front view with feet (c) back view with feet**

**Making the pulley joint:**

- Cut out a 2 1/4" x 1 1/4" x 1/2" aluminum block.
- Drill a 3/8" hole in the center of the block like in figure 8.3 a.

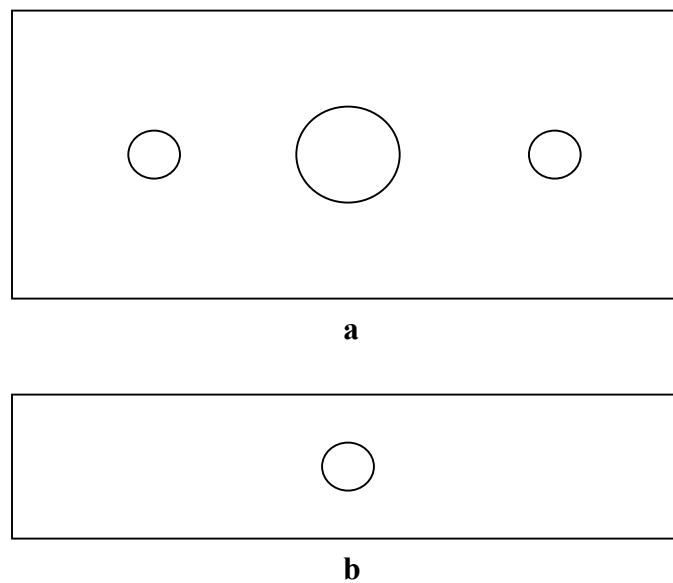


**Figure 8.3 aluminum block (a) side view (b) top/bottom view**

8. Drill two smaller holes on opposite sides of the center hole. See figure 8.3 b.
9. Drill two holes in the top and bottom centers and tap the holes to thread them.
10. Line the block up with the pulley wheel like in figure 8.4 and drill holes through the pulley wheel on opposite sides of the center hole like in step 8.
11. Drill a small hole through the top and bottom lip of the pulley wheel slightly above the bottom of the groove.

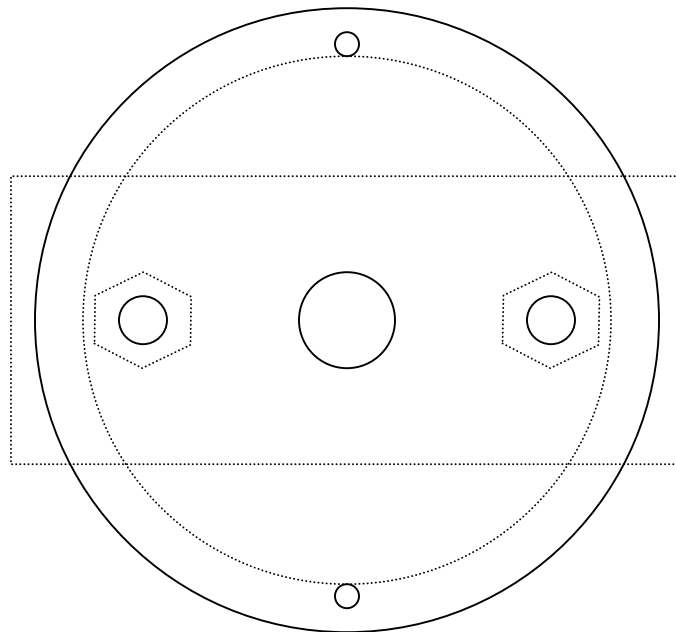


**Figure 8.4 Pulley wheel with holes drilled and aluminum block outline**

12. Drill a 3/8" hole in the body for the 5 1/2 " length 3/8" diameter bolt about 3/4" away from the side of the front legs and in the center of the body's sides. See figure 8.5.

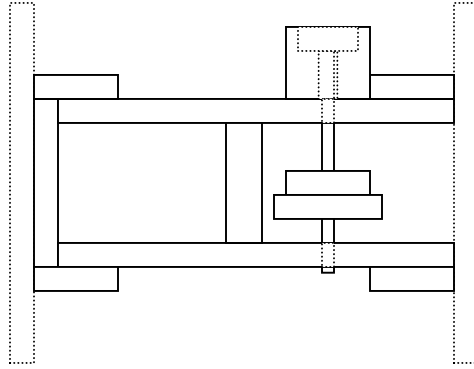


**Figure 8.5 Top view of platform**

**Connecting the Potentiometer:**

13. Make a circular piece of  $\frac{1}{2}$ " length hard wood to screw into half of the 1" length  $\frac{3}{8}$ " diameter nut so that it is extremely tight (figure 8.6). Just find a dowel rod that fits the whole and screw it in.
14. Once the wood is screwed in about half way into the nut, cut off the end of the dowel rod sticking out.
15. Once the wood is in place, drill a small hole about a fraction smaller than the shaft size of the potentiometer and cram the shaft of the potentiometer in the hole.

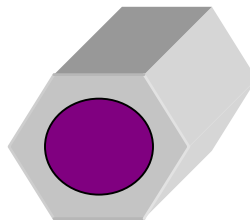
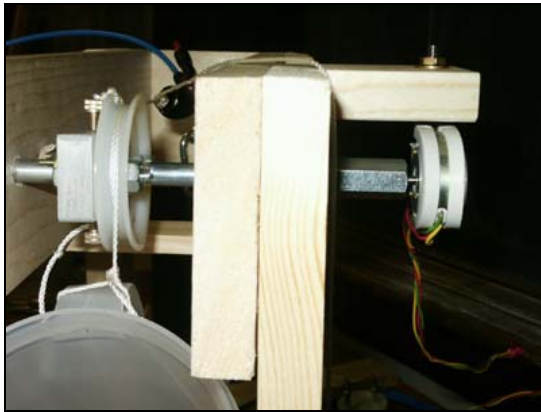


**Figure 8.6 1" length  $\frac{3}{8}$ " diameter hex nut with hard wood screwed into the nut**

16. Slide the 5 ½" length 3/8" diameter bolt through the body's 3/8" holes and slide the aluminum block and pulley onto the bolt like in figure 8.7 a.
17. Bolt the pulley wheel and block together using the outside holes.
18. Screw in two stops in the top and bottom piece of aluminum to hold the wheel and block tight on the bolt. See figure 8.7.



**a**



**b**

**Figure 8.7 Assembling the pulley (a) front view showing pulley connected to aluminum block and steel bolt (b) top view of platform showing the stops screwed into the aluminum block**

19. Screw the 3/8" regular hex nut onto the bolt so that the bolt can continue to rotate freely
20. Next, screw the 1" length 3/8" diameter nut with potentiometer on the end of the bolt so that it is tight against the other nut.
21. Fix a piece of 1 x 4 wood to hold the potentiometer in place and screw it in the body from the inside. See figure 8.7 for reference.

22. Drill a hole in the wood for a small bolt to slide through wood and the rubber padded clamp end to hold the potentiometer in place.
23. Screw the 1 x 4 piece of wood to side of the body so that it is flush with the top and next to the leg like in figure 8.7 b.

**Wooden arm:**

24. Cut a 14" piece of 1" x 3" wood out.
25. Drill holes through the wood to match up with the holes in the aluminum block like in figure 8.8.

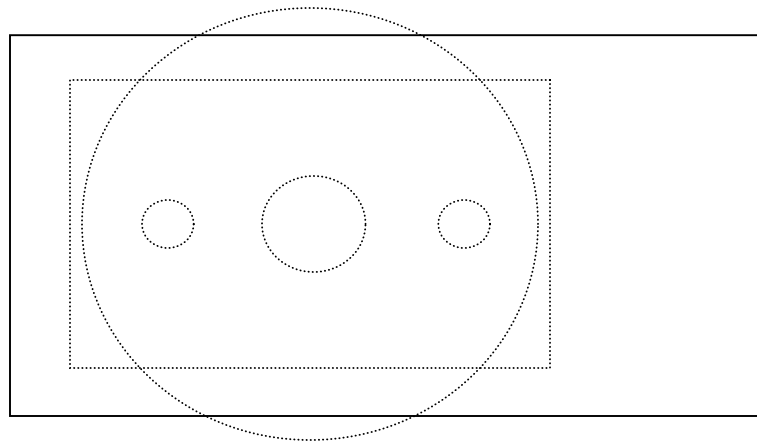


**Figure 8.8 Wooden armholes with aluminum block and pulley wheel outlined**

**Muscle Attachment:**

26. Slide spring link around the air muscle loop with the inlet end and connect the link to top the eyebolt like in figure 8.9 a.
27. Tie nylon rope around the other loop and wrap the other end clockwise around the pulley once or twice.

28. Tie the excess end of rope that is wrapped around the pulley through the top hole made in step 11. See figure 8.9 b.
29. Repeat steps 25 – 27 for the bottom antagonist muscle except wrap the rope counterclockwise around the pulley wheel and tie the excess end through bottom hole on the pulley wheel that was made in step 11.

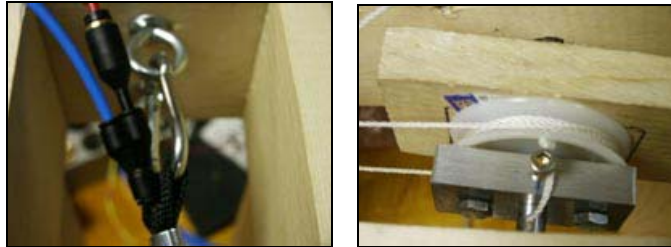


**Figure 8.9 Attaching air muscles to device (a) rear muscle attachment to spring link (b) muscle attachment to pulley wheel**

## 8.2 Controller and Experiment code

### 8.2.1 Main.h and Main.c

#### 8.2.1.1 Main.h

```
// Main.h
// author Carey Merritt

void main(void);
void buttons_init(void);
void bang_flexion(void);
void bang(void);
void sampleLength(void);
void samplePressure(void);
void sampleLeakage(void);
void sampleExhaust(void);
void sampleFlow(void);
void wait(unsigned long t);
```

#### 8.2.1.2 Main.c

```
// main.c
// author Carey Merritt
```

```

#include "sfr83v100.h"      /* SFR register definition */
#include "main.h"          /* main.c definition */
#include "timer.h"
#include "ad.h"
#include "board.h"
#include "serial1.h"
#include <stdio.h>

#define v1IN p12_0        // inlet valve for muscle 1
#define v1EX p12_1        // exhaust valve for muscle 1
#define v2IN p12_2        // inlet valve for muscle 2
#define v2EX p12_3        // exhaust valve for muscle 2

volatile unsigned long system_counter = 0;
volatile unsigned int ad0_value = 0, ad4_value = 0, ad6_value = 0;
volatile unsigned int ad7_value = 0;

volatile unsigned char button_1;    // Button 1 pressed flag
volatile unsigned char button_2;    // Button 2 pressed flag
volatile unsigned char button_3;    // Button 3 pressed flag

unsigned const char clear[] = "                \0";
unsigned const char UART_NOFLICKER1[] = {'\r', '□', '[', '1', 'A', 0};
unsigned const char UART_NOFLICKER2[] = {'\r', '□', '[', '2', 'A', 0};

unsigned int pressure[6000];
char out[80];
unsigned int test = 0;

void main(){

    float degreeF;
    int degreeI;
    float m = 0.342787f;    // slope of rotary pot degrees per ad_value

    // for rotary pot there is a dead zone from 335 - 360 degrees so the
    // rotary pot should be offset from zero to calibrate. The degree offset
    // from zero should be subtracted from the calculation to shift the value
    // back. This way we can avoid the deadzone.

    // Set BCLOCK to divide by 1 (Full Speed) from the default divide by 8
    prc0 = 1;    // Unlock the System Clock Control Register
    mcd = 0x12; // Set the divide ratio to 1.

    prc0 = 0;    // Lock the System Clock Control Register

    // Start the 32Khz crystal sub clock
    prc0 = 1;    // Unlock the System Clock Control Register
    cm04 = 1;    // Start the 32KHz crystal
    prc0 = 0;    // Lock the System Clock Control Register

    ta0_init();    // Initialize Timer TA0 (Tick Clock)
    buttons_init();
    ad_init();    // Initialize the A/D Converter
    init_uart();

    // initialize on board LED's and set data direction for output
    pd8_0 = 1;    // set green led4 for output
    pd7_4 = 1;    // set up port P7_4 as output (Yellow LED/ LED)
    pd7_2 = 1;    // set red led for output
    LED2 = 0;

```



```

LED3 = 0;
LED4 = 0;

// set data direction for pins to control pneumatic solenoid valves
pd12_0 = 1;    // set data direction register for pin12_0 output
pd12_1 = 1;    // set data direction register for pin12_1 output
pd12_2 = 1;    // set data direction register for pin12_2 output
pd12_3 = 1;    // set data direction register for pin12_3 output
v1IN  = 0;    // A38 on 150 DIN (P120/OUTC30)
v1EX  = 0;    // B38 on 150 DIN (P121/OUTC31)
v2IN  = 0;    // C38 on 150 DIN (P122/OUTC32)
v2EX  = 0;    // A39 on 150 DIN (P123/OUTC32)

// The Pressure sensor 1 is on AN6/P106 and A34 on 150 DIN
// The Pressure sensor 2 for the triceps is located on AN4/P104
// The Rotational sensor is on AN7/P107 and B34 on 150 DIN

while(1){

    // button handler
    LED2 = !p8_2;
    v1IN = !p8_2;

    LED3 = !p8_3;
    v1EX = !p8_3;

    //LED4 = !p8_4;
    //v2IN = !p8_4;

    v2EX = !p9_7;

    // if button 3 pressed then run test routine
    if(!p8_4){
        //bang();
        bang_flexion();
        //flexion();
        //bicepTest();
        //sampleExhaust();
        //samplePressurePWM();
        //samplePressure();
        //sampleLeakage();
        //sampleFlow();
        //generateSquareWave();
        //sampleLength();

        // output length and pressure
        /*
        if(test == 0){
            sprintf(out,"%d %d \r\n",ad7_value,ad6_value);
            writeString(out);
            test = 1;
        }
        */

        //bicepTest();

    }
    else {
        test = 0;
    }
}

```

```

        //writeString(UART_NOFLICKER1);

        //pressure = ((float)ad6_value - 40.96f)/9.0779f;
        //if(pressure < 0.0f)
        //    pressure == 0.0f;
        //sprintf(out, "%d %d\r\n",ad4_value,ad6_value);
        //writeString(out);
        //bang();
        wait(101);

        //display_ad(0,ad6_value,"AD6=\0");    // display pressure
        //display_ad(0,ad0_value,"AD0=\0");
        //display_ad(64,ad7_value,"AD7=\0");    // display angle
    }
}

// bang_flexion is the main control algorithm presented in the thesis
void bang_flexion(){
    int error;
    int pmax = 585;           // maximum of 60 psi converted to adc
    int pmin = 91;          // maximum of 10 psi converted to adc
    int pldesired, p2desired;
    int pinc = 2;
    int desired = 40;
    unsigned char b1toggle = 0;
    unsigned char b2toggle = 0;

    // while button 4 has not been pressed
    while(p9_7){
        // toggle between flexion and extension modes based on
        // button presses on button 1 and 2
        if(!p8_2){
            if(!b1toggle){
                LED2 = 1;
                LED3 = 0;
                b1toggle = 1;
                b2toggle = 0;
                desired = 40;
            }
        }
        else if(!p8_3){
            if(!b2toggle){
                LED2 = 0;
                LED3 = 1;
                b1toggle = 0;
                b2toggle = 1;
                desired = pmax;
            }
        }
    }
    pinc = ad0_value/100;    // set increment based on on-board pot value

    // signal generator based on button 1 or 2
    if(b1toggle)
        desired = desired + pinc;
    else if(b2toggle)
        desired = desired - pinc;

        // signal conditioner to make sure desired is less
        // than max psi and greater than min psi
    if(desired > pmax){

```

```

        desired = pmax;
        pldesired = pmax;
        p2desired = pmin;
    }
    else if(desired < pmin){
        desired = pmin;
        pldesired = pmin;
        p2desired = pmax;
    }
    else {
        pldesired = desired;
        p2desired = pmax - desired;
        if(p2desired < pmin)
            p2desired = pmin;
    }

    // calculate the error for the bicep
    error = pldesired - (int)ad6_value;

    // use the error to decide which valves to open
    // and allow for a 3 PSI threshold
    if(error < -30){
        v1IN = 0;
        v1EX = 1;
    }
    else if(error > 30){
        v1IN = 1;
        v1EX = 0;
    }
    else {
        v1IN = 0;
        v1EX = 0;
    }

    // calculate the error for the tricep
    error = p2desired - (int)ad4_value;

    // use the error to decide which valves to open
    // and allow for a 3 PSI threshold
    if(error < -30){
        v2IN = 0;
        v2EX = 1;
    }
    else if(error > 30){
        v2IN = 1;
        v2EX = 0;
    }
    else {
        v2IN = 0;
        v2EX = 0;
    }
    wait(71);
}

// bang() is a similar control algorithm to bang_flexion
// that converts the angle of the potentiometer to a
// desired pressure for the bicep.
void bang(void){
    int error;
    int desired;

```

```

int pmax = 585;          // maximum of 60 psi converted to adc
int pmin = 91;          // maximum of 10 psi converted to adc
int pldesired, p2desired;

while(1){
    desired = ad0_value + 40;          // set desired to pot value plus 40
                                        // (0 PSI) to make sure that the value
                                        // is a pressure value
    // make sure angle is less than max psi
    if(desired > pmax){
        pldesired = pmax;
        p2desired = pmin;
    }
    else if(desired < pmin){
        pldesired = pmin;
        p2desired = pmax;
    }
    else {
        pldesired = desired;
        p2desired = pmax - desired;
        if(p2desired < pmin)
            p2desired = pmin;
    }

    error = pldesired - (int)ad6_value;

    // use the error to decide which valves to open
    // and allow for a 3 PSI threshold
    if(error < -30){
        v1IN = 0;
        v1EX = 1;
    }
    else if(error > 30){
        v1IN = 1;
        v1EX = 0;
    }
    else {
        v1IN = 0;
        v1EX = 0;
    }

    error = p2desired - (int)ad4_value;

    // use the error to decide which valves to open
    // and allow for a 3 PSI threshold
    if(error < -30){
        v2IN = 0;
        v2EX = 1;
    }
    else if(error > 30){
        v2IN = 1;
        v2EX = 0;
    }
    else {
        v2IN = 0;
        v2EX = 0;
    }

    wait(71);
}

```

```

}

// waits for a time t in ms
void wait(unsigned long t){
    unsigned long waitTime = system_counter + t;
    while(waitTime > system_counter);
}

// sample length for 6 seconds
void sampleLength(void){
    int i;
    unsigned long waitTime;
    system_counter = 0;           // reset system counter

    for(i = 0; i < 6000; i++){
        pressure[i] = ad7_value; // sample angle
        // wait 1ms
        wait(11);
    }

    // output to uart
    for(i = 0; i < 6000; i++){
        sprintf(out, "%d %d \r\n",i,pressure[i]);
        writeString(out);
    }
}

// sample pressure from 0 to max PSI when opening the valve
void samplePressure(void){
    int i;
    unsigned long waitTime;
    system_counter = 0;           // reset system counter
    v1IN = 1;
    for(i = 0; i < 2000; i++){
        pressure[i] = ad6_value; // sample angle
        // wait 1ms
        wait(11);
    }

    v1IN = 0;
    v1EX = 1; // exhaust valve
    wait(20001); // wait 2 seconds
    v1EX = 0; // close exhaust valve

    // output to uart
    for(i = 0; i < 2000; i++){
        sprintf(out, "%d %d \r\n",i,pressure[i]);
        writeString(out);
    }
}

// sample pressure after filling up the muscle with air and closing the valve
void sampleLeakage(void){
    int i;
    unsigned long waitTime;
    system_counter = 0;           // reset system counter
    v1IN = 1;
    wait(10001); // open valve and wait for 1s for it to fill up
}

```

```

v1IN = 0; // turn off valve and measure leakage - output every 1/2 (500ms) sec

for(i = 0; i < 240; i++){ // (60*2)*2 -> 2 mins of half second samples
    // output to uart
    sprintf(out, "%d \r\n",ad6_value);
    writeString(out);
    wait(5001); // wait half a second
}

v1EX = 1;
wait(15001); // wait 1.5 seconds for the air muscle to exhaust
v1EX = 0;

}

// sample pressure from a max PSI after filling up the muscle with
// air and exhausting the muscle
void sampleExhaust(void){
    int i;
    unsigned long waitTime;
    system_counter = 0; // reset system counter
    v1IN = 1;
    wait(30001); // open valve and wait for 1s for it to fill up
    v1IN = 0; // turn off valve and measure leakage - output every 1/2 (500ms) sec
    wait(51);
    v1EX = 1;
    for(i = 0; i < 6000; i++){
        pressure[i] = ad6_value;
        // wait 1ms
        wait(11);
    }
    v1EX = 0;

    // output to uart
    for(i = 0; i < 6000; i++){
        sprintf(out, "%d %d \r\n",i,pressure[i]);
        writeString(out);
    }
}

// samples the flow state when both valves are open
// measurements begin after the muscle is filled with air
void sampleFlow(void){
    int i;
    unsigned long waitTime;
    system_counter = 0; // reset system counter
    v1IN = 1;
    wait(20001); // open valve and wait for 1s for it to fill up
    v1EX = 1; // turn on exhaust valve for flow state and measure pressure
    for(i = 0; i < 1500; i++){
        pressure[i] = ad6_value;
        // wait 1ms
        wait(11);
    }
    v1IN = 0;
    v1EX = 0;

    // output to uart
    for(i = 0; i < 1500; i++){

```

```

        sprintf(out, "%d %d \r\n", i, pressure[i]);
        writeString(out);
    }
}

// initializes the 4 on board buttons
void buttons_init(void)
{
    asm("FCLR I"); // Disable all interrupts

    pu24 = 1;      // Turn on the pullups for ports 8_0 through 8_3
    pu25 = 0;      // Turn on the pullups for ports 8_4, 8_6 and 8_7
    pd8_2 = 0;     // Set port 8_2 (button 0) to an input
    pd8_3 = 0;     // Set port 8_3 (button 1) to an input
    pd8_4 = 0;     // Set port 8_4 (button 2) to an input
    int0ic = 0x03; // Set button 0's interrupt level to 3
    int1ic = 0x03; // Set button 1's interrupt level to 3
    int2ic = 0x03; // Set button 2's interrupt level to 3

    // Set the initial values of the button flags and debounce timers
    button_1 = 0;
    button_2 = 0;
    button_3 = 0;

    asm("FSET I"); // Enable all interrupts
}

```

## 8.2.2 Serial1.h and Serial1.c

### 8.2.2.1 Serial1.h

```

/*****
*
*   File Name:    serial1.h
*
*   Content:     Header file for the RS232 Serial Port driver for UART0 of
*               the M32C/80's MCU.
*****/

#ifndef MAIN_CLOCK
#define MAIN_CLOCK    (unsigned long)20e6 // Main clock crystal speed 20MHz
#endif
#define BAUDRATE    115200 // UART0 baud rate
#define DIV_RATE    0      // Valid entries are 0, 1, 2... Where:
                          // 0 = clock divide rate of 1,
                          // 1 = clock divide rate of 8,
                          // 2 = clock divide rate of 32

#define XMIT_BUFFER_SIZE    80 // Transmit buffer size in bytes.
#define RECEIVE_BUFFER_SIZE 80 // Receive buffer size in bytes.

// Calculate Bit Rate Register Value
// Setting UART0 bit rate generator for 9600 baud
// example: 129 = 20MHz / (16*(n+1)*9600) - 1      :   f1 => n=0
#if DIV_RATE == 0
#define BRG_REG_VALUE (unsigned char)((MAIN_CLOCK/(BAUDRATE*16*1))-1)
#elif DIV_RATE == 1
#define BRG_REG_VALUE (unsigned char)((MAIN_CLOCK/(BAUDRATE*16*8))-1)

```

```

#elif DIV_RATE == 2
#define BRG_REG_VALUE (unsigned char)((MAIN_CLOCK/(BAUDRATE*16*32))-1)
#endif

// Some handy MACROS *****
#define TXEPTY 0x8 /* transmit register empty */
#define TE 0x1 /* transmit enable */
#define TI 0x2 /* transmit buffer empty */
#define RE 0x4 /* receive enable */
#define RI 0x8 /* receive complete */

#define ACK 0x40
// #define BUSY 0x20
#define FAULT 0x10
#define RESET 0x8
#define STROBE 0x4
/*****/

// Interrupt Processing Functions
#pragma INTERRUPT rcev_isr // Receive Interrupt Handler.
void rcev_isr(void);

#pragma INTERRUPT xmit_isr // Transmit Interrupt Handler.
void xmit_isr(void);

void init_uart(void); // Initial Serial UART0 of M32C/80's MCU.
int char_rcev(void); // Test for presence of char in receive queue.
char rcev_char(void); // Receive single char from receive serial queue.
void writeString(char * str);
void uart_xmit(char c);

```

### 8.2.2.2 Serial1.c

```

//serial1.c
#include <string.h>
#include "sfr83v100.h" /* SFR register definition */
#include "serial1.h"
#include "board.h"

// QUEUE STRUCTURES
char Ser_RCEV_q[RECEIVE_BUFFER_SIZE];
int SRECV_IN, SRECV_OUT;

void init_uart(void){

    int trash;
    ps0_7 = 1; // set port 6_7 to TxD0 function page

    ulmr = 0x05; // 8 bits, Internal clock, one stop bit, Parity
disabled, sleep mode deselected.
    //ulbrg = BRG_REG_VALUE; // bite rate generator register - 0 (n+1)
    ulbrg = 10; // 10 is for 115000bps baud
    ulc0 = 0x10; // f1(main clock), no CST/RST, TXD is CMOS output,
transmit on falling edge, MSB first.

    // Initialize Queues
    //SXMIT_IN = 0; // Init queues indexes.
    //SXMIT_OUT = 0;
    SRECV_IN = 0;

```



```

SRECV_OUT = 0;

ulrb = 0; // clear transmit buffer register
ulc1 = u0c1;

ulc1 |= RE; // receive enable
trash = ulrb; // clear receive buffer by reading it
ulc1 &= 0x0b; // receive disable

_asm("fclr i"); // disable interrupts

slric = 0x02; // UART1 receive interrupt control register -
priority = 2

ulc1 |= RE; // receive enable
ulc1 |= TE; // transmit enable

_asm("fset i"); // enable interrupts
}

//Interrupt handler for the receive buffer
void rcev_isr(void){
    static char received;
    LED3 ^= 1; // toggle yellow LED3
    received = ulrb;
    Ser_RCEV_q[SRECV_IN] = received;
    if(++SRECV_IN >= RECEIVE_BUFFER_SIZE)
        SRECV_IN = 0;
    ulc1 |= RE; // receive enable
}

void xmit_isr(void){

}

void writeString(char * str){
    int temp;
    temp = strlen(str);
    while(temp--){
        // wait for data to be grabbed by remote connection i.e. data is still on
the transmit buffer
        while(( ulc1 & 0x02) == 0);
        ulrb = (unsigned short) *str++;
    }
}

// transmit a single character
void uart_xmit(char c){
    // wait for data to be grabbed by remote connection i.e. data is still on the
transmit buffer
    while(( ulc1 & 0x02) == 0);
    ulrb = c;
    LED4 ^= 1;
}

//Receive single char from receive serial queue.
char rcev_char(void){ // Receive single char from receive serial queue.

    char data;
    if(SRECV_OUT != SRECV_IN){
        data = Ser_RCEV_q[SRECV_OUT];
    }
}

```

```

        if(++SRECV_OUT >= RECEIVE_BUFFER_SIZE)
            SRECV_OUT = 0;
        return data;
    }
    else
        return 0xff;
}

//returns 1 if received data is in the receive queue. Checks queue buffer for
receive data.
int char_rcev(void){
    if(SRECV_OUT == SRECV_IN)
        return 0;
    else
        return 1;
}

```

## 8.2.3 adc.h and adc.c

### 8.2.3.1 adc.h

```

// ad.h
// author: Carey Merritt

#pragma INTERRUPT ad_int // define ad_int() to be an interrupt routine
void ad_int(void); // AD conversion interrupt routine

void ad_init(void); // initialize the A/D converter

```

### 8.2.3.2 adc.c

```

// ad.c
// author: Carey Merritt

#include "sfr83v100.h" // SFR register definition
#include "main.h" // Include the ain header file for any definitions
#include "ad.h" // Header definitions for this file

extern unsigned int ad0_value;
extern unsigned int ad4_value;
extern unsigned int ad6_value;
extern unsigned int ad7_value;

unsigned char channel;

/*****
Name: AD_init
Parameters: None
Returns: None
Description: Initializes the A/D converter to a single mode 10 bit conversion
using the sample and hold circuit and using the fAD/2 conversion
clock. Also set up the A/D converter to convert channel AN0
*****/
void ad_init(void)
{
    //_asm("fclr i");
}

```

```

ad0con0 = 0x80; // Set the AD to AN0 input, One shot Mode,
               // Software trigger
               // and a fAD/2 conversion clock

ad0con1 = 0x28; // Connect Vref and set the AD to a 10bit conversion
ad0con2 = 0x01; // Enable the Sample and hold circuit
ad0ic = 6;      // Set the interrupt priority level to 6

pd9_7 = 0;     // Set the A/D pin to an input //for ADTRG

channel = 0;
adst_ad0con0 = 1;

//_asm("fset i");
}

//This is that ad completion interrupt routine.
void ad_int(void){

switch (channel){
case 0:
    ad0_value = ad00;          // onboard pot
    channel = 4;
    break;
case 4:
    ad4_value = ad04;
    channel = 6;
    break;
case 6:
    ad6_value = ad06;
    channel = 7;              // next channel is channel 7
    break;
case 7:
    ad7_value = ad07;
    channel = 0;              // next channel is channel 0
    break;
default: break;
}

ad0con0 = 0x80 | channel;
adst_ad0con0 = 1;           // start next conversion
                           // clear interupt flag is handled by hardware
}

```

## 8.2.4 Board.h

```

// board.h
// author Carey Merritt

/*****
*
*   File Name:    board.h
*
*   Content:     Macros for access to items on the M32c/83 evaluation board
*****/

#define LED2 p7_2
#define LED3 p7_4
#define LED4 p8_0
#define LED5 p15_1

```

## 8.2.5 Timer.h and Timer.c

### 8.2.5.1 Timer.h

```
// timer.h
// author Carey Merritt

#pragma INTERRUPT ta0_int // define ta0_int() to be an interrupt routine
void ta0_int(void);      // Timer A0 interrupt routine

void ta0_init(void);
```

### 8.2.5.2 Timer.c

```
// timer.c
// author Carey Merritt

#include "sfr83v100.h" // SFR register definition
#include "main.h"      // Include the main header file for any definitions
#include "timer.h"    // Header definitions for this file

// Redefine the variables that these routines need to use but are defined
// in another module
extern volatile unsigned long system_counter; // background counter

int time_cnt = 0;

/*****
Name:      ta0_int
Parameters: None
Returns:   None
Description: This is the timer A0 interrupt routine. It updates the timer count
              every timer a0 interrupt (every milisecond).
*****/
void ta0_int(void){
    system_counter++;
}

/*****
Name:      TAO_init
Parameters: None
Returns:   None
Description: Initializes the timer A0 interrupt
*****/
void ta0_init(void){
    _asm("fclr i");
    ta0mr = 0x40; // Set Timer A to a Timer operating at f8
    //ta0 = 1999; // Set the timer to fire every lms
    ta0 = 2499;  // Set the timer to fire every lms
    ta0s = 1;    // Start the timer
    ta0ic = 2;   // Set the interrupt Priority level to 2
    _asm("fset i");
}
```